OPTIMIZATION OF FLEXIBLE SPECTRUM IN OPTICAL TRANSPORT NETWORKS

By

Duncan Kiboi Boiyo

Submitted in fulfilment of the requirements for the degree of

PHILOSOPHIAE DOCTOR

in the faculty of Science at the Nelson Mandela Metropolitan University

April 2017

Promoter

Prof. Tim Gibbon

Co-promoters

Dr. Romeo Gamatham

Prof. Andrew Leitch

Dedication

This thesis is dedicated to my family and the Sabaot community.

“For whoever seeketh light, God granteth”

Declaration

I, Duncan Kiboi Boiyo, student number: 214197484, hereby declare that the thesis for PhD in Physics is my own work and that it has not previously been submitted for assessment or completion of any postgraduate qualification to another University or for another qualification.

Signature: 

Date: 22nd February 2017

Acknowledgement

This journey would have been the longest had it not been for the best, steadfast concern, positive criticism, discussions, guidance and support from my promoters, research mates at the NMMU's Centre for Broadband Communication (CBC), friends and family. Firstly, I wish to thank my promoter Prof. Tim Gibbon for giving me a chance to work under his supervision. His experience and knowledge in the field of optics and high speed fibre communication were of great importance to this work. I am also greatly indebted to my co-promoters Prof. Andrew Leitch and Dr. Romeo Gamatham for their time and positive input to my studies. To my former supervisors; Dr. David Waswa, Prof. Samuel Rotich and Prof. George Amolo, thank you very much for the humble grooving that you provided.

I am also grateful to Nelson Mandela Metropolitan University (NMMU) and their Physics Department in offering me a chance and financial support to complete my PhD studies. Through your support, the local and international conferences that I attended were so valuable for the experience, progress and completion of this work. Thank you Alta McCleland for your unending and excellent support and assistance to the Centre for Broadband Communication during my entire period of study.

I would like to sincerely acknowledge research funding and equipment support from the following organizations: SKA, ALC, CSIR-NLC, NRF, DST, Cisco, Telkom, Dartcom, THRIP and Ingoma Services. Thank you for supporting my quest to see the "light".

To the members of the NMMU's CBC and friends; Dr. Rotich, Dr. Chabata, Wassin, Isoe, Phumla, Dr. Kwarikunda, Kagiso, Lucean, Okullo, Dr. Bosire, Hilda, Agnes, Sister Anne, Tereziah, John, Michelle, Jane and Immaculate, you all became part of my immediate family. I am also indebted to NMMU's volleyball and Postgraduate soccer teams for the healthy training and league matches. I thank God for these amazing families.

To my family and two kids Arnold and Chepkorir, you gave me a reason for working extra hard. Your prayers, sacrifices, encouragement and inspiration were so helpful. To my parents, siblings and friends, those frequent calls, texts and chats were valuable.

And to God, I give praise and thanksgiving for the care, safety, wisdom, life, love, kindness and daily provisions.

Kongoi missing', Asante sana, Thank you, Dankie, Enkosi

Contents

List of Figures

List of Tables

Abstract

The ever-increasing demand for broadband services by end-user devices utilising 3G/4G/LTE and the projected 5G in the last mile will require sustaining broadband supply from fibre-linked terminals. The eventual outcome of the high demand for broadband is strained optical and electronic devices. The backbone optical fibre transport systems and techniques such as dense wavelength division multiplexing (DWDM), higher modulation formats, coherent detection and signal amplification have increased both fibre capacity and spectrum efficiency. A major challenge to fibre capacity and spectrum efficiency is fibre-faults and optical impairments, network management, routing and wavelength assignment (RWA). In this study, DWDM and flexible spectrum techniques such as wavelength assignment and adjustment, wavelength conversion and switching, optical add and drop multiplexing (OADM) and bitrate variable transmission have been experimentally optimized in a laboratory testbed for short- and long-haul optical fibre networks.

This work starts by experimentally optimising different transmitters, fibre-types and receivers suitable for implementing cost effective and energy efficient flexible spectrum networks. Vertical cavity surface-emitting lasers (VCSELs) and distributed feedback (DFB) lasers have been studied to provide up to 10 Gb/s per channel in 1310 nm and 1550 nm transmission windows. VCSELs provide wavelength assignment and adjustment. This work utilises the non-return-to-zero (NRZ) on-off keying (OOK) modulation technique and direct detection due to their cost and simplicity. By using positive intrinsic negative (PIN) photo-receivers with error-free BER sensitivity of -18±1 dBm at the acceptable 10^{-9}-bit error rate (BER) threshold level, unamplified transmission distances between 6 km and 76 km have been demonstrated using G.652 and G.655 single mode fibres (SMFs).

For the first time, an all optical VCSEL to VCSEL wavelength conversion, switching, transmission at the 1550 nm window and BER evaluation of a NRZ data signal is experimentally demonstrated. With VCSEL wavelength conversion and switching, wavelength adjustments to a spectrum width of 4.8 nm (600 GHz) can be achieved to provide alternative routes to signals when fibre-cuts and wavelength collision occurs therefore enhancing signal continuity. This work also demonstrates a technique of removing and adding a wavelength in a bundle of DWDM and flexible channels using an OADM. This has been implemented using a VCSEL and a fibre Bragg grating (FBG) providing a wavelength isolation ratio of 31.4 dB and $\sim 0.3\ dB$ add/drop penalty of 8.5 Gb/s signal. As a result, an OADM improves spectrum efficiency by offering wavelength re-use.

Optical impairments such as crosstalk, chromatic dispersion (CD) and effects of polarization mode dispersion (PMD) have been experimentally investigated and mitigated. This work showed that crosstalk penalty increased with fibre-length, bitrate, interfering signal power and reduced channel spacing and as a result, a crosstalk-penalty trade-off is required. Effects of CD on a transmitted 10 Gb/s signal were also investigated and its mitigation techniques used to increase the fibre-reach. This work uses the negative dispersion fibres to mitigate the accumulated dispersion over the distance of transmission. A 5 dB sensitivity improvement is reported for an unamplified 76 km using DFB transmitters and combination of NZDSF true-wave reduced slope (TW-RS) and submarine reduced slope (TW-SRS) with + and – dispersion coefficients respectively. We have also demonstrated up to 52 km 10 Gb/s per channel VCSEL-based transmission and reduced net dispersion. Experimental demonstration of forward Raman amplification has achieved a 4.7 dB on-off gain distributed over a 4.8 nm spectral width and a 1.7 dB improvement of receiver sensitivity in Raman-aided 10 Gb/s per wavelength VCSEL transmission. Finally, 4.25-10 Gb/s PON-based point to point (P2P) and point to multipoint (P2MP) broadcast transmission have been experimentally demonstrated. A 10 Gb/s with a 1:8 passive splitter incurred a 3.7 dB penalty for a 24.7 km fibre-link.

In summary, this work has demonstrated cost effective and energy efficient potential flexible spectrum techniques for high speed signal transmission. With the optimized network parameters, flexible spectrum is therefore relevant in short-reach, metro-access and long-haul applications for national broadband networks and the Square Kilometre Array (SKA) fibre-based signal and data transmission.

Keywords: *Optical transport networks, DWDM, flexible spectrum, VCSELs, DFB, wavelength conversion, OADM, Raman amplification, signal impairments, signal transmission, Optical fibre broadband networks.*

List of acronyms

ACO-Ant-colony optimization

ADC-Analogue to digital converter

APD-Avalanche photodiode

B2B-Back to back

BER-Bit error rate

BERT-Bit error rate tester

BPF-Band-pass filter

BPSK-Binary phase shift keying

BT-Bias tee

BVT-Bandwidth variable transmitter

CD-Chromatic dispersion

DBR-Distributed Bragg reflector

DCF-Dispersion compensating fibre

DD-Direct detection

DFB-Distributed feedback

DGD-Differential group delay

DOP-Degree of polarization

DWDM-Dense wavelength division multiplexing

EA-Electrical amplifier

EAM-Electro-absorption modulator

EDFA-Erbium doped fibre amplifier

ER-Extinction ratio

FBG- Fibre Bragg grating

FTTX-Fibre to the home/building/premise/node/dish/hut

FUT-Fibre under test

FWM-Four wave mixing

GMPLS-General multi-purpose label switching

GPON-Gigabit passive optical network

GVD-Group velocity dispersion

IA-RWA-Impairment-aware routing and wavelength assignment

IDF-Inverse dispersion fibre

InAlGaAs-Indium Aluminium gallium arsenide

InGaAsP-Indium Gallium arsenide phosphide

ISI-Inter symbol interference

ITU-T-International telecommunication union

LDC-Laser diode controller

LED-Light emitting diode

MAN-Metro-access network

MMF-Multimode fibre

MZM-Mach-Zehnder modulator

NMS-Network management system

NRZ-Non-return-to-zero

NZDSF-Non-zero dispersion shifter fibre

OADM-Optical add and drop multiplexer

OEO-Optical-electrical-optical

OLT-Optical line terminal

ONU-Optical network unit

OSNR-Optical signal to noise ratio

OSPF-Optical shortest path first

P2MP-Point to multipoint

P2P-Point to point

PC-Polarization controller

PCE-Path computation element

PIN-Positive intrinsic negative

PMD-Polarization mode dispersion

PMF-Polarization maintaining fibre

PON-Passive optical network

PPG-Programmable pattern generator

PRBS-Pseudo random binary sequence

QAM-Quadrature amplitude modulation

QoS-Quality of signal

QoT-Quality of transmission

QPSK-Quadrature phase shift keying

RF-Radio frequency

RFI-Radio frequency interference

ROADM-Reconfigurable optical add and drop multiplexer

SDN-Software defined network

SKA-Square Kilometre Array

SMF-Single mode fibre

SMSR-Side mode suppression ratio

SOA-Semiconductor amplifier

SOP-State of polarization

SPM-Self-phase modulation

SRS-Stimulated Raman scattering

TDM-Time division multiplexing

TEC-Thermo-electric cooler

TFR-Timing and frequency reference

TIA-Trans impedance amplifier

TL-Tunable laser

TW-RS-True Wave-reduced slope

TW-SRS-True wave-submarine reduced slope

VCSEL-Vertical cavity surface-emitting laser

VOA-Variable optical attenuator

WDM-Wavelength division multiplexing

XPM-Cross-phase modulation

ZDSF-Zero dispersion shifted fibre

Chapter 1

1.0 Introduction

The tremendous increase in demand for bandwidth by fixed and mobile devices, smart-homes/vehicles/healthcare, cloud computing and data centres has stretched the demands on optical transport networks. The devices will require sustaining broadband supply from fibre-linked terminals. Most European, American and Asian countries have had successful fibre installed to the home/building/premises (FTTX) connections using passive optical networks (PONs) for individual and/or institutional users that rely on high speed connectivity in their daily operations. Due to the high capacity and reach of an optical fibre over copper and free-space transmission, backbone network architectures have focused on achieving enhanced sensitivity, reach and capacity by taking advantage of developments in semiconductor lasers, optical fibres and detectors. Different modulation formats and multiplexing techniques have greatly increased capacity and spectrum efficiency as well as minimizing signal impairments that occur over length of an optical fibre-link. Advanced modulation formats greatly improve spectrum efficiency by increasing the number of transmitted bits per symbol. However, advanced modulation formats are limited by the poor signal to noise performance and this results in low bit receiver sensitivity. As a result, the traditional on-off keying (OOK) and phase-shift keying (PSK) modulation formats have been optimized for long distance transmission. In increasing fibre capacity, dense wavelength division multiplexing (DWDM) has been used to aggregate several channels with channel spacing range of 25 GHz to 100 GHz and transmitting them over a single fibre. However, a trade-off between capacity and distance is required since adjacent channels are affected by inter-channel crosstalk, optical nonlinear effects and the fixed DWDM grid system that introduces underutilization of spectrum. For metro-access networks (MANs) using either point to point (P2P) or point to multipoint (P2MP), routing and spectrum assignment (RSA), channel collisions and switching and real-time fault detection and repairs poses a great challenge to signal continuity for fixed DWDM systems.

Different fibre-based network topologies require optimized speeds, capacity, reach and device performances. From short-reach to long-haul signal transmission, fibres have been used to create an inter-continental network using marine cabling and the layout of national broadband networks (NBNs) that depends entirely on backbone fibre connections.

Optical fibre networks have created a faster data transfer, control and monitoring and timing and reference frequency (TRF) signals in megaprojects such as the Square Kilometre Array (SKA) Project, South Africa, a global telescope for scientific study of the universe. Since optical fibres are immune to electromagnetic interference (EMI), the more sensitive RF timing signals for accurate measurements and synchronization in the SKA are therefore best transmitted over fibres rather than copper and free-space. Distance is also a major factor in the SKA Project since signal transmission will cover over 3000 km baselines to incorporate other partner countries which makes optical fibre transport an important element in realization of the project. The correlator dishes of the MeerKAT will be distributed within 12 km with real-time signal transmission. This creates the SKA fibre to the dish (FTTD network.

This thesis presents viable techniques for optimizing high speed optical fibre transport networks for short-reach, metro-access and long-haul broadband networks. Energy and cost effective techniques for providing efficient spectrum utilization are presented. Focus has been emphasized on the various techniques for implementing flexible spectrum networks such as tunable transmitters, different bit-rates, wavelength conversion and switching, optical add and drop multiplexing (OADM), dense wavelength division multiplexing (DWDM) and considering signal impairments to optimize quality of signals at the 1310 nm and 1550 nm transmission windows. Wavelength tunable, directly modulated, high bandwidth, low cost and low power consuming vertical cavity surface-emitting lasers (VCSELs) and distributed feedback (DFB) lasers as well as highly sensitive positive intrinsic negative (PIN) photo-receivers have been used.

Signal impairments such as chromatic dispersion, polarization mode dispersion (PMD) and crosstalk occurring in different single mode fibres (SMFs) have been considered and compensated for optimized fibre-reach and high capacity short and long distance transmission. Dispersion has been minimized by considering fibres with low dispersion effects at the 1310 and 1550 nm transmission windows while dispersion compensation has been achieved by using fibres with negative dispersion properties. Moreover, fibre-reach has been extended by utilising forward Raman amplification on VCSEL-based 10 Gb/s signal transmission. Wavelength conversion and switching has for the first time been experimentally demonstrated using 1550 nm window VCSELs to provide wavelength re-routing during fibre-cuts and channel collisions. OADM multiplexing has been demonstrated using a FBG to increase spectrum capacity by providing wavelength drop and

channel re-use. Up to 10 Gb/s PON-based P2P and P2MP high speed signal broadcast has been optimized passive splitters.

This study has for the first time, to the best of our knowledge, experimentally demonstrated and evaluated a cheaper, energy efficient and simple VCSEL-to-VCSEL wavelength conversion and switching at the 1550 nm window that reduces channel collisions and wavelength blocking probability. We have combined wavelength tunability, conversion, switching, DWDM with flexible spacing, OADM and mitigated signal impairments to create an optimised reconfigurable flexible spectrum for use in next generation networks. Distances of 500 m to 76.8 km have been considered to emulate short-access to long-distance signal transmission. This study has been implemented in a laboratory testbed at the Nelson Mandela Metropolitan University's Centre of Broadband Communication, Port Elizabeth, South Africa.

1.1 Thesis Outline

This thesis is structured as follows; Chapter 1 provides an introduction to optical communication systems and network topologies for short and long-haul point-to-point (P2P) and point-to-multipoint (P2MP) in metro-access, national broadband networks and the SKA fibre network. Chapter 2 describes state of the art equipment, advantages and disadvantages of flexible spectrum in optical fibre networks. It also discusses managing network properties using control and monitoring algorithms in a control plane. The various components of a flexible spectrum network are illustrated in chapter 3. The state of the art components such as VCSELs, DFB lasers, modulation techniques, photo-receivers, types of fibres and optical effects that limit the quality of a signal such as fibre attenuation, dispersion, PMD and crosstalk are introduced. Chapter 4 discusses examples of backbone optical fibre networks and their architecture such as the South African and Australian national broadband networks (NBNs) and the SKA-South Africa optical fibre network. Chapter 5 to 9 give experimental and simulated research findings as performed in a laboratory testbed.

Chapter 5 demonstrates performance evaluation of VCSEL and DFB lasers for use at the 1310 and 1550 nm transmission windows. Wavelength tunability, low power consumption and direct modulation to transmit up to 10 Gb/s per channel/wavelength is reported. The PIN photo-receiver has been optimized for short and long-distance transmissions. Wavelength tunability of a VCSEL has been presented as one technique of wavelength assignment of nominal central wavelengths at the transmitter of a flexible

spectrum network. Chapter 6 describes a novel base technique for achieving purely optical wavelength conversion and switching and transmission using a pair of VCSELs operating at the low 1550 nm transmission window and bit error rate (BER) evaluation. Chapter 7 demonstrates a cheap and efficient OADM implementation for use at an optical node for receiving and inserting a new data signal into the available channel. This therefore enhances wavelength re-use and spectrum efficiency. Chapter 8 characterises and compensates signal impairments such as crosstalk, dispersion and polarization in a fibre-link to enable high speed and undistorted signal transmission. Chapter 9 provides an experimental demonstration of how fibre-links, wavelength assignment and optimized bit-rate transmission can be transmitted for short, metro-access, hops in long-haul, long-haul and broadcast optical fibre networks. Chapter 10 concludes with a summary of this thesis.

Chapter 2:

2.0 Flexible Spectrum and its Challenges in Optical Fibre Transport Systems

This theory chapter provides detailed information on the elements, opportunities and challenges experienced in implementing flexible spectrum networks. Advantages such as efficient and effective utilization of available spectrum in high speed signal transmission over fibre are highly emphasized. From bandwidth variable transmitters (BVTs), dense wavelength division multiplexing (DWDM), high fibre capacity to receiver technology for application to short and long-haul networks been studied. Comparisons between fixed DWDM and flexible spectrum fibre networks and ways of integrating these networks have also been provided. Technology of controlling and managing network parameters using either a central or distributed control plane comprising of algorithms is described to provide an insight of resource optimization and self-reconfiguration networks.

2.1 Background to Flexible Spectrum

The demand for real-time interactive communication has astronomically driven the global network traffic and stretched the hardware requirements. From clustered data storages instruments generating 10 Gb/s to terabit scale data flow, requires hundreds of Gb/s high speed backbone optical paths. Recent innovations focusing on transmission, medium and receiver technologies such as advanced modulation techniques, multiplexing, coherent detection and digital equalization have been predicted to improve fibre capacity and spectrum efficiency [1]. Not only is the bitrate per wavelength increased but also fibre-reach.

Dense-wavelength division multiplexing (DWDM) is one of the main techniques used to increase fibre capacity by having several wavelengths traversing within a single fibre-strand. The channel spacing in a fixed DWDM system are 25 GHz, 50 GHz, 100 GHz and multiples of 100 GHz [2]. Indeed, these spacing have historically evolved by simply sub-dividing the 100 GHz by successive factors of two [2]. To increase spectrum efficiency by avoiding wastage of unutilized or underutilized spectrum, flexibility is key. In flexible spectrum networks, flexibility encompasses dynamic configuration of link parameters such as modulation techniques, bitrates, wavelength switching, routing and spectrum assignment (RSA) and forward error correction (FEC) [1], [3], [4]. In a typical flexible grid network,

through algorithms, a network itself chooses arbitrary data channels and assigns sections of spectrum and the suitable path/route. Moreover, the selected channels have mixed modulation formats, bitrates and bandwidth that are optimized for specific channel requirements [5]. By slicing the spectrum, sub-and super-channels with 12.5 GHz to 500 GHz slot widths can be created [6], [7].

2.1.1 Terminologies used in Flexible Grid System

The following are the accepted terminologies used in flexi-grid system [2]:

(a) Frequency grid: - this is a set of reference frequencies used to define the allowed nominal frequencies and a typical central frequency granularity of 12.5 GHz.

(b) Nominal central frequency: - Refers to each of the allowed frequencies defined in the flexible DWDM grid. A nominal central frequency can be built from the following expression;
$193.1\ THz + n \times 0.00625\ THz$, where *n* is either a positive or negative integer and $193.1\ THz$ is the ITU-T "Anchor Frequency".

(c) Frequency slot: - is a frequency range that is allocated to a slot within a flexible grid and is not available to other slots. It is defined by the nominal central frequency and the slot width.

(d) Slot width: - In a flexible grid, this is defined as the full width of a frequency slot.

(e) Nominal central frequency granularity: - It is the spacing between successive allowed nominal central frequencies and is set to 6.25 GHz. This is equivalent to channel spacing in fixed DWDM systems.

(f) Slot width granularity: - Is equal to 12.5 GHz and defines the spectral size of the slot width.

These terminologies are illustrated in figure 2.1.

2.2 Application of Flexible Spectrum in Optical Transport Networks

In solving global internet traffic, DWDM systems have been found to increase the optical fibre capacity and spectrum efficiency. This has been realized by reducing the channel spacing from 2.5 THz (20 nm) in the traditional coarse wavelength division multiplexing (CDWM) to 25-100 GHz as implemented in DWDM systems [2], [8]. One of the ways of implementing flexible spectrum in existing optical fibre-links is to have multi-bitrates allocated to different frequency slots so as to achieve a variable transponder. By choosing

the right nominal central frequencies and slot widths, flexible grid systems can be integrated into the existing 25 GHz, 50 GHz, 100 GHz and multiples of 100 GHz grid systems.

The multi-bitrate optical systems are achieved by using modulation formats such as on-off keying (OOK), binary phase shift keying (BPSK), quadrature amplitude modulation (QAM) and their higher-order multiples [9], [10], [11]. Indeed, 100 Gb/s and 400 Gb/s bitrate have been demonstrated using polarization multiplexed-quadrature phase shift-keying (PM-QPSK) and polarization multiplexed-16-quadrature amplitude modulation (PM-16QAM) to fit into the existing 50 GHz grid system [6], [11]. Slot widths of the flexible frequencies can be configured to satisfy channel requirements and the available spectrum. Depending on how it is used, "flexibility" may actually be used to describe a fixed and channelized grid [12]. From the DWDM central frequencies, nominal central frequencies can be created based on $193.1\,THz + n \times 0.00625\,THz$ and slot width multiples of $12.5\,GHz \times m$ as illustrated in table 2.1 and figure 2.1. The channels are chosen in such a way that the nominal central frequencies do not overlap. Overlapping channels introduces inter-channel crosstalk [13].

Table 2.1: An example of the nominal central frequencies in the fixed DWDM grid that the flexible grid can fit into [2].

Nominal central frequencies (THz) for spacings of:				**Approximate nominal central wavelengths (nm)**
12.5 GHz	**25 GHz**	**50 GHz**	**100 GHz**	
193.2375	-	-	-	1551.4197
193.2250	193.225	-	-	1551.5200
193.2125	-	-	-	1551.6204
193.2000	193.200	193.20	193.2	1551.7208
193.1875	-	-	-	1551.8212
193.1750	193.175	-	-	1551.9216
193.1625	-	-	-	1552.0220
193.1500	193.150	193.15	-	1552.1225
193.1375	-	-	-	1552.2229
193.1250	193.125	-	-	1552.3234
193.1125	-	-	-	1552.4239
193.1000	193.100	193.10	193.1	1552.5244

193.0875	-	-	-	1552.6249
193.0750	193.075	-	-	1552.7254
193.0625	-	-	-	1552.8259
193.0500	193.050	193.05	-	1552.9265
193.0375	-	-	-	1553.0270
193.0250	193.025	-	-	1553.1276
193.0125	-	-	-	1553.2282
193.0000	193.000	193.00	193.0	1553.3288

An example of flexible grid system is as shown in figure 2.1. Two flexible channels with 50 GHz (m= 4) slot widths are created at the anchor frequency, 193.1 THz (n= 0) and 193.05 THz (n= -8) respectively. Further flexibility is illustrated by slicing the spectrum to 75 GHz by allocating 6 slots at n= 19 and n= 31 [2]. The available spectrum can be used as a guard band between the 50 GHz and 75 GHz channels to prevent frequency overlap. All the different channels in a flexible grid system have different modulation formats and bitrates to allow contiguous wavelengths and avoid spectrum fragmentation [1], [14].

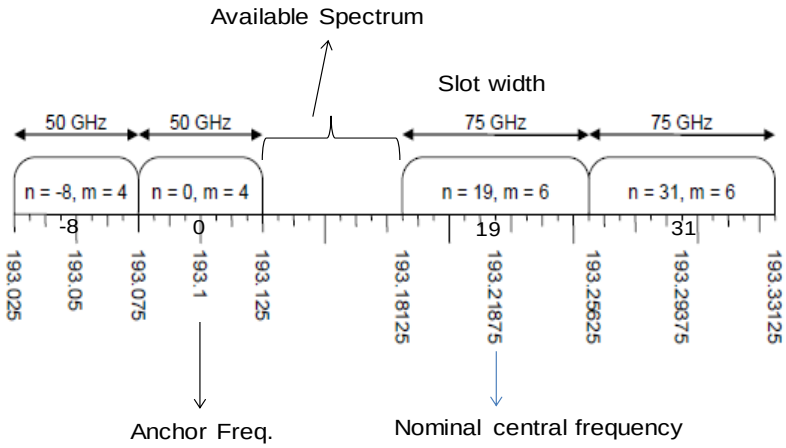

Figure 2.1: An example of flexible grid system and different frequency slots [2].

For efficient spectrum usage, the available spectrum can be allocated to additional channels by either creating a single channel with a 50 GHz size (n= 8, m= 4) or two channels with 25 GHz slot widths at n= 10 and n= 6. In both scenario, a 6.25 GHz is left unallocated. The remaining 6.25 GHz can be used as a guard band.

2.2.1 Opportunities for Flexible Spectrum Networks

a) Spectrum Efficiency

The main advantages of flexible spectrum are the ability to defragment the spectrum to dense 12.5 GHz spacing and also join contiguous frequency slots forming arbitrary slot sized

channels. This has been enhanced by the implementation of the Liquid Crystal on Silicon (LCoS) devices for large-scale flexible spectrum deployment [15]. Virtual network properties of a flexible spectrum at a network node can be dynamically configured using software implemented LCoS-based wavelength selective switching (WSS). This is done by switching any number of channels to any arbitrary output ports. Spectrum efficiency is also enhanced by allocating smaller amounts of spectrum to lower bandwidth signals that do not necessarily require an entire 50 GHz slot in the DWDM fixed grid system [6], [16]. The multi-bitrate transponders in flexible networks greatly reduce the spectrum usage by utilizing advanced modulation formats for a small symbol rate to achieve above 100 Gb/s with less than 100 GHz spectral width [15]. Higher capacity per channel on a narrow bandwidth using QPSK, OFDM, 8PSK and 16QAM also increases spectrum efficiency [7].

b) Routing and Resource Allocation

Flexible spectrum has optimized transmission distance in optical transport networks (OTNs) by adapting routing and resource allocation algorithms to attain realistic transmission distances with penalties at the acceptable bit error rate (BER) and minimising the number of transponders used [17]. Super-channels utilizing orthogonal frequency division multiplexing (OFDM) have been used to create with 12.5 GHz spaced subcarriers, 10-400 Gb/s channels using different symbol-rates for multi-bitrate carriers [18]. The spectrum-sliced elastic optical path network (SLICE) has been reported to eliminate the current wavelength-routed optical path networks and in the frequency-domain, provide efficient and flexible wavelength routed OTNs. The SLICE has been used to sub-divide spectrum into sub-wavelength and super-wavelength adjacent channels utilizing OFDM technology [1]. As a result, SLICE can be used to shrink or expand the spectrum depending on demand for bandwidth to offer dynamism where traffic is needed [19].

c) Energy and Cost Efficiency

The energy efficiency in terms of Watt/Gb/s is determined by power consumption per link capacity of transmitters, active link components such as optical cross-connects, ROADMs and receivers. Cost efficiency is optimized by considering the cost of equipment (CapEx) and the operational costs (OpEx) in running the network [19]. Operational costs are always difficult to predict since they encompass variety of factors such as costs of a central office, device running electricity costs and labour costs [20], [19]. It is therefore, economically

efficient to achieve both spectrum and capacity efficiency within a cost and efficient network architecture. Fibre-reach, spectrum efficiency, routing and spectrum assignment (RSA) and quality of signal are all optimized to reduce the energy and costs of a network link [21].

2.2.2 Challenges in Flexible Spectrum Networks

a) Spectrum Fragmentation

There has always been a spectrum continuity constraint associated with WDM systems, which dictates the availability of a vacant channel in a selected path for an established source-to-destination connection. This is done to ensure that the costly optical-electrical wavelength conversion is avoided [15]. In a flexible spectrum system, the problem of spectrum continuity becomes much of a concern since contiguous and non-contiguous spectrum slots are available. This results in isolated frequency slots with varying slot widths that increases channel blocking probability when spectrum is needed by a channel with an unknown order of connection demand. Despite the availability of spectrum, traffic demands might therefore be blocked [22]. Several approaches that reduce blocking probabilities and at the same time ensure spectrum efficiency have been studied and reported. These techniques include spectrum defragmentation and reallocation of the central frequencies of non-contiguous slots to form a gridless frequency system [23]- [24].

b) Switch in Time and Controllability

The implementation of flexible spectrum and introduction of bitrate variable transponders have added an extra complexity in the design and implementation of control and configuration of flexible grid systems [15]. Since transmission bitrates and slot sizes are self-determined by transponders, a real-time, constraint-aware control plane is needed to advertise and control network properties [14]. Feasibility studies have reported that ROADMs provide a real switch-in time that can reduce the costly of fixed WDM optics, blocking probability and reduce the CapEx by 30 % [6]. Moreover, RSA capabilities of the network are to be done in real-time with traffic requests from end-users by developing an advanced channel monitoring system [25]. However, it has been reported that it is difficult to implement the existing routing and wavelength assignment (RWA) algorithms in fixed WDM systems utilizing OFDM networks, even in fixed bitrates [17]. As a result, implementing a flexible spectrum with densely spaced subcarriers and contiguous grids with OFDM results in spectrum overlap. Utilizing RWA and RSA algorithms to optimize

wavelengths might be difficult to achieve. Complexities are even further added when physical layer impairments (PLIs) affecting the optical signal such as noise, chromatic dispersion (CD), attenuation, crosstalk and non-linear effects are considered [26]. The ideal flexible spectrum network should be able to reconfigure and adapt to changing impairments without use of rigid lookup tables.

2.3 State of the Art Equipment and Industry Implementation of Flexible Spectrum

As previously described, flexible spectrum is characterized by subsystems with flexible grid characteristics. These subsystems include different wavelengths, DWDM links, optical fibres, tunable transmitters and receivers, layer switching elements and electro-optic network components [27]. As reported in [2], the granularity of 6.25 GHz may not typically accommodate all the components of a flexible network into the frequency slots of a flexi grid. However, these components can be adjusted to fit into the possible slot widths and positions and having 25 GHz (slot widths multiples of even **m** only) [27]. As a result, the state of the art equipment used to implement flexible spectrum can be integrated with the existing fixed grid components. The following sections describe some of the elements and subsystems of a flexible spectrum network.

a) Bandwidth Variable Transponders (BVTs)

Bandwidth variable transponders (BVTs) have the capability of adjusting the transmission bitrates and the respective modulation formats. This expands or contracts the bandwidth depending on the traffic demand [28]. This has been effected by utilizing the spectrally efficient modulation formats such as 8PSK, 16QAM and 64QAM for short-reach transmission to achieve above 100 Gb/s super-channels. However, for long-haul transmission, more robust and less spectrum efficient modulation techniques such as OOK, BPSK, QPSK and OFDM are used to obtain 1-40 Gb/s speeds per channel [28], [29]. To further improve spectrum efficiency, advanced forms of BVTs have been proposed such as the sliceable BVTs (SBVTs) that utilize Nyquist WDM (NWDM) with carrier spacing closer to the Nyquist frequency [30]. However, advanced NWDM and OFDM require electrical external signal modulation with complex digital signal processing (DSP) for pulse re-shaping, filtering, data recovery, PLI compensation and signal equalization [31]. To increase spectrum efficiency, the unused subcarriers and spectrum can be turned off [28].

In metro-access and longer-reach flexible networks, the cost-effective and less complex direct modulation or externally modulated transmitters are used. The external modulators used to obtain up to 40 Gb/s speeds include the Mach-Zehnder modulator (MZM) using OOK and BPSK modulation techniques which are common to tunable semiconductor laser sources [32]. Path computation and wavelength assignment is provided by wavelength tunability in semiconductor lasers such as VCSELs and DFB transmitters. Their signal detection and data recovery is based on the less complex direct detection (DD) using a positive intrinsic negative (PIN) photodiode with a trans-impedance amplifier (TIA) or the high sensitivity Avalanche photodiode (APD) [32].

b) Bandwidth-variable Optical Cross-Connects (BV-OXCs)

Optical cross-connects (OXCs) have found applications in modern WDM communication systems to by-pass individual or several wavelength inputs to multiple output ports in an optical node of a network [33]. The two techniques of implementing OXCs include hybrid and the all-optical switching. For the hybrid approach, an electrical OXC is used for optical-electrical-optical data conversion while all-optical switching is used to directly channel incoming wavelengths to designated output ports [34]. The operational requirements, efficiency (number of ports) and insertion losses determine the most appropriate OXCs to be used in a WDM system [34].

To adapt to the demands of a flexible spectrum, bandwidth variable OXCs (BV-OXCs) provide an end-to-end connection, sufficient spectrum optical paths with optimised switching and RSA. Indeed, BV-OXCs and BVTs have been demonstrated in the SLICE technology without optical-electrical-optical (OEO) conversion [17], [35]. However, there is no industrial implementation of BV-OXC in a real network that has so far been reported. A lab demonstration of BV-OXC has been done to determine the best and optimized path computation element (PCE) where modulation formats, spectrum and the forward error correction (FEC) parameters are not only included as constraints as in the fixed grid systems, but are all described in the PCE [4]. Furthermore, RSA and PLIs are included to select an optimized path. The main challenge in OXCs is inter-channel crosstalk [36].

c) Reconfigurable Optical Add and Drop Multiplexers (ROADMs)

In communication networks, routers are used to by-pass wavelengths between separate networks. An intelligent way of managing WDM channels has been the introduction of

several types of OADMs. Depending on the degree of nodes, OADMs have been categorized into; fixed OADM (FOADM), blocker OADM (BOADM), reconfigurable (ROADM) and tunable OADM (TOADM) [37]. Different manufacturing techniques are used to design ROADMs and they include; microelectromechanical systems (MEMs), liquid crystal devices (LCDs), LCoS and planar lightwave circuit (PLCs) [38]. ROADMs provide an opportunity of either adding, dropping and allowing optical wavelengths to pass through a node (express) using wavelength selective switching (WSS) providing up to 4 to 40 port ranges. ROADMs are either but not limited to colourless (any wavelength), directionless (using software control plane, inbound and outbound routing), gridless (all sub- and super-channels) or contentionless (no wavelength blocking as traffic is rerouted) [39]. In a typical deployment, ROADMs enable remote control of add and drop wavelengths at each node while ensuring that addition of any wavelengths does not affect the existing channels at that node.

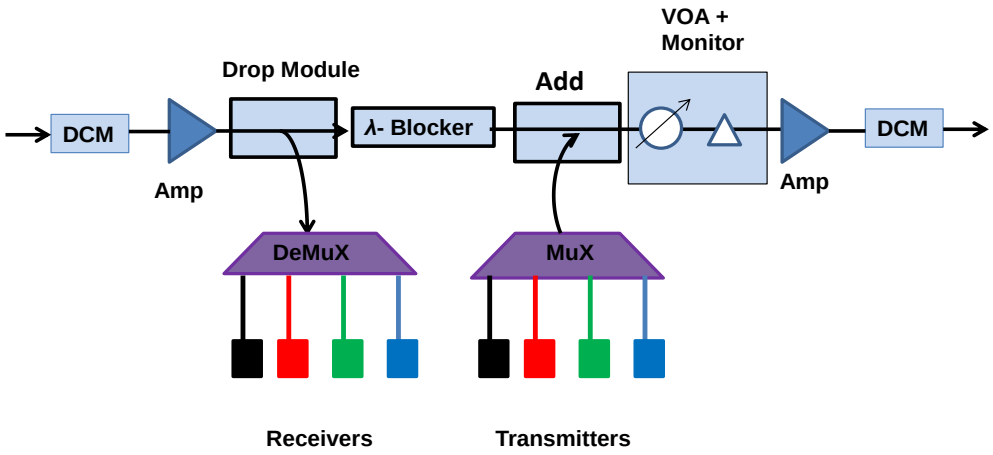

Figure 2.2: A block diagram of a ROADM with in-built multi functionality: dispersion compensating module (DCM), amplifier (amp), multiplexer (MUX), demultiplexer (DeMuX), wavelength blocker, Add/drop modules, variable optical amplifier (VOA) and power monitoring (Monitor) [35].

An example of a ROADM with in-built multi-functionality for creating an arbitrary network node is shown in figure 2.2. A bundle of incoming DWDM/flexible signals undergo a dispersion compensating module (DCM) that provides dispersion managed signal for pre- and post-amplification (amp) in an east-west scheme. A ROADM consists of add and drop modules that is designed for dropping and adding new wavelengths using WSS demultiplexers and multiplexers. Moreover, a variable optical attenuator (VOA) and a monitor are connected to the device to adjust and monitor the optical power of each wavelength.

Some of the requirements of a flexible network are having a flexible spectrum, WSS, flexible optical channel management (OCM), colourless multiplexer/demultiplexer, hybrid Raman-EDFA amplifiers and advanced network management control [25]. ROADMs therefore eliminate the costly OEO regeneration that is common with OXCs and add more control and flexibility to a network using a single platform [38]. Moreover, ROADMs support purely fast optical switching that are less expensive than the high speed electronics. As a result, CapEx and OpEx are greatly reduced when ROADMs are implemented. The efficiency of RSA can be improved by using add/drop capability where a demultiplexer routes only the selected wavelength to a local drop. This reduces the complexity and cost of the amplifier power and incorporating coherent receivers for colourless demultiplexing [25]. With respect to flexible grid systems, gridless ROADMs may have difficulties fitting into the ITU-T flexible grids with 12.5 GHz granularity especially in OFDM-based BVT where subcarriers are sometimes spaced in MHz [19].

2.4 Application of Flexible Spectrum in Optical Fibre Networks

The application of a flexible, gridless and bidirectional flexible spectrum for point-to-point (P2P) and point-to-multipoint (P2MP) in existing and future network topologies promises to attain an optimized trade-off between capacity and reach. Sub-channels and super-channels that transmit at 1 Gb/s to 400 Gb/s range and spectrum efficient bit-rates using BVTs and optimized receivers are interesting features of a flexible spectrum network. In the following sections, short and long-reach networks are studied to provide feasibility for flexible spectrum in metro-access networks, DWDM and long-haul fibre links spanning between 1 to 1000’s km.

2.4.1 Metro-Access Networks (MANs)

A typical application of a flexible spectrum in an incoming long-haul DWDM signal entering a ring metro-access network (MAN) where a ROADM controls the ingress and the egress wavelengths at a network node is as shown in figure 2.3. From the central office (CO) of a network, a ROADM configures and reconfigures the RSA of the network for optimized QoS and penalty while ensuring that spectrum efficiency and self-healing network is realized. Route and transmission restoration can be achieved by using directionless ROADMs, thereby reducing requirement for additional BVTs in multiple nodes of a complex network [31]. Indeed, the WSS capability of the ROADM is used to terminate (drop) wavelengths when the particular source-to-destination communication is ended.

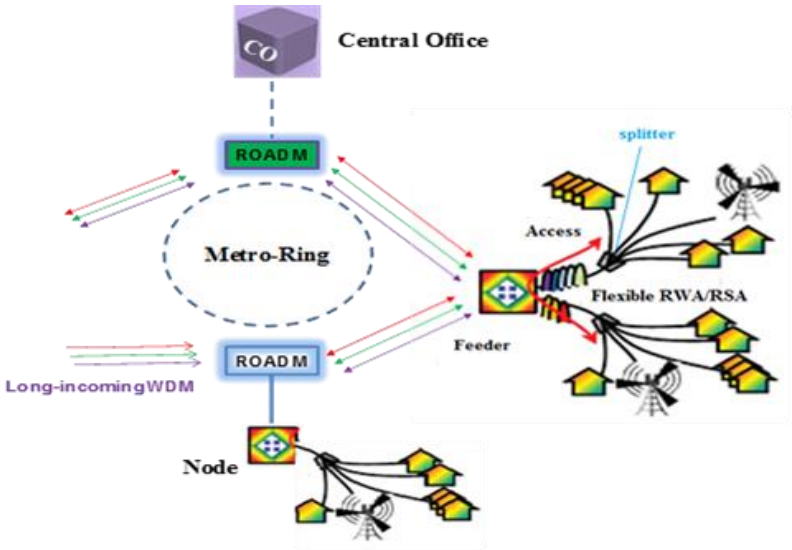

Figure 2.3: A network implementation of a ROADM in a typical ring metro access networks showing a long incoming network DWDM link and end user access [38].

For spectrum efficiency, a ROADM enables wavelength reuse where a new demand for spectrum is initiated. Moreover, in the event of fibre faults or cuts, the directionless ROADM can be used to reroute channels to their destinations via an adjacent node. To avoid channel overlap, the advantage of gridless flexible spectrum and ROADMs ensure that the wavelengths can be switched to new wavelengths.

For metro-access transmitters, elastic transponders can be used to provide optimized transmission with a trade-off between capacity, fibre-reach and QoS [40]. Some signals can hop over several optical nodes comprising of BV-OXCs without the signal being "lost" along the transmission.

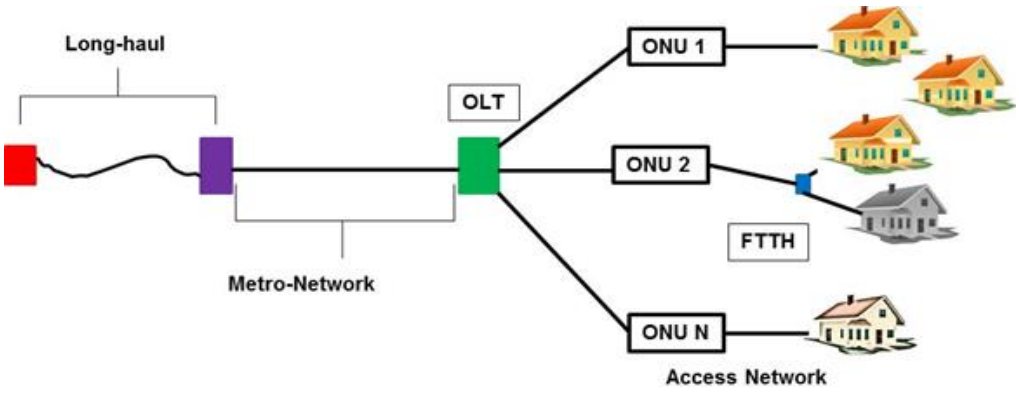

Figure 2.4: Illustration of long incoming signal and the connection into metro access network comprising of a central office (CO) with an optical line terminal (OLT), optical network units (ONUs) and the access users.

A metro-access network may contain either P2P or P2MP for single or multi-wavelength distribution services. As a result, a ROADM can be used to effectively reconfigure an access

network from the control plane located at the CO of a passive optical network (PON) as shown in figure 2.4. Both resource and signal provisioning of the different requests can therefore be effectively monitored.

2.4.2 Dense Wavelength Division Multiplexed (DWDM) Networks

For DWDM networks with 25-100 GHz spacing, for efficient spectrum utilization, sub- and super-channels can be created by arbitrary bandwidths that fit into the ITU-T grid systems. Since DWDM increases fibre capacity, PONs, MANs and long distance fibre networks can all utilize the hybrid DWDM and flexible spectrum systems. Instead of the fixed channel spacing, the flexible spectrum can be used to subdivide the spectrum into 25 GHz and multiples of 25 GHz such as 25, 50, 75 and 100 GHz spacing. These DWDM signals can transmit at 1 Gb/s to 100 Gb/s with OOK, BPSK, QPSK, DQ-PSK and mQAM modulation formats and fitting them into 25-100 GHz frequency slots available multiplexers and demultiplexers. Moreover, 400 Gb/s super-channels made up of four (4) multiples of 100 Gb/s signals can be multiplexed to create a super-channel [3], [11], [28].

2.4.3 Long-haul Networks

The multi-bitrate and flexible spectrum signals have found a lot of interest in both short and long distance backbone fibre transmissions. This is done by optimizing the link parameters such as capacity and reach. Xtera company have created a new line-card that can be used in fixed and flexible grids with adjustable QPSK, 8QAM and 16QAM to provide 100-400 Gb/s channels. With a 61 nm spectrum, optically amplified 40 Tb/s was transmitted for 1,500 km fibre [41]. Compensation techniques for dispersion and other fibre PLIs and sensitive APD receivers can be used in coherent detection to increase transmission distance [42]–[44].

2.5 Network Optimization Using Algorithms and the Control Plane

One of the main advantages of flexible spectrum is the realization of a virtual control plane that can be used to remotely configure and optimize the hardware of a network to suit the traffic demands. Recent attention has shifted to towards providing feasible solutions for multi-layer network controls in both physical and software domains. As a result, the work of a control plane includes network management, configuration and exchange of network parameters contained in a routing table. This therefore makes the control plane “the brain” of a network [45]. A control plane intelligently collects the information about devices’ source to destination, available routes, distance/reachability, link load and in the software

domain, prioritizing, de-prioritizing or blocking specific packets. This is implemented by using sets of algorithms and protocols in a software considering the availability of resources, arrival time and demands of individual packets. In terms of location in a network, control planes are either centralized or distributed [45]. This results in the network properties being monitored and configured either over the entire network or in between instantaneous locations where adjustments are to be effected. The advantage of deploying a distributed control plane is that, more scalable solutions can be realized since data and control planes are interconnected by virtual application programmable interfaces (APIs). An example of a distributed control plane is the OpenFlow control plane [45], [46], [47].

A control plane includes a path computation element (PCE) and traffic engineering database (TED) which enable determination of route and service requests in a network in the software domain [48]. A testbed has experimentally demonstrated a real-time control plane that manages the modulation formats, routing and spectrum allocation. This has been achieved while maintaining OSNR, QoS, BER and high spectrum efficiency of the link [14].

Some of the resource allocation and optimization algorithms and protocols have been reported and they include; the particle swarm optimization (PSO), the local search, simulated annealing, genetic algorithms (GA), game theory and the ant colony optimization (ACO). These algorithms control the bitrates, transmitted signal power and the number of end-users that are active in a single link connection. This is done to maximize capacity and the available resources in an optical transport network [49]. The algorithms and protocols focus on implementing dynamic impairment-aware- RWA (IA-RWA), optical shortest path first (OSPF), general multi-purpose label switching (GMPLS) protocols and PCE protocols that incorporate physical impairments affecting an optical signal [48]. However, with the dynamic shift from fixed to flexible spectrum, optimization algorithms should not only focus on RWA but also on flexible routing and gridless conditions.

A heuristic method, adaptive frequency assignment-collision avoidance (AFA-CA) has been reported where the order of received traffic demands are processed in sequence to minimize spectrum exhaustion as well as predictive approach that avoid potential link collisions during congestion [50]. For spectrum utilization, maximize path spectrum consecutiveness (MPSC), maximize total link spectrum consecutiveness (MTLSC) and maximize heaviest link spectrum consecutiveness (MHLSC) algorithms have been reported. These algorithms have been used in dynamic resource provisioning and have showed low blocking probabilities [51]. Moreover, simulation results based on ACO-RSA has reported

lower blocking, less complexity and higher adaptability to different bitrates for slot-based spectrum allocation in flexible networks utilizing bandwidth variable switching nodes [52].

In general, control and data planes and network management systems(NMS) have been used to develop software defined networks (SDNs) to offer dynamism in complex networks. For instance, Google and Coriant have deployed their own SDN to effectively and efficiently monitor their global data centres [45], [53].

2.6 Summary

This chapter describes several advantages and challenges facing flexible spectrum networks in achieving dynamic allocation of spectrum, routing and wavelength allocation, spectrum and energy efficiency and network resource control. From transmitter-fibre-receiver optimization to providing signal continuity, several networks topologies in which flexible spectrum can be implemented and integrated with the existing fixed spectrum for P2P and P2MP networks in single and DWDM fibre links have been discussed. The next chapter introduces different components and techniques used to implement flexible spectrum networks.

Chapter 3:

3.0 Implementation of Flexible Spectrum in Optical Fibre Networks

This chapter describes the theory of different technologies that can be used to implement optical communication systems ranging from transmitters to receivers. Two directly modulated lasers distributed feed-back laser (DFB) and the vertical cavity surface-emitting lasers (VCSELs), as well as their advantages and applications in flexible spectrum networks are discussed. Direct and indirect modulation techniques and photodetectors such as positive intrinsic negative (PIN) and the Avalanche photodiode (APD) are reported. Optical fibre and factors affecting a signal such as polarization mode dispersion (PMD), chromatic dispersion (CD), crosstalk and attenuation are also described. Finally, network nodes used to route and reroute channels in a multi-node network topology are discussed. These nodes include; wavelength division multiplexers (WDM), optical add and drop multiplexers (OADMs), passive optical splitters, wavelength converters and switches and the reconfigurable optical add and drop multiplexers (ROADMs).

3.1. Optical Communication System

An optical communication link consists of a transmitter, physical medium and a receiver. A transmitter converts an electrical stream of bits into an optical light signal that is transmitted through a medium and received by an optoelectronic device (receiver) which converts the optical signal back to the electrical form [54]. At the transmitter, bits are added into a modulator which encodes and drives an optical signal that is then launched into a medium for transmission. The commonly used main media of signal transmission are optical fibre, free-space and copper [55]. For optical fibre, a receiver comprises of a photodetector which converts the optical signal back to an electrical form which is then fed to a demodulator that separates the signal state changes and their timing. The electrical signal is then decoded and constructed into the original stream of bits for presentation to the end-user [56].

Communication media are categorized into guided (fibre and copper) and unguided (free-space). Free-space and copper transmissions are pre-dominantly used in the near end-user locations with the optical fibre forming the backbone in long-distance transmission [57]. The main advantage of free-space transmission is the mobility of end-user devices and

has therefore replaced copper wires in most existing and modern network links. It is however noted that both copper and RF free-space transmissions are limited by lower speeds, shorter distances and susceptibility to electromagnetic(EM) interferences [58]. An optical fibre is a stand-out medium for optical communications due to its high transmission speeds, immunity to EM interferences, high capacity per fibre-strand and low attenuation in long distance transmission. This makes optical fibre transport supreme over other media of communication for short and long distance high speed broadband connections [57], [59].

3.1.1. Optical Transmitters

In optical fibre communication systems, an optical transmitter converts an electrical input signal into an optical signal for coupling it into a fibre. It mainly comprises of a continuous wave (CW) optical source which include a light-emitting diode (LED) or a semiconductor laser source [60]. Most semiconductor lasers emit light through stimulated excitation of the laser cavity as a result of an external drive current and can emit up to ~100 mW (~20 dBm) optical power. The emitted light has a narrow spectral width due to its coherent nature, which makes it capable for high speed and long distance transmission [60]. Wavelength tunability within the active gain region of a semiconductor laser can be achieved by varying the injected current so as to adjust the size of the grating [60]. An example of a semiconductor laser source is the vertical cavity surface-emitting laser (VCSEL). VCSELs are compact in size, wavelength stable, wavelength tunable, low power, high bandwidth and is directly modulated [61]-[62]. The capability of directly modulating the VCSEL using an input electrical signal reduces the complexity of requiring an additional external modulator. Moreover, the ability to adjust the transmission wavelength of the VCSEL makes it also ideal for wavelength division multiplexed (WDM) systems and wavelength conversion.

3.1.2. Vertical Cavity Surface-Emitting Laser (VCSEL)

Vertical cavity surface-emitting lasers (VCSELs) are semiconductor sources that emit a light beam that is perpendicular to the planes of an active region or perpendicular from the top surface of the cavity. Other convectional lasers such as edge-emitting lasers (EEL) emit an optical beam from the surface of the chip [63], [64].

The structure of a VCSEL comprises of an active gain medium sandwiched by two distributed Bragg reflector (DBRs) mirrors. The active region receives an injected drive-in current through an oxide aperture or proton injection while emitting a beam that is

perpendicular to this active region [65]. The longitudinal mode spacing (Δλ) between successive modes is given by;

$$\Delta\lambda = \frac{\lambda^2}{2\eta_{eff}L_{eff}} \quad \ldots\ldots\ldots\ldots\ldots\ldots\ldots\ldots\ldots\ldots\ldots\ldots \quad 3.1$$

where λ is the lasing wavelength, η_{eff} is the average refractive index of the top p-type and lower n-type mirrors and L_{eff} is the total cavity length which comprises of the thickness of the active region and the electric field penetration depth in the DBR structure. The typical longitudinal mode spacing of a VCSEL is 30 nm, while an EEL has a 0.3 nm spacing. If the gain profile of the VCSEL and the stop-band of the DBR is considered to achieve an extremely short cavity length, the VCSEL will therefore only lase in a single longitudinal mode as compared to the EEL [65]. The structure of a VCSEL showing the DBRs, the electrodes, mode-fields, the active region and the perpendicular emission of an optical beam is shown in figure 3.1.

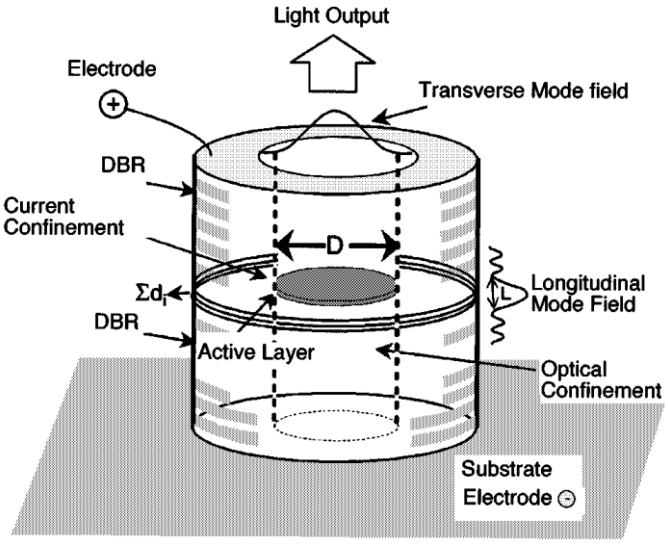

Figure 3.1: The structure of a VCSEL [66].

Several techniques have been used to improve current confinement within a predefined area of a VCSEL so as to reduce the threshold current level. They include mesa etching of the top mirror, ion implantation to achieve high resistive semiconductor regions, or selective oxidation on the semiconductor layer using aluminium content. Selective oxidation reduces the optical losses experienced on the laser cavity by decreasing the threshold current while proton implantation has been used to fabricate commercial VCSELs for their reliability and production [64]. The mesa diameter for single mode and multi-mode VCSELs is 23 μm and 28 μm respectively. This therefore results in reduced mesa capacitance. In terms of aperture, a single mode VCSEL with a 3 μm diameter and a multi-mode with a 6 μm diameter have

been reported [67]. The increased aperture diameter in multi-mode VCSELs increases the number of excited transverse modes [67]. With sufficiently high injection currents, modal gain results in multi-mode operation enabling them for 25 Gb/s and extended reach [68]. To drive the VCSEL, electric current is injected on the Ohmic contacts of the top and bottom epitaxial layers of the substrate. The threshold current can be lowered to sub-100 μA range by reducing the diameter of the VCSEL to a few μm. The low current (in mA range) required to drive a VCSEL makes it a low power consuming laser. By operating the VCSEL above the threshold level, the VCSEL has a constant current-power relationship. However, a rollover characteristic is seen at higher currents (above saturation level) due to internal heating of the VCSEL. Unlike the EELs, it is safe to use the VCSEL up to the maximum output power since its power density remains within the $^{kW}/_{cm^2}$ and can therefore not induce optical damage to the semiconductor material [64], [66].

Frequency chirping and dispersion are the two major defects experienced by VCSELs during normal operation. Chirping is the instantaneous change of wavelength with varying optical powers. This results in time dependent instantaneous frequency changes. Dispersion dictates how the optical spectrum of a laser broadens during fibre transmission. A number of techniques for reducing and limiting chirping have been reported. These techniques involve injection-locking and filter offsetting to narrow the spectrum [69]. The relationship between chirping Δv and the optical power P is expressed by equation 3.2.

$$\Delta v(t) = -\frac{\alpha}{4\pi}\left(\frac{d}{dt}\ln P(t) + kP(t)\right) \quad \text{3.2}$$

where the first term represents the transient chirp that relates to the time derivative of power P, the second term is the adiabatic chirp due to instantaneous optical power, α is the line enhancement factor and k is related to the geometry of the device and its non-linear gain [69].

Directly modulated and 10-40 Gb/s bit-rate VCSELs lasing at 1310 nm and 1550 nm windows have already been produced and commercialized [62], [70], [71]. In this study, VCSELs from Raycan company are used as transmitters. The material composition of these VCSELs are InAlGaAs, InGaAs and InAlAs which offers the VCSEL high reliability, reflectivity, low-loss current confinement, reduced thermal impedance and low series resistance for long wavelength emissions [66], [70]. The emission wavelength of the Raycan VCSEL can be adjusted by varying the drive-in bias currents. The Raycan VCSEL, bias and temperature control and electrical radio frequency (RF) input signal as used in this study are shown in figure 3.2.

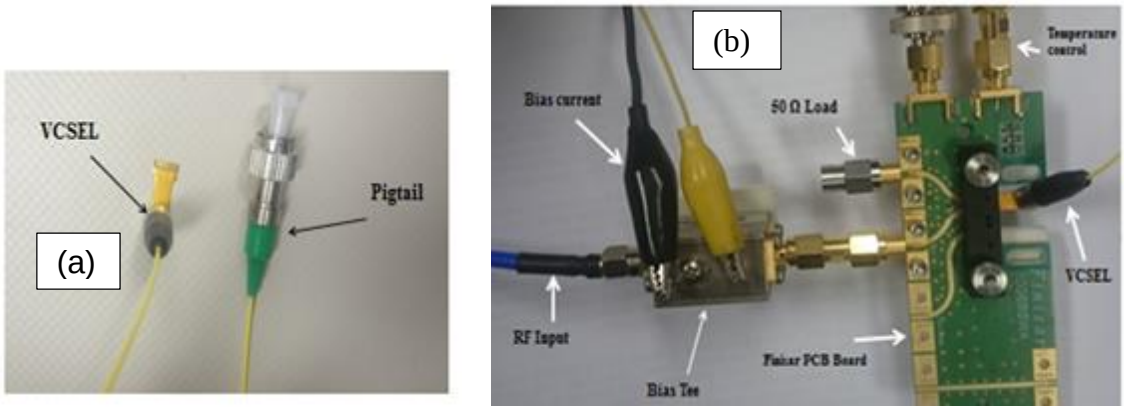

Figure 3.2: Pictures of (a) a VCSEL and pigtail (b) mounted on a printiable circuit board (PCB) with an input modulation RF via a bias tee, with input bias current and temperature control and a termination 50 Ω resistor.

Pictures taken at the NMMU' Centre for Broadband Communication laboratory showing the assembly of the 1310 and 1550 nm VCSELs as used in this study is shown in figure 3.2. The assembly consists of printable circuit boards (PCBs) that are used to mount the VCSEL and also enables injection of drive current via the anode and the cathode of the bias tee. The PCB also enables the connection of an external thermo-electric controller (TEC) to control the temperature of the VCSEL cavity during operation. The 50 Ω termination is used to enable the VCSEL for single drive only.

3.1.3. Distributed Feed-back (DFB) Lasers

The distributed feed-back (DFB) is a semiconductor laser with a corrugated structure within the cavity that allows only specific wavelengths to oscillate and emit. As a result, a narrow linewidth optical beams are emitted which make the DFB lasers ideal for closely packed DWDM signals [20]. DFB lasers emitting at the 1310 nm and 1550 nm transmission windows have been manufactured.

The emission wavelength is selected by the Bragg wavelength of the distributed feedback which is dependent on the temperature of the cavity. DFB lasers have $\sim 18\, mA$ threshold current, 4 mW (6 dBm) optical output power and a high side-mode suppression ratio (SMSR) of approximately 45 dB [72]-[73]. As a result, DFB lasers have higher threshold currents and optical power as compared to VCSELs as shown in figure 3.4.

In terms of modulation, recent advances have enabled direct modulation of DFB lasers to attain up-to 40 Gb/s and due to the narrow linewidth, long-haul transmission have also been attained. The main advantages of a DFB laser over VCSELs is that a DFB laser is

slightly affected by chirping and therefore has better wavelength stability and higher optical power. The emission wavelength of a DFB can be tuned by changing the cavity temperature.

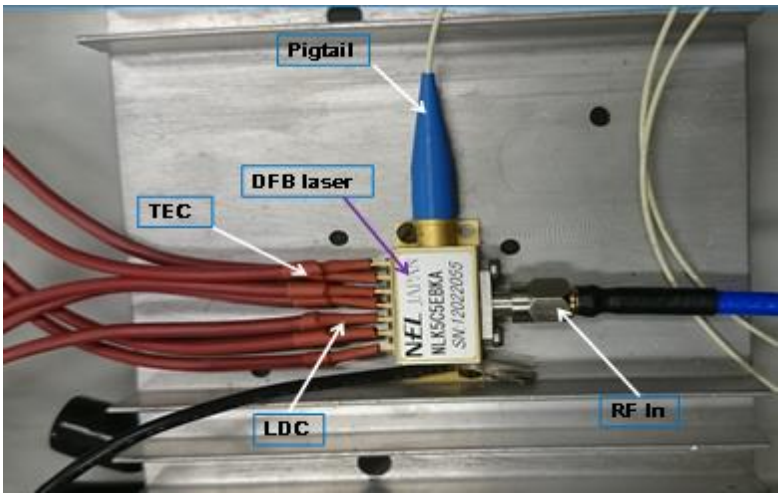

Figure 3.3: A picture of directly modulated DFB laser with laser diode controller (LDC), thermos-electric control (TEC), input modulation RF and output signal fibre pigtail.

In this experimental study, a 1550 nm internally/directly modulated DFB was used. The temperature and biasing controls is as shown in figure 3.3. The modulated output optical signal is emitted via a fibre pigtail as shown in the picture taken at the laboratory.

3.1.4. Modulation

The entire process of modulation involves changing the physical property of the optical light which is either the amplitude or the frequency (including phase). As a result, the two simplest, cheap and common modulation formats are intensity or amplitude modulation (AM) and frequency modulation (FM). Other modulation formats include; polarization, phase and spatial light modulators [9], [74].

In most semiconductor lasers, the output power of the laser varies directly with an input bias current. Directly modulated lasers utilize intensity modulation which involves the turning on and off of the light signal with an input electrical signal [20]. The on and off state of the laser is determined by the logic state of the input electrical signal. When digital data is used to modulate a laser, the “1”-bit corresponds to an on-state while the “0”-bit corresponds to an “OFF” state [75]. The input electrical signal used for direct modulation can either be analogue or digital signals. The ideal way of operating a directly modulated laser is to apply an offset current to bias the laser above its lasing threshold and to operate below the rollover current levels. Between the lasing threshold and saturation levels (mid biasing point), the laser attains a constant slope as shown in figure 3.4.

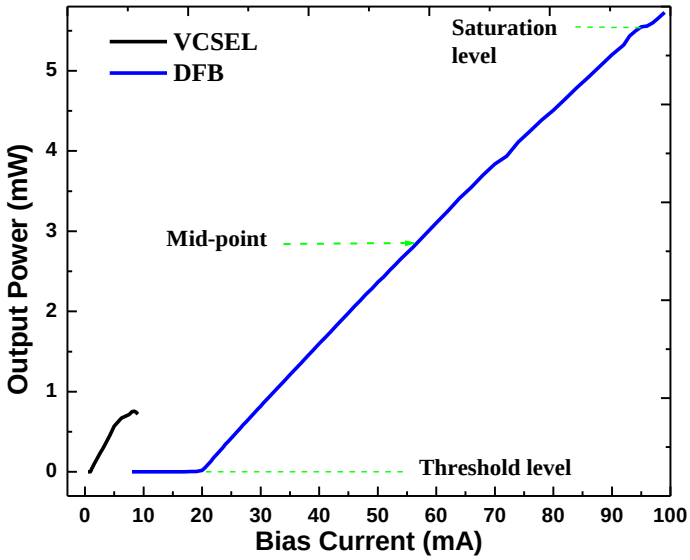

Figure 3.4: The input current-output power characteristics of a typical VCSEL and DFB lasers.

An ideal turn on/off during modulation is achieved when the laser is biased at the mid biasing point of the laser current-power characteristics. This is done so as to avoid under- and over-modulation of a laser that might result in electrical signal chirping, transients and reduced lifetime of the laser [75]. Direct modulation is mostly used in DFB, VCSEL and Fabri-Perot lasers and have a $50\ \Omega$ load termination to match the series resistance of the device [76].

In fibre transmission, instantaneous frequency chirping arises from a change in refractive index of an optical fibre due to change in carrier density resulting in high signal dispersion. Dispersion becomes a major limiting factor in directly modulated high speed VCSEL transmissions due to chirping [69]. In optical fibres, dispersion introduces uncertainty at the receiver due to the cumulated chromatic dispersion over distance of transmission. The eventual constraint on the receiver is the reduction in receiver sensitivity [75], [77]. It is possible to achieve high bit-rates of 10 Gb/s and beyond in VCSELs using direct modulation.

External modulation involves an external modulator which changes the physical property (amplitude, phase/ frequency) of the optical wave. The most common configuration is having an external modulator between the optical laser source and the fibre. The most well-known external modulators operating at the low attenuation 1550 nm window include the electro-absorption modulator (EAM) and the Mach-Zehnder modulator (MZM).

Although they are complex and expensive, EAM and MZM produces a high quality signal, low/zero chirp and speeds up to 40 Gb/s [11], [75].

3.1.5. Receivers

A receiver comprises of a photodetector, filter, an electrical amplifier and a demodulator that extracts the original data that was transmitted. Signal receivers mainly rely on a photodetector to convert the optical signal to an electric current. This makes the photodetector an essential component in an optical fibre communication system The requirements for optimized photodetectors are: high sensitivity, wide bandwidth, low noise, low cost and high reliability [78]. In their operation, a photodetector receives the transmitted optical signal and converts it with minimum loss possible, to an equivalent electrical signal that can be used by the normal end-user devices such as telephones, computers, televisions and distribution terminals such as mobile cell-towers. The emergence of high-speed optical fibre transmission, low attenuation and dispersion at the 1310 and 1550 nm transmission windows has led to the development of photodetectors operating within this window.

In receiving a transmitted signal, direct or indirect detection is performed. Direct detection techniques are normally done on intensity/amplitude modulated signals with on-off keying (OOK) or non-return to zero (NRZ) formats. Indirect and coherent detection techniques are used to demodulate multi-level signal involving change in amplitude, frequency, phase or polarization of an optical signal [72]. For a phase modulated signal with binary phase shift keying (BPSK), the interferometric technique involving a local oscillator (LO) at the receiver is used to match the signal frequency while phase-locking the signal [56], [79]. Signal recovery can also be performed using interferometric-type setup by delaying one arm of the signal and allowing it to interfere with itself [11]. The quality of modulated and transmitted bits of data are analysed using either bit error-rate (BER) measurements or eye-diagrams [20], [80].

3.2. Optical Fibre and Signal Impairments

Optical fibres have tremendous applications in modern day high speed communication systems due to their high capacity, low optical loss, less distortion, high data security and high immunity to electromagnetic interference (EMI). Fibres are optimized for different transmission environments and topologies such as aerial, buried and marine deployments. In terms of transmission distances, fibres have been deployed to enable backbone short distance

metro-access and long-distance signal transmission for offering telephone, video, high definition-television and mobile data to the premises, enterprises and to institutions [72].

In terms of geometry, an optical fibre consists of a core, cladding and a protective jacket. The material composition of the core and the cladding ensures that the optical signal remains within the core during transmission by utilizing the basic principle of total internal reflection.

During propagation, an optical pulse maintains the following propagation equation obtained from solving the Schrodinger equation [72], [77];

$$\vec{P} = \varepsilon_o(\chi + \frac{3}{2}\frac{\chi^{(3)}}{c\epsilon_o\eta_o}I)\vec{E} \quad \text{.....3.3}$$

and the change in refractive index due to intensity;

$$\eta = \eta_o + \eta_2\frac{P}{A_{eff}} = \eta_o + \Delta\eta \quad \text{.....3.4}$$

where $\vec{P}$ is the electric polarization as a function of the electric field $\vec{E}$, ε_o is the vacuum permeability, χ and $\chi^{(3)}$ are 1st and 3rd order magnetic susceptibility, *c* is the vacuum speed of light, η_o and η_2 are passive and high intensity-dependent refractive indexes [77]. The 1st and 3rd order magnetic susceptibilities are responsible for linear and nonlinear effects when an optical signal wavelength λ is propagated through fibre. Indeed, non-linear effects result from the high optical power *P* which is dependent on the effective core area of the fibre (A_{eff}) and are cumulative over length of the fibre with a non-linear coefficient, $\gamma = \frac{2\pi\eta_2}{\lambda A_{eff}}P$. The linear effects include chromatic dispersion, attenuation while fibre non-linearity and phase changes results in four-wave mixing (FWM), self-phase modulation (SPM), cross-phase modulation (XPM), stimulated Raman scattering (SRS) and stimulated Brillouin scattering (SBS) [59] [72].

Depending on their manufacture and applications, optical fibres are either; single mode fibres (SMF) or multimode fibres (MMF). SMFs offer long distance transmission since signal propagation is in single mode only at 1310 nm and 1550 nm transmission windows. Whereas, MMFs are best suitable for short reach and mainly transmit at 850 nm [59].

Based on in-built tolerance to dispersion, PMD and attenuation, different types of SMFs exist. Dispersion being a major limiting effect in optical signals has been minimized by tailoring dispersion profiles of the fibres during manufacture. This has been done by shifting dispersion towards zero waveguide dispersion wavelengths. As a result, fibres have been optimized to operate at zero dispersion 1310 nm wavelength for ITU-T G.652 and 1550 nm for zero dispersion shifted fibre (ZDSF) G.653 and non-zero dispersion shifted fibre (NZDSF) G.655 fibres with typical 3 ps/(nm.km) dispersion [81]. The presence of small

and tolerable amounts of dispersion is necessary to offset non-linear effects such as FWM [81], [82]. The attenuation coefficients of the G.652 are 0.4 dB/km while G.655 has a 0.2 dB/km attenuation. Therefore, in terms of reach, G.655 fibres are best suited for long distance single wavelength or for DWDM back-borne transmission at the 1550 nm transmission window. Moreover, G.657 fibres are tailored for application in fibre-to-the-home (FTTH) based on its tolerance to PMD and bending.

3.2.1. Optical Attenuation

There are several factors that degrade the quality of signal and distance in optical communication systems. These include attenuation, linear and the intensity-dependent non-linear effects. Indeed, neglecting dispersion and non-linear effects within the optical medium, the transmitted power of the signal is given by the following equation;

$$P_o = P_i e^{(-\alpha L)} \quad \text{..... 3.5}$$

where P_o and P_i are the output and input powers respectively, α is the attenuation coefficient in dB/km and L is the length of the fibre. From the manufacturing perspective, fibres have an attenuation profile that is both wavelength and distance dependent. The attenuation coefficient is given by;

$$\alpha\left({}^{dB}/_{km}\right) = -\frac{10}{L} Log_{10}\left(\frac{P_o}{P_i}\right) \quad \text{..... 3.6}$$

From the traditional assumption that an optical fibre portrays a near perfect signal transmission, loss of signal power arises due to both intrinsic and extrinsic effects. Intrinsic attenuation results from power absorption and Rayleigh scattering within the fibre core while extrinsic effects result from the waveguide dependence of power. Causes of extrinsic attenuation include core/cladding losses, bending-losses, splice and connector losses.

Fibres have been designed to reduce material absorption that results from the OH-ions within the fibre by eliminating the impurities. As a result, low water-peak fibres that enable long-distance transmission at the 1310 nm and 1550 nm windows have been designed and manufactured [82]. As a result, signal attenuation resulting from absorption and extrinsic losses have been minimized to typical values of 0.2 dB/km [56], [82].

3.2.2. Chromatic Dispersion (CD)

An optical signal propagating in an optical fibre is guided by both the refractive index and the wavelength dependence of material which makes sure that light is confined within the core of a fibre. In the time domain, chromatic dispersion (CD) makes light pulses to

propagate at different speeds resulting in pulse broadening. This phenomenon occurs in almost all types of optical fibres. The optical pulse broadening results from the finite spectral linewidth of the optical laser source and the modulated carrier [20], [59].

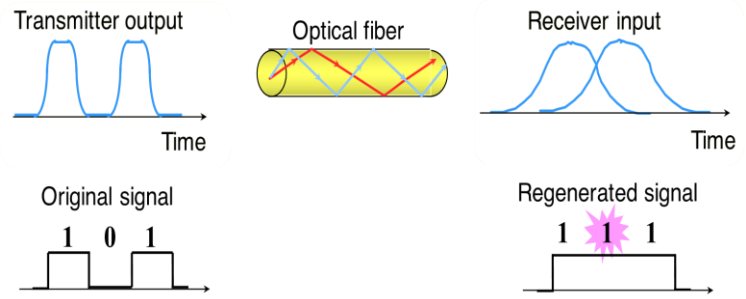

Figure 3.5: Effects of dispersion on transmitted signal and data bits [20], [83].

With a smaller linewidth, an optical signal becomes more coherent and therefore minimizes wavelength spreading [84]. However, when an optical signal is propagated through a fibre, the spectrum is broadened by increased cumulative dispersion effects due to increased length resulting in inter-symbol interference [85]. The received signal is distorted as shown in figure 3.5. Dispersion causes the optical pulses to broaden and creates an error-bit when data bits are modulated into the signal. As a result, the receiver detects a "HIGH" or a "1" instead of a transmitted "LOW" or "0" bit [20].

Different types of fibres portray varying CD properties at the 1310 nm and 1550 nm transmission windows. The temporal spreading of an optical pulse is quantitatively represented by wavelength and distance dependent dispersion coefficient in ps/(nm.km) and a dispersion slope in $\mathrm{ps}/(\mathrm{nm}^2.\mathrm{km})$ [77].

3.2.3. Compensation of Chromatic Dispersion

Minimization, management and compensation of dispersion effects remains an important optimization reach-capacity priority in optical fibre communication networks. The degree to which pulse overlap and eventual error-bits are created in an optical fibre link can be compensated at different stages of signal transmission at the transmitter, in-line and compensation at the receiver-end. For the pre-compensation technique at the transmitter stage, pre-chirp coding is done so as to compensate chirping related dispersion effects that arise in lasers with chirping [20], [86]. In-line compensation involves using dispersion compensating fibres (DCF), optical filters fibre Bragg gratings (FBGs). In DCF technique, a highly negative dispersion fibre with up to -100 ps/(nm.km) dispersion coefficient is used to cancel out the cumulative positive dispersion effects associated with G.652 and G.655 fibres in the link [43]. Inverse dispersion fibres (IDF) have equal but negative dispersion

properties to the conventional SMFs [87]. This technique remains to be the most efficient, easy to implement and cost-effective at the 1550 nm transmission window. Indeed, ZDSF fibres are not effective for long-haul and DWDM transmission since FWM and XPM becomes detrimental. As a result, the NZDSF fibres with minimal CD not only increase the fibre-reach but also minimizes FWM and XPM effects throughout the transmission [56]. In terms of connectivity, the IDF or DCF fibre is always connected after the high dispersion SMF. The relationship between the accumulated dispersion D_{link} effects over a fibre-link whose length is L_{link} and the negative dispersion compensating fibre is given by [72],[81], [20];

$$[\, L_{link} \times D_{link}) + (L_{IDF\ or\ DCF} \times D_{IDF\ or\ DCF})] = Residual\ Dispersion \ldots\ldots\ldots \quad 3.7$$

Post-compensation involves use of electrical dispersion compensation (EDC) using digital signal processing (DSP) where at the receiver; the electrical signal undergoes electrical data correction and equalization. Moreover, forward error-correction (FEC) techniques are also used in signal recovery. Together with narrow bandwidth filters, DSP can be implemented to achieve an offline dispersion compensation [43], [88]. However, a major drawback of EDC and DSP is the large amounts of electronics and overload on the hardware since it depends on the computation speed.

Of the described compensation techniques, a more viable and reliable process is the purely optical inverse dispersion fibre (IDF) technique since it can also be used to extend the reach of the fibre and is less costly as well. This is implemented by combining two fibres with relatively equal but opposite dispersion coefficients. As a result, dispersion is mitigated and the length of the fibre is extended [44].

3.2.4. Polarization Mode Dispersion (PMD)

Despite the single mode nature of SMFs, light propagates in two polarization modes (fast and slow axis) with almost identical propagation speeds. Due to the geometrical structure and random fibre imperfections such as bends and environmental effects, the optical pulses however propagate at different speeds since an optical fibre has random and varying refractive indices. This phenomenon is referred to as birefringence and leads to a time delay between the fast and slow axes. The propagation time delay is called the differential group delay (DGD), $\Delta\tau$ and results in pulse broadening and overlap. This phenomenon results in polarization mode dispersion (PMD).

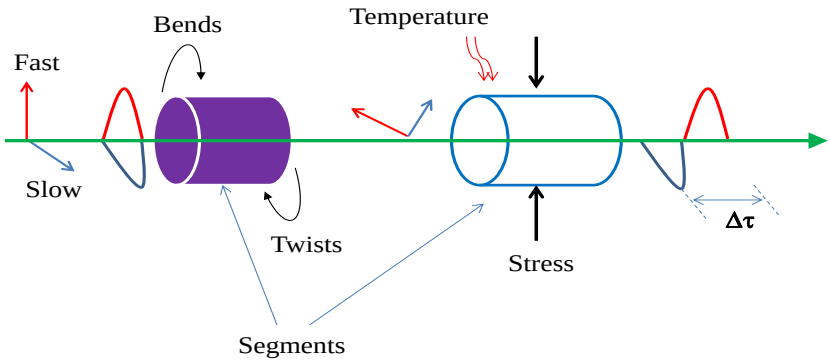

Figure 3.6: Illustration of fast and slow axis due to birefringence, segments of fibre, external causes of PMD and the pulse differential group delay (DGD), Δτ [72], [81], [84].

The extrinsic PMD effects results from the fibre vibrations, temperature changes, wind, cabling stress and connector mode coupling due to several segments of fibre as shown in figure 3.6 [81]. For undisturbed transmission, the symmetrical and circularity of the core maintains the physical properties of the fibre. However, for a disturbed fibre, the symmetrical change in the states of polarization (SOPs) of the signal within the core is broken resulting in PMD. In terms of data transmission, PMD induces error-bits due to the bit-overlap and therefore degrades the signal.

In optical fibre communication systems, the PMD coefficient as a result of total DGD due to intrinsic and extrinsic conditions is expressed as;

$$PMD = \frac{DGD}{\sqrt{L}} \quad \text{..... 3.8}$$

where PMD is the PMD coefficient and L is the length of the fibre. Therefore, PMD coefficient is expressed in ps/√km [72].

3.2.5. Mitigation of Polarization Mode Dispersion

Change in the states of polarization has become an important element in designing optical fibre-based sensors due to the fast response to external parameters that induce change in SOPs. Since the changes in the polarization is random and unpredictable in time, it is therefore important to stabilize, correlate and track input-output change in polarization states of a signal. Different methods of controlling, monitoring, stabilizing and maintaining polarization have been reported [86].

Dynamic control of polarization involves tracking and controlling SOPs using a set of arranged wave-plates with periodic polarization orientations. Another technique of stabilizing PMD is by using a polarization maintaining fibre (PMF) with a high in-built

birefringence that maintains the orientation of a highly polarized optical signal [56]. Algorithms in DSP have also been suggested to track and compensate overall PMD effects in the entire fibre-link [11]. Ultimately, PMD problem is solved by using low-PMD modern fibres and dispersion robust modulation techniques [9]. The typical PMD coefficient in most modern fibres is ≤ 0.02 ps/√km for low mode coupling and 0.04 ps/√km in the fibre-link design [82], [89], [90].

3.2.6. Crosstalk

The interaction between adjacent optical signals can be classified into linear and non-linear types. This depends on the intensity and frequency levels of the respective signals. The main causes of crosstalk are SPM, XPM, FWM and inter-symbol interferences within an optical path [9] [77]. The levels of crosstalk are affected by the signal's optical power, bitrates, channel spacing, distance of transmission and the receiver filter bandwidth [59], [91], [92]. The eventual effects of crosstalk are inter-symbol interference (ISI) resulting in error-bits. This therefore strains the receiver in distinguishing the receiver bits in high speed modulated signals [9]. As much closer channel spacing increases spectrum efficiency in DWDM and flexible spectrum networks, a trade-off between crosstalk penalties and channel spacing should be considered [2]. For contiguous channels, a guard-band is often allowed to separate channels so as to minimize inter-channel crosstalk [74], [2], [93].

3.3. Examples of Optical Nodes in a Flexible Spectrum Optical Network

In a fibre-linked network, nodes are made up of either active or passive components that direct incoming and outgoing wavelengths. They comprise of devices that handle single or/and multiple wavelengths and by either optical or electrical techniques, are capable of maintaining the QoS, routing, wavelength switching, bandwidth selection and assignment and network adjustment due to fibre-faults. Some of the components used to create an optical node in a reconfigurable flexible spectrum network include; wavelength division multiplexer and demultiplexer, optical add and drop multiplexer (OADM), wavelength conversion and switching and reconfigurable optical add and drop multiplexers (ROADM).

3.3.1. Wavelength Division Multiplexer (WDM)

Wavelength division multiplexers (WDM) are filter-based components used to combine several wavelengths into a single SMF fibre. WDMs are also bidirectional in that they can be used to separate individual wavelengths at the receiver-end as demultiplexers. By

combining several wavelengths into a single fibre, WDMs increase the capacity of the fibre [20], [94]. The current filter-based DWDMs can accommodate between 40-160 channels spaced at 25 GHz, 50 GHz and 100 GHz within the ITU-T grid systems. All the channels within the WDM and DWDM grid systems can be integrated into the flexible spectrum since all the wavelengths are assigned respect to the anchor wavelength 1552.5 nm (193.1 THz).

The operational bandwidth of WDMs enables amplification of the signals using the Erbium-doped fibre amplifiers (EDFA) to extend the reach of the fibre. However, amplification-related signal impairments may arise such as inter-channel interference and crosstalk due to non-linear effects [72], [74]. Therefore, bit-rates, channel spacing, signal powers, modulation formats, types of fibres and CD compensation should be optimized for better performance. In overall, DWDMs have therefore greatly increased spectrum efficiency and at the same time fibre capacity.

3.3.2. Optical Add and Drop Multiplexer (OADM)

Optical add and drop multiplexers (OADMs) are based on the fibre Bragg gratings (FBGs) which offer reflectance of wavelength that matches the Bragg wavelength λ_B while transmitting the rest of the WDM wavelengths [95]. The difference between OADMs and WDMs is that OADMs allow an additional optical signal satisfying the Bragg condition to be added into an existing WDM transmission. An OADM is therefore used to both multiplex and route a wavelength into and out of an SMF fibre [72]. A bundle of WDM wavelengths that pass through an OADM are often referred to as the cut-through channels while the rest are add/drop channels [94].

In a flexible network, an OADM can therefore be used to terminate a connection once the signal arrives at the destination while assigning the available wavelength and bandwidth to a new user. This therefore increases efficiency since no unutilized or underutilized wavelengths can exist in the network [37].

3.3.3. Wavelength Conversion and Switching

In a typical optical fibre network, incidences of wavelength collisions can be experienced and result in inter-channel interference. However, these collisions can be eliminated by utilizing flexible wavelength converters that are cost and energy efficient. At an optical node, an incoming wavelength can be converted to a new wavelength and therefore avoid the probability of channels colliding. Several techniques have been used to achieve wavelength collisions and they include; optoelectronic conversion, laser converters and coherent

converters [96]. Of the reported techniques, the optoelectronic conversion utilizes optical-electrical-optical (OEO) conversion which is expensive to implement since more electrical components are required.

An all-optical wavelength conversion can be attained by using non-linear optical grating based on a fibre-loop, cross-gain modulation, cross-phase modulation and FWM-based semiconductor optical amplifier (SOA) [97]. A key element of optical wavelength conversion is the ability to adjust the wavelength of converting semiconductor lasers. Different tunable lasers have been used and they include; the micro-electro mechanical external cavity lasers (MEM-ECL), the MEM-VCSEL and the multi-section DFB lasers. It has however been reported that achieving optical injection locking in MEM-ECL and MEM-VCSEL laser cavity is difficult and therefore attaining wavelength conversion using these lasers requires in-depth study and implementation [98]. For a flexible spectrum networks, wavelength conversion and switching of data signals from one wavelength to the other enables wavelength reuse in WDM signals [99].

3.3.4. Reconfigurable Optical Add and Drop Multiplexer (ROADM)

Colourless, gridless, directionless and contentionless reconfigurable optical add and drop multiplexers (ROADMs) are used to offer dynamic control of the channels and spectrum in an optical fibre network. The colourless property enables wavelengths to be switched and assigned variable bandwidth depending on the state of a network as determined by its control plane. The in-depth description of ROADM structure and configuration has been explained in section 2.3 of chapter 2. Bit-rate variable transponders (BVT) with different modulation formats providing spectrum efficient transmissions have been used. At a network node, the wavelengths can be dropped or added in any direction of the network. In most cases, reconfiguration algorithms contained in the control plane of the network are used to dynamically route, assign wavelength and spectrum to channels.

3.4. Link Power Budget

Typically, an optical signal experiences attenuation as it propagates over an entire fibre-link. Passive components in the link such as optical couplers, isolators, connectors, beam splitters, WDMs, filters, circulators, polarization controllers and rotators have insertion losses (IL) that aggregately reduce the optical power of a signal [100]. As a result, the output power of the signal will determine the fibre-reach and affects the sensitivity of the receivers [85]. Therefore, before transmitting a signal over the fibre, it is always recommended to perform

a power budget of the entire link during the network design [20] [72]. The receiver sensitivity P_{sens} in terms of dBm is given by;

$$P_{sens} = P_{tr} - IL_T - Penalty - M \ldots\ldots\ldots\ldots\ldots 3.9$$

where P_{tr} is the transmitter power, IL_T is the total component insertion losses, M is the link margin (for extending reach) and *Penalty* is the power penalty due to link impairments such as dispersion, crosstalk, PMD and non-linear effects [72], [101].

3.5. Summary

For optimum signal transmission, proper choice of components and implementation techniques is vital to attain an end-to-end communication. Cheaper and low power consuming wavelength tunable optical transmitters such as DFB and VCSELs and PIN and APD photo-receivers operating at both 1310 nm and 1550 nm transmission windows have been explained. In terms of optical power and chirping, a DFB laser is best suitable for long distance transmission as compared to the VCSEL which is better for DWDM systems due to its wavelength tunability. Signal impairments associated with an optical fibre such as chromatic dispersion, PMD, attenuation and crosstalk and the power budget in the optical link have been discussed. The different methods of minimizing and compensating both linear and non-effects affecting the signal have also been explained. Network optical nodes such as WDMs, OADMs, ROADMs, passive optical splitters and wavelength converters and switches have been discussed.

In this study, the optical nodes for our flexible spectrum network depended on the availability of the cost effective and efficient components in the Centre for Broadband Communication (CBC) at the Nelson Mandela Metropolitan University (NMMU), South Africa. The next chapter provides a description of different broadband networks in South Africa, Australia and the fibre network as applied in the major telescope project, The Square Kilometre Array (SKA) -South Africa.

Chapter 4:

4.0 Flexible Spectrum for the Square Kilometre Array Project, South Africa and the South African and Australian National Broadband Networks

This chapter describes network designs, architecture and topologies for the South African National Broadband Network (NBN), the Australian NBN and the fibre network in the Square Kilometre Array (SKA) Project-South Africa. The intercontinental marine backbone optical fibres connecting these networks are described as well as the inland backbone fibre deployment serving broadband suppliers and end-users in the metro-access networks (MANs) and also remote end-users at over 100 km distances. A description of how existing fixed spectrum systems and flexible spectrum designs can be integrated to improve fibre capacity, reduce re-installation costs and improvement of spectrum efficiency is also discussed. Cheaper and long lasting energy efficient solutions are also suggested for implementation in different topologies.

4.1. South African National Broadband Networks

The South African National Broadband Networks (SA-NBNs) play a greater role in improving the country's educational, health, gross domestic product (GDP) and economic growth by providing a platform for national, provincial and municipal coordination and improvement of socio-economic welfare. The core values of the SA-NBN is to provide an open access, robust and cost effective, and ubiquitous broadband for effective coordination of the government institutions and private sectors [102], [103].

The SA-NBN consists of optical fibres which forms the backbone of the country's telecommunication services. This network architecture has been used to connect several cities including Cape Town, Port Elizabeth, East London, Bloemfontein, Johannesburg, Pretoria and Durban using a 10 Gb/s ring network topology [104]. The main gaps in the South African broadband connectivity arises from both the infrastructural challenges that affect spectrum, reach, availability and cost. The biggest gap is in the metro-access connectivity that requires stable and high capacity feeder optical fibre transport to aid the more successful on-site Local Area Networks (LANs) and 3G/4G/LTE fixed and mobile terminals. From 1993, South African fibre deployment was connected by the South Atlantic-

2 (SAT-2) which provided up to 560 Mb/s and from 2001, the South Atlantic-3 (SAT-3), West African Submarine Cable (WASC) and South Africa Far East (SAFE) submarine cables provided up to 440 Gb/s for 13,500 km. SAFE has linked South Africa and Asia with India and Malaysia as the landing points [105], [106].

Currently, the South African fibre communication networks are fed by undersea fibre consortia such as the East African Submarine Cable system (EASSY), Sea Cable System (SEACOM) and the West African Cable System (WACS). Precisely, in the western coast, WACS's entrance into South Africa is through Yzerfontein which is near Cape Town while SAT-3, SAFE and SEACOM connect through Mtunzini near Durban. The incoming bandwidth from these companies range from 0.8 Tb/s to 14.5 Tb/s traversing over thousands of kilometres [107]. This has greatly improved the fibre backbone connectivity with the existing SAT-2 and SAT-3 cables. The fibre connecting South Africa from the submarine cables is shown in figure 4.1.

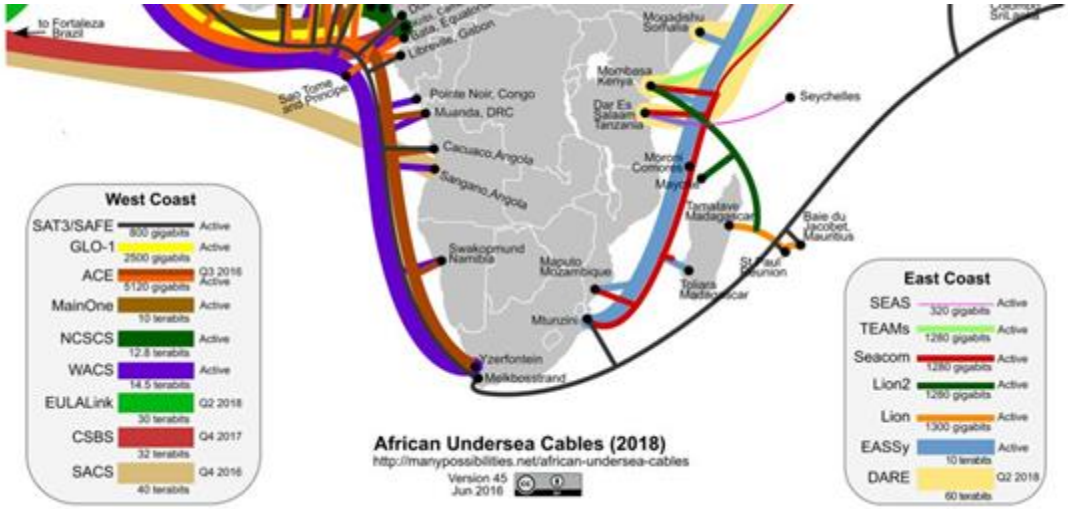

Figure 4.1: Undersea optical fibres feeding South Africa from the West and East Coasts; WACS and SAT 3 via Yzerfontein, Cape Town and SAFE, SEACOM and EASSY through Mtunzini in Durban [107].

In terms of coverage, 86% of the South African population live within 10 km of an optical fibre node. This therefore makes the South African government increase the budget so as to offer rural network access using both wireless and fibre deployment to health, educational sectors, public and private users [103]. The distribution of backbone optical fibre deployment in major cities within South Africa and learning and research institutions is shown in figure 4.2. Extensions of backbone fibre extensions to the interior major cities and their surroundings are provided by companies such as Dark Fibre Africa (DFA), Telkom and

Neotel-South Africa [108]. Moreover, with collaboration with the Tertiary Education and Research Network (TENET), the South African National Research Network (SANReN) have connected over 139 educational institutions and research centres across the country with bandwidth range of 1-10 Gb/s as shown in figure 4.2 [108].

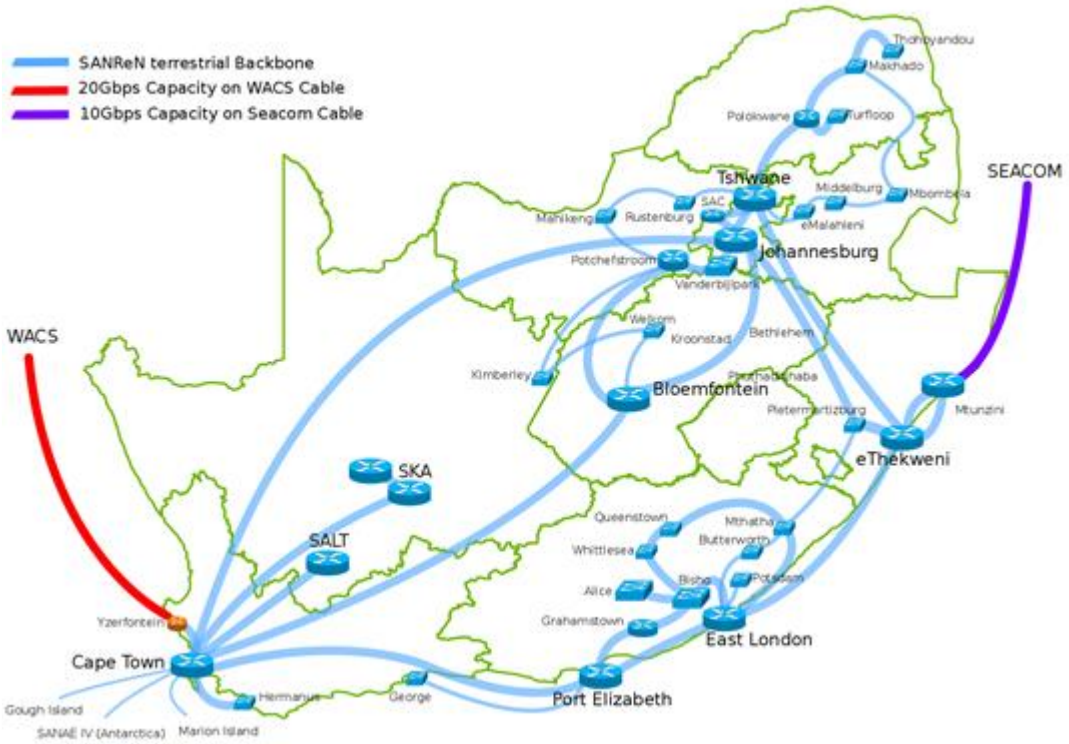

Figure 4.2: The ingress West Africa Cable Systems (WACS) and Sea Cable System (SEACOM) and 10 Gb/s ring fibre network between Cape Town, Port Elizabeth, Bloemfontein, Durban, Johannesburg and Pretoria. And Point to Point (P2P) between Cape Town and The South African Large Telescope (SALT) and The Square Kilometre Array (SKA) sites [104], [109].

An extensive fibre connection to major cities covering between 95-1000 km distances and their respective access networks to research institutions and universities is shown in figure 4.3. This metro-ring networks are linked by ≤10 Gb/s fibres providing services to the local universities and research centres.

For metro-access networks, South African broadband users are served by operators such as Telkom, Vodacom, Netleo, MTN, Cell C, DFA, Fibrehoods, Link Africa, and Internet Solutions [108], [110]. Depending on the capacity, network topology and geographic distribution, services are distributed either using optical fibre or wireless connections. The last mile access provides connections to end-user devices such as phones, PCs, TVs,

Telepresence Units (TPUs) and CCTV cameras. In South Africa, the last mile services are provided by Telkom's ADSL, 3G and LTE mobile operators and Neotel's CDMA, WiMaX and LTE services.

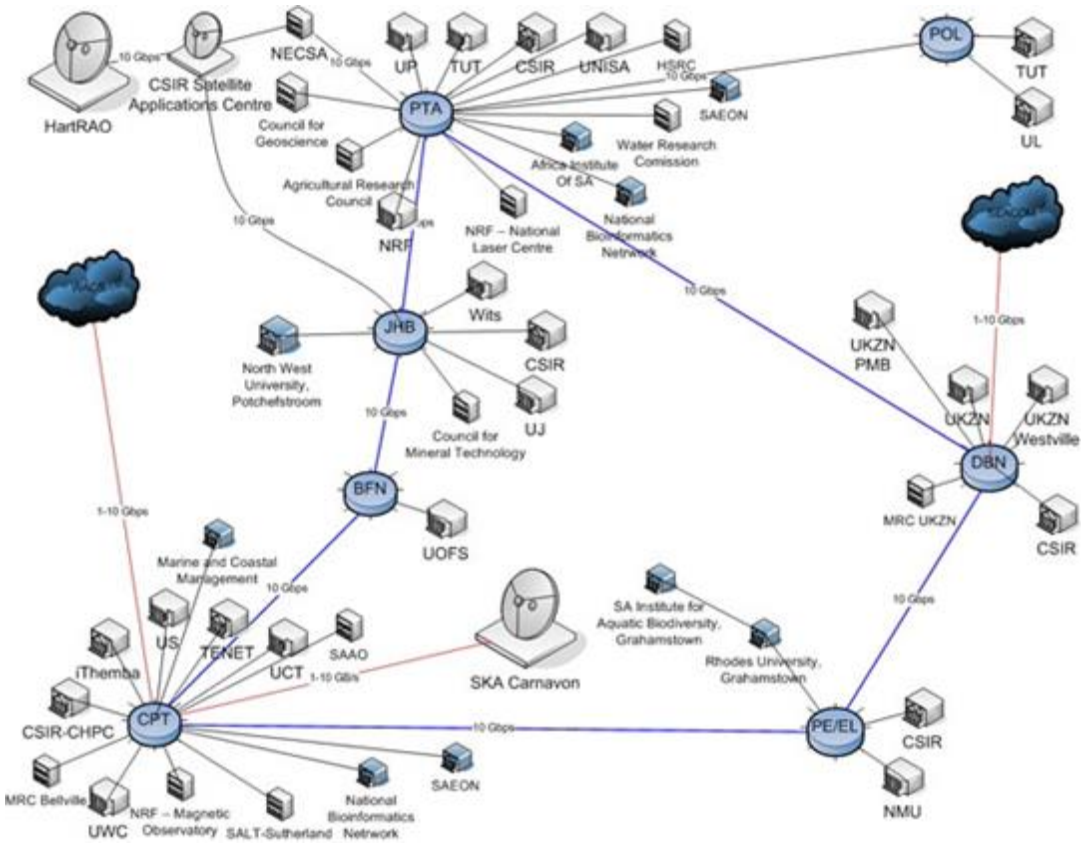

Figure 4.3: A ring fibre network between Cape Town (CPT), Port Elizabeth (PE)/East London (EL), Durban (DBN), Pretoria (PTA), Johannesburg (JHB) and Bloemfontein (BFN) their metro access fibre networks to universities and research institutions. The incoming sea cable to CPT (WACS) and DBN (SEACOM) [108].

The vision of the South African Broadband Policy is to provide efficient and extended services such as government e-services to the municipalities and access connected communities. Through research and development, South Africans are being empowered with global competitive knowledge to provide vibrant and creative hardware and software that provide content and applications to the needs of the society. In terms of coverage, by 2020, the South African NBN plans to connect 80-100% of schools, health facilities and public sector facilities with 10-100 Mb/s [103], [111].

In meeting demands for fibre connectivity to rural and geographically/economically isolated parts of South Africa, new technologies that offer high spectrum utilization, capacity and long distance fibre transmissions are required to provide backbone for broadband

signals. This can be realized through innovations and implementations of tested techniques such as advanced modulation formats, DWDM systems, coherent detection and the recently interesting flexible spectrum technology. Indeed, advanced modulation formats such as the DQPSK, mQAMs and mPSK have been reported to provide transmission speeds of up to 100 Gb/s and OFDM to create 400 Gb/s super-channel [6], [21], [41]. For the metro-access and long unamplified backbone networks, cheaper and energy-efficient transmitters such as the VCSELs can be used to create 10 Gb/s networks to transmit signals up to 80 km [69]. With high capacity fibre communication networks, efficient, effective, scalable and reliable signal distribution services to the end-user for the last mile 3G, LTE, Wireless and fibre-to-the-home/base-station/building/hut (FTTX) will meet the country's need to revolutionize broadband applications for socio-economic growth.

4.2. Australian National Broadband Network (NBN)

The Australian National Broadband Network (Aus-NBN) is a national and a wholesale-only network that provides its users with open-access connectivity facilitated by fixed line, satellite and broadband connection retailers or service providers. It was started by the Broadband Advisory Group (BAG) in 2003, advising the Federal Government to engage industry to initiate the NBN. Most of the backbone broadband connectivity in Australian is fibre-based, which has completely replaced copper due to its low capacity, corrosion and excessive requirement for insulation gel. The main prototype for the NBN is to have a purely fibre-to-the-premise (FTTP) to offer more than 100 Mb/s to the end-user [112]. For fixed wireless networks, 2.3 and 3.4 GHz radio spectrums will be used to provide LTE wireless outside the fibre connected areas to 4% of the population. In terms of cost, the Australian Federal government plans to spend A$37.4 billion. By January 2016, there have been 736,052 active NBN fibre, satellite and wireless services [113].

The Aus-NBN comprises of five domains; the End-user, access, aggregation and backbone, service edge and core, and application and content [114]. End-user connections are facilitated by access technologies such as passive optical networks (PONs), Gigabit-PON (GPONs), 3G, LTE and satellite. The PON and GPON links consist of optical network interface (ONI) which is the end-user termination point while at the central office (CO), routing and switching of channels is done by an optical line terminal (OLT). Access connectivity requires three fibre transport system; the distribution fibre network (DFN), local fibre network (LFN) and the premise fibre network (PFN). The main integral component of

implementing FTTX is the actual fibre deployment which forms the backbone to all the metro-access connections [115].

Figure 4.4 shows the DWDM signals over fibre in a ring topology with respective access connections using FTTX, wireless network terminals (WNT) and Ethernet access switch (EAS). The Aus-NBN Co DWDM fibre network is made up of several DWDM nodes located at the point of intersection with access networks to provide a bidirectional traffic movement.

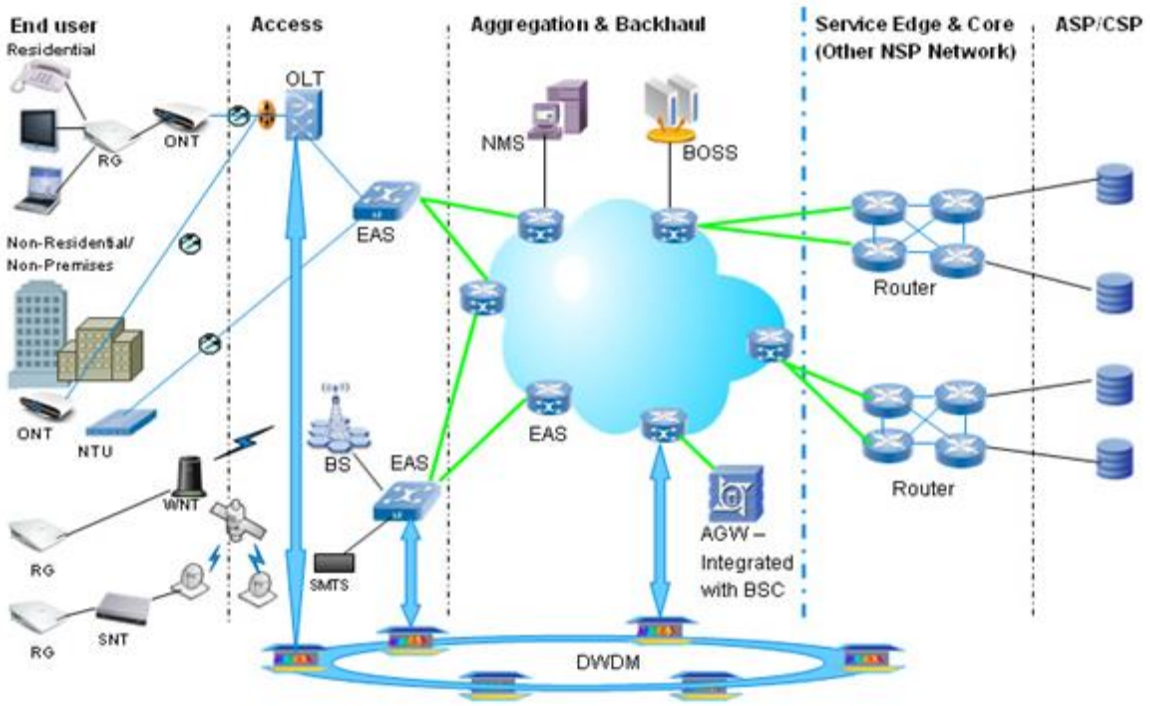

Figure 4.4: The overall Australian National Broadband Network (Aus NBN) architecture showing long haul backbone DWDM over fibre and the access to end user connectivity [114].

As shown in figure 4.4, the Aus-NBN has two types of DWDM nodes. The ROADMs and the optical line repeaters (OLRs) with inbuilt amplifiers, wavelength selective switches and add/drop filters. As a result, ROADM technology has been used to transit wavelengths, extract data from a user and inject into an optical interface (add) and to extract a wavelength (drop) from a DWDM link and transfer it to the user interface. In implementing reconfigurable networks, 8-96 channel ROADMs that support 40 Gb/s per wavelength and in future rising to 100 Gb/s have been used. Different network topologies have also been deployed; the standalone and overlapping physical rings, point-to-point spur links and point-to-point standalone links.

A network management system (NMS) is used to implement remote software configuration of customer personnel equipment (CPE) and has the information about the network properties that are impairment-aware to detect and correct a network fault [114]. By having an intelligent NMS, costs can greatly be reduced since fault detection and recovering a connection does not require a physical technician to perform the repairs [114].

4.3. The Square Kilometre Array (SKA), South Africa Fibre Network

The Square Kilometre Array (SKA) Project is a global scientific unit that is aimed at providing in-depth answers about the universe by creating a very powerful and more sensitive radio telescope for astronomy. Upon completion, the projected traffic from the SKA dishes will be 100 times the current global internet traffic and will have a super-computer that is more sensitive than one hundred million computers for signal and data processing [116]. The South African SKA will be located in the Karoo region of Western Cape and will host 3,000 dish antennas. Indeed, the MeerKAT which is a precursor to the SKA, will have 64 dishes. Other African countries involved with the SKA include; Kenya, Madagascar, Namibia, Mauritius, Ghana, Zambia, Mozambique and Botswana [116], [117].

The backbone of the SKA is the signal and data transport (SADT) networks which will interface the entire system and therefore poses the greatest design challenge. The over 40 Gb/s of data from each dish to the Karoo Array Processing Building (KAPB) station and the eventual hundreds of Pb/s will require advanced techniques and optical fibre capabilities to transmit this enormous data. Moreover, real-time control and monitoring and timing signals will require extensive and reliable fibre connectivity and development of algorithms and software to remotely track each antenna.

Figure 4.5 represents a schematic of the SKA fibre network from individual dish antennas to the rest of the world. This fibre network topology corresponds to the typical telecommunication network as described in chapter 2, where data signals are exchanged in a bidirectional manner between the end-user (antennas), the KAPB and the control office [118]. From KAPB to the individual dish-antennas, the fibre network can be compared to a PON network topology where a 1.712 GHz timing and reference frequency (TFR) signal is transmitted from the KAPB/central office (CO) in a downstream direction while the antennas transmit data signals in an upstream direction within ~12 km distance [119], [120]. There is a total of 170 km of buried fibres connecting KAPB and a single antenna with a maximum

distance of 12 km. Indeed, the network represents both point-to-point (P2P) and star topologies. The collected data will be transmitted from Karoo to the science data processor (SDP) in Cape Town, South Africa for over 800 km and to astronomers outside South Africa [118], [121].

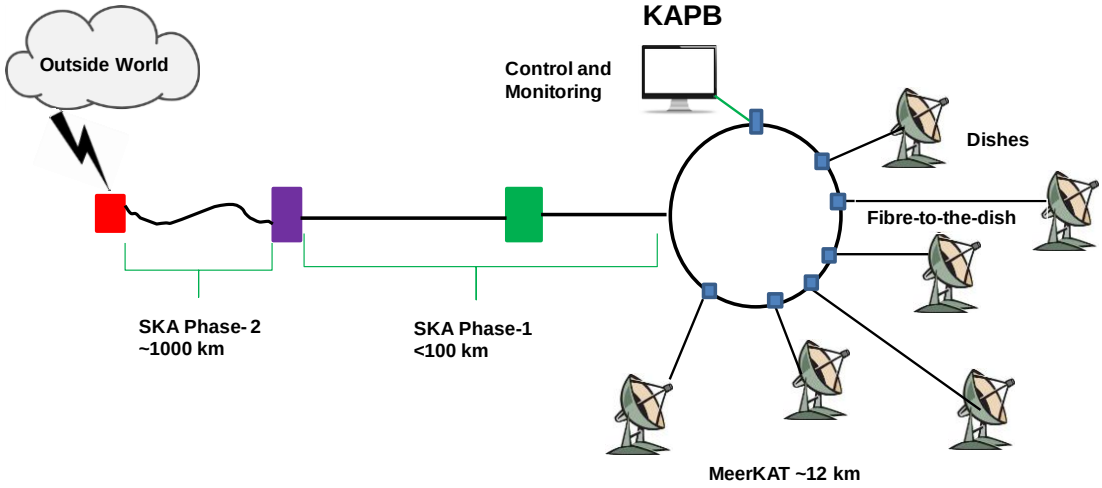

Figure 4.5: An illustration of the SKA fibre network; 12 km Fibre to the dish (FTTD) to the Karoo Array Processing Building (KAPB) and <100 km to SKA Phase 1 and SKA Phase 2 to the Outside World of Astronomers. A monitoring and control plane to track data and timing signals is also shown.

Since the SKA Project will require precise synchronizing in real-time, local TFR clock signals have to be stable to reduce signal loss and to ensure that there is minimum drift and timing mismatch during data correlation [121]. The SADT will generally utilize advanced optical fibre transport technologies to transmit the enormous data for long distances. DWDM and optimized transmitter-fibre-receiver designs will form the backbone of SADT [122]. Advanced modulation formats such as mPSK, DQPSK, mQAM and OFDM and coherent detection will be used. With these technologies, sub- and super-channels transmitting at 1-100 Gb/s and 1.088-14.5 GHz clock signal frequencies for short and long distances will be achieved [118].

For spectrum efficiency and capacity, colourless-grid system and other advantages of the flexible spectrum as discussed in chapter 2, the SKA fibre network can be designed with ROADM-technology, BVT and wavelength tunable transmitters to achieve a reconfigurable network. Data and clock signal distribution to and from the antennas and to the processing stations can also be remotely tracked using control and monitoring algorithms contained in a control plane in the Karoo and in Cape Town. With wavelength and data switching capabilities of the flexible spectrum network, troubleshooting, network healing during

fibre-faults can be done without physical repairs [122]. As a result, data and clock signal transmission can be optimized for the short fibre-reach to the long SKA spiral arms [123]. Cheaper, wavelength stable and energy efficient transmitters such as DFB and VCSELs could be used to transmit these signals due to their lower power consumption, direct modulation, wavelength tunability and ability to transmit high speed signals for long distances without regeneration.

4.4. Summary

In this chapter, distribution of spectrum in South African national broadband network (SA-NBN), Australian national broadband networks (Aus-NBNs) and the Square Kilometre Array (SKA)-South Africa has been reported. Integration of different types of signal distribution services such as optical fibre, satellite and wireless to homes, educational/research institutions, public sectors, premises, mobile cell towers and consumer gadgets (computers, smartphones, HD-TV, TPUs and CCTVs) have also been reported. Indeed, backbone optical fibre distribution to P2P and complex mesh and P2MP networks transmitting both data and timing signals for short and long-haul distances using existing fixed and flexible grid systems has also been discussed. The several advantages of flexible spectrum in optical fibre networks could be used to increase the efficiency, capacity and remote management of the network and to optimize link properties to suit the demand of broadband and connectivity. Fibre capacity and spectrum efficiency on existing fibre networks can be improved by utilizing DWDM, advanced modulation formats, coherent detection, ROADM technology, flexible spectrum and control planes to implement cost and energy efficient Next-Gen optical fibre networks. The following chapter provides the first experimental results for optimizing transmitter-receivers, types of fibres, different bit-rates, DWDM systems and distance of transmission.

Chapter 5:

5.0 Transmitter and Receiver Technology for Flexible Spectrum

This chapter provides experimental demonstration of various types of optical transmitters and receivers that can easily be integrated into high speed flexible spectrum networks. These transmitters and photo-detectors are cost-effective, reliable, reconfigurable and efficient for high capacity spectrum utilization. We present vertical cavity surface-emitting lasers (VCSELs) and distributed feed-back (DFB) laser transmitters that offer up to 10 Gb/s signal transmission in single or wavelength division multiplexed (WDM) systems. Indeed, signal transmission performance for these transmitters are reported using eye-diagrams, bit error-rate (BER) measurements and penalties for short and long-haul transmission.

5.1. Vertical Cavity Surface-Emitting Laser (VCSEL) Technology for High-Speed Optical Systems

The characteristics and advantages of VCSEL technology for high speed signal transmission as described in chapter 3 are experimentally endorsed in the following sections. Central nominal wavelength tunability and ability for direct modulation and detection for optimized high speed signal transmission in DWDM systems and switching are demonstrated.

5.1.1. VCSEL Biasing and Wavelength Tunability

The biasing and the ability to tune the emission wavelengths of 10 Gb/s VCSELs were experimentally demonstrated and reported as seen in figure 5.1. The output power of the VCSEL was measured as the bias current was increased from 0 mA to 9.8 mA. As seen in figure 5.1 (a), the threshold current of the VCSEL was seen to be at 0.9 mA while the saturation current was seen to be at 8 mA. Above 8 mA, the output power of the VCSEL reduced as the current was further increased. As a result, the best operational bias points for the VCSEL is between the threshold and saturation current points (the linear region). During modulation, the VCSEL was biased at the middle of the linear region (4.45 mA) to provide a complete ON-OFF modulation swing. By operating the VCSEL up to the 8 mA saturation current point, the maximum optical output power was -1.3 dBm. The bias current was

restricted to 9.8 mA (without modulation) so as to avoid damaging the normal performance of the VCSEL.

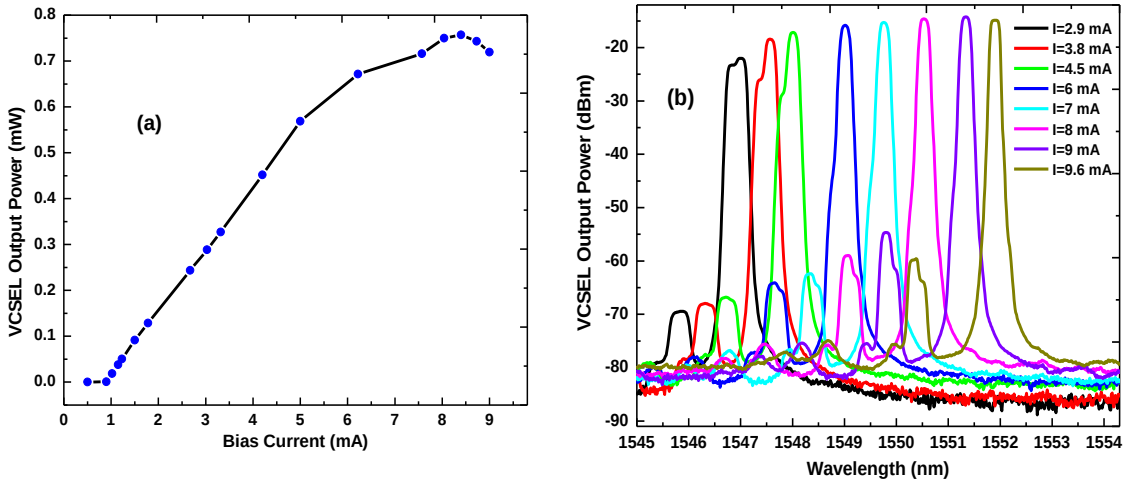

Figure 5.1: Experimental characterization of the VCSEL. (a) Biasing of the VCSEL with increase in bias current and (b) Wavelength tunability.

The central nominal wavelength tunability was another important characteristic of the VCSEL. The VCSEL was biased above its threshold current to give sufficient output power. Indeed, the emission wavelength was tuned from 1547 nm to 1551.9 nm by increasing the bias current from 2.9 mA to 9.6 mA. This implied that by biasing the VCSEL with 2.9-9.6 mA, a 4.9 nm (612.5 GHz) wavelength tunability range was achieved. Therefore, we can create 10 Gb/s tunable channels operating within a 612.5 GHz bandwidth using VCSELs which can allow 12 DWDM channels at a 50 GHz spacing. This characteristic of the VCSEL makes it an important component for Dense-WDM and flexible spectrum applications and in systems where wavelength tuning is required.

5.1.2. Experimental Demonstration of High Speed VCSEL Transmission

Transmission capabilities of 10 Gb/s 1310 nm and 1550 nm VCSEL are presented in this section. This was done to investigate transmission capabilities of the VCSELs within the 1310 nm and 1550 nm transmission windows. The experimental demonstration of direct modulation and detection was performed and is illustrated in the experimental setup shown in figure 5.2. VCSEL biasing was performed by varying the current using the laser diode controller (LDC) and directly modulating the VCSEL with a 8.5-11.3 Gb/s non-return-zero (NRZ) pseudo-random binary sequence (PRBS 2^7-1) from a programmable pattern generator (PPG) via a bias-tee (BT). The bit error-rate tester (BERT) generated patterns with variable modulation depths and a maximum RF output voltage, $V_{r.m.s.}$ of

0.354 V. The VCSEL was biased above the threshold current. The modulated signal from the VCSEL was then transmitted over a fibre-under test (FUT). In this experiment, the FUT comprised of different types of fibre with varying lengths, attenuation, PMD and dispersion properties. A variable optical attenuator (VOA) was used to vary the optical signal power into the photodiode (PD) to emulate the typical losses in a fibre-link.

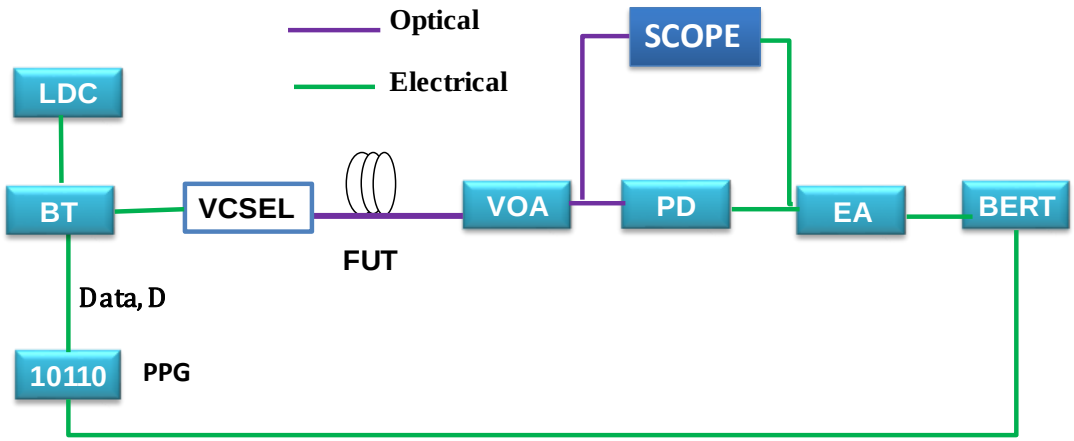

Figure 5.2: An experimental set up for VCSEL transmission where PPG is the programmable pattern generator, BT is the bias tee, LDC is the laser diode controller, FUT is the fibre under test, VOA is the variable optical attenuator, PD is the photodiode, EA is an electric amplifier and BERT is the bit-error-rate tester.

The receiver comprised of a PD and a 10 GHz electrical amplifier (EA). This EA was used to amplify the electrical signal to meet the operational requirements of the BERT. The quality of the transmitted signal was evaluated by eye-diagrams and BER measurements using an oscilloscope and BERT respectively. The BERT determined the number of errors received and compared the errors to the total number of transmitted bits. A 531-707 MHz clock signal from the PPG was used to synchronize the 8.5-11.3 Gb/s transmitted and received data signals. Finally, the quality of the optical signal was characterized by observing the optical spectrum, electrical data patterns, eye-diagrams, BER measurements and penalties.

To demonstrate direct modulation of a VCSEL, a 1550 nm VCSEL was modulated with a 10 Gb/s PRBS pattern from a PPG and a PIN photodiode was used as a photo-receiver. A 5.5 mA bias current was applied to the VCSEL and RF modulation voltage range of 0.194-0.347 $V_{r.m.s.}$ used. These voltages were the root-mean square (r.m.s) values of the peak-peak voltages. Indeed, 3-12 dB electrical attenuators were used to match the RF modulation voltages with the $V_{r.m.s.}$ of the VCSEL so as to achieve above 50% modulation index. The eye-diagrams measured at -16.2 dBm of optical power representing the

modulated signal with 0.194 $V_{r.m.s.}$ and 0.347 $V_{r.m.s.}$ is shown in figures 5.3 (a) and (b). As seen in the diagrams, the power (in mWatt) increased implying that the eye-opening increased with an increase in modulation voltage. The extinction ratio (ER) was 9.2 dB and 10.4 dB for 0.193 V and 0.347 V modulation voltages respectively.

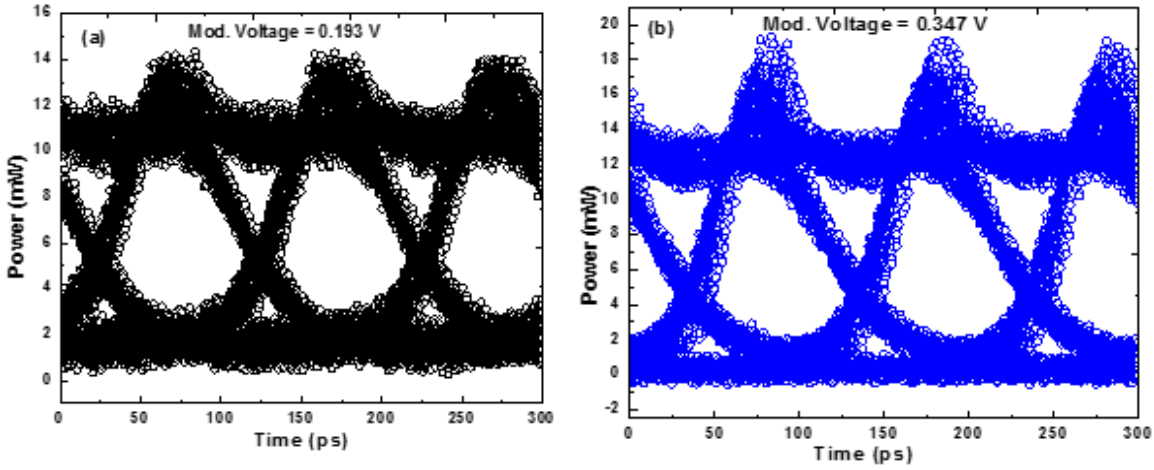

Figure 5.3: Eye diagrams for an optical signal modulated at 10 Gb/s with (a) 0.193 V and (b) increased chirping for 0.347 V root mean square (r.m.s.) modulation voltages. The eye diagrams were measured at -16.2 dBm of the optical power.

A wide and open eye represented an error-free modulation. When the eye was open, the receiver was able to distinguish between the '1' and '0' and therefore few errors were detected. However, the over-shoots in the "1" -level of the eye-diagram was as a result of VCSEL chirping. This was observed when the modulation voltage was increased to 0.347 $V_{r.m.s.}$ as shown in figure 5.3 (b). The increased voltage resulted in a change in the refractive index of VCSEL cavity thereby changing the emission frequency of the VCSEL as shown in figure 5.4 (a). By modulating the VCSEL with an analogue sine wave of 0.347 V, the wavelength change was measured to be 0.1 nm. An analogue sine wave was used to investigate the transition in the whole period of the signal instead of the instantaneous "1" or "0" bit transitions.

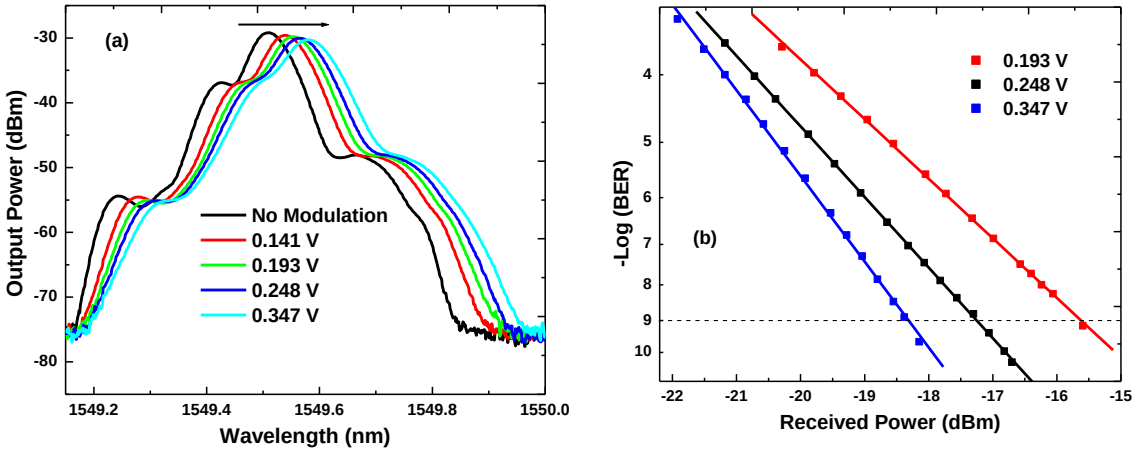

Figure 5.4: (a) illustration of wavelength drift due to increased modulation voltages leading to frequency chirping (b) the BER measurements showing improved receiver sensitivity due to increased modulation voltages 0.193-0.347 V.

When the BER measurements were done at a threshold of 10^{-9}, an increase in the modulation voltage resulted in improved received sensitivity as shown in figure 5.4 (b). The sensitivity for a 0.193 V was seen to be -15.6 dBm while a 0.347 V had a -18.3 dBm. This represented a 2.7 dB improvement in the PIN receiver sensitivity when the modulation voltage was increased from 0.193 V to 0.347 V as this increased the ER of the received signal. It was therefore important to identify the optimal modulation voltages that reduced the effects of chirping and at the same time increased the eye-opening and sensitivity. This was necessary since chirping introduces high dispersion effects on a transmitted signal [69]. Despite the high ER as a result of increase in modulation voltages, transmission of a modulated signal with high ER may not be ideal for minimizing chromatic dispersion. A trade off of ER and chromatic dispersion penalty must therefore be considered.

5.1.3. 1310 nm and 1550 nm VCSEL 10 Gb/s Signal Transmission

The 1310 nm and 1550 nm transmission windows used in high-speed optical fibre communication systems were investigated to determine the optimized fibre-reach for different types of fibres and transmission speeds. Signals were transmitted using 1310 nm and 1550 nm 10 Gb/s VCSELs and detected using the same PIN photodiode. The presence of chirping in the VCSEL and chromatic dispersion (CD) in the fibre introduces bit-errors and hence power penalties during transmission. Different fibre-types also experience different attenuation values as described in chapter 3.

A 1310 nm VCSEL was biased at 8.6 mA and lased at 1306 nm and the output power was measured to be -2.4 dBm and modulated with a 10 Gb/s PRBS data and transmitted over

a G.652 fibre for various distances. The PIN receiver sensitivities for the back-to-back (B2B) and transmission over 6-18 km fibre are shown in figure 5.5 (a). The 1310 nm wavelength is regarded as a zero (0) dispersion transmission wavelength with 0.3 dB/km attenuation in G.652 fibres [81].

The sensitivity for the B2B, without transmission was seen to be at -19.6 dBm. After transmitting the signal for 6 km, the sensitivity reduced to -19.3 dBm. A small dispersion penalty of 0.3 dB was incurred. By increasing the transmission distance to 18 km, the sensitivity reduced to -18.5 dBm representing a 1.1 dB penalty. Error-free transmissions were realized for all the 6-18 km transmission over the G.652 fibre.

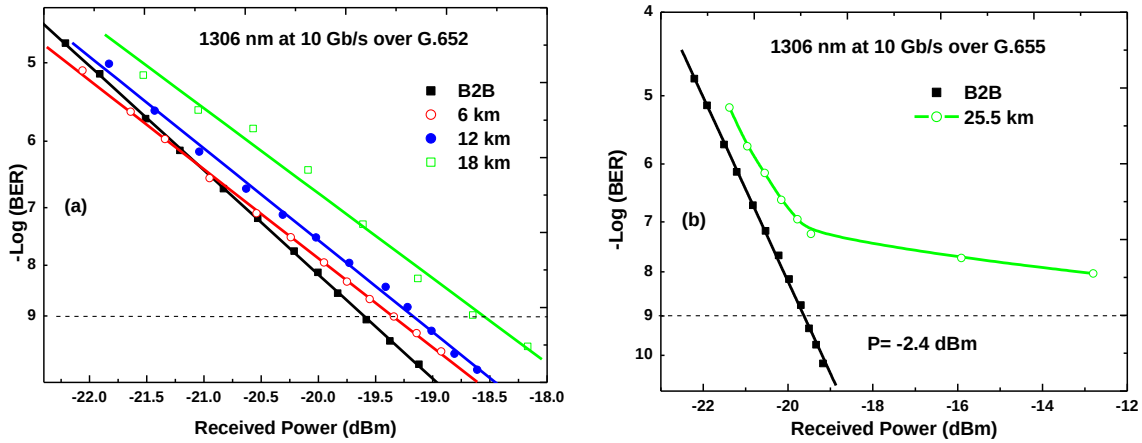

Figure 5.5: An illustration of 10 Gb/s signal transmission over at 1306 nm transmission wavelength. (a) Error-free transmission over 6-18 km G.652 fibre and (b) Error-floor over 25.5 km G.655 fibre.

When the same 1306 nm VCSEL was used to transmit a 10 Gb/s signal over a 25.5 km G.655 fibre with a 0.2 dB/km attenuation, an error-floor was reached as shown in figure 5.5 (b). The error-floor is the region in which the BER flattens and the receiver is unable to distinguishably separate the received "1" and "0" bits [72]. It is also the point at which the BER fails to cross the telecommunication 10^{-9} BER threshold as seen in figure 5.5 (b). The error-floor was due to the high dispersion (>798 ps) effects that affected the signal resulting in the increased number of error-bits received.

It is therefore evident to conclude that 1310 nm signal transmission are best suited for long distance G.652 fibre since dispersion effects are lower at the 1310 nm transmission window.

The 1550 nm low attenuation transmission window was also studied and reported. A VCSEL biased at 7.5 mA with optical output power of -3.8 dBm and lasing at 1550.4 nm was used. A 10 Gb/s data pattern was used to modulate the VCSEL and transmitted over

25.5 km G.655 and 6-12 km G.652 fibres and BER performance reported as shown in figures 5.6 (a) and (b).

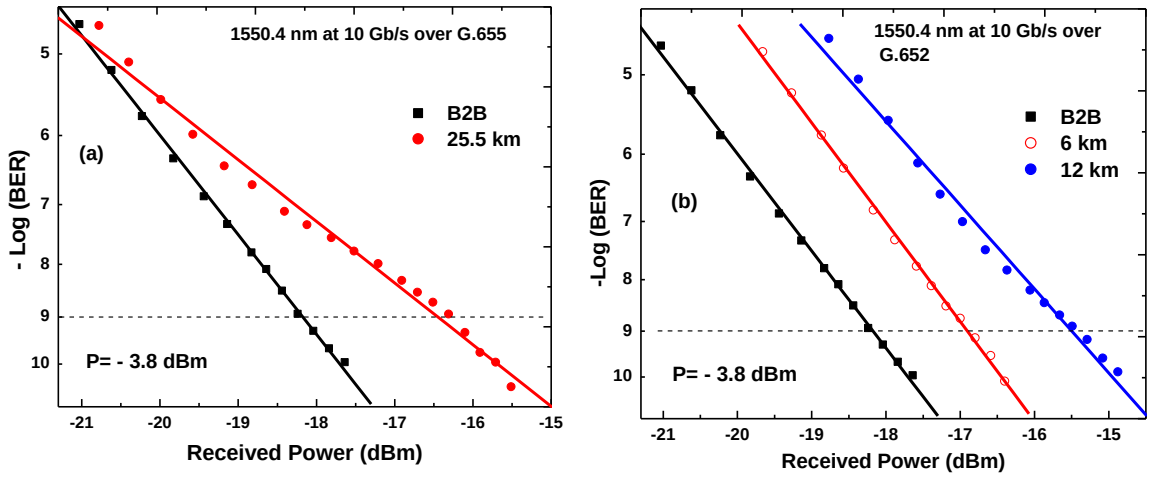

Figure 5.6: Experimental BER measurements for 10 Gb/s transmission over (a) G.655 and (b) G.652 fibres at 1550.4 nm.

The PIN receiver sensitivity for B2B was seen to be -18.2 dBm. When the signal was transmitted over 25.5 km G.655 fibre, the sensitivity reduced to -16.5 dBm. This reflected a 1.7 dB power penalty as shown in figure 5.6 (a). The reduction in receiver sensitivity was as a result of the 140.25 ps dispersion in the G.655 fibre.

For transmission over G.652 fibres, the 1550.4 nm 10 Gb/s signal was transmitted for 6 km and 12 km and the BER measurements shown in figure 5.6 (b). A 1550.4 nm transmission experienced a 17 ps/(nm.km) dispersion slope in a G.652 fibre as discussed in chapter 3. The signal experienced 102 ps and 204 ps dispersion over the 6 km and 12 km fibres respectively. The sensitivity for 6 km was -16.9 dBm and 12 km was seen to be at -15.5 dBm. Penalties of 1.3 dB and 2.7 dB were incurred for 6 km and 12 km transmission respectively. The high dispersion resulted in more error-bits being received and therefore limited longer distance transmission over the G.652 fibre.

In high speed signal transmission using VCSELs, fibre links should be optimized for to achieve both reach and error-free transmission within the 1310 nm and 1550 nm transmission windows. As this becomes the basis for single wavelength, DWDM and flexible spectrum channels in typical networks.

5.1.4. Dense Wavelength Division Multiplexing (DWDM) Technology Using VCSELs to Increase Capacity

A single strand of an optical fibre can be used to transmit several wavelengths that have been combined together using WDM technology. Each wavelength can be assigned to a dedicated

destination thereby increasing the capacity of the fibre transmission. In this study, wavelength tunability in VCSELs was used to experimentally demonstrate a WDM optical communication system fitting into the 50 GHz and 100 GHz grid systems. Two band-pass filter-based multiplexers and demultiplexers were used to combine and separate the wavelengths respectively. By changing the bias currents as previously illustrated in figure 5.1 (b), the emission wavelengths of the VCSELs were tuned to match the nominal central wavelengths in 50 GHz and 100 GHz multiplexers/demultiplexers for fixed and flexible grid systems.

When a 50 GHz multiplexer (MUX) was used to combine wavelengths with equal bandwidth, the 50 GHz channel spacing allowed twice the number of channels as compared to a 100 GHz MUX. As a result, spectrum capacity and efficiency were improved. However, closer channels may interfere due to pulse broadening that results from chromatic dispersion in the fibre. It was therefore prudent to set a trade-off between attaining spectrum efficiency and at the same time minimizing crosstalk effects.

An experimental demonstration of WDM technology using VCSELs is shown in figure 5.7. Two 1550 nm VCSELs were modulated with 10 Gb/s PRBS data. Indeed, VCSEL 1 was modulated with a data D while VCSEL 2 was modulated with an inverse data $\overline{\mathrm{D}}$. This was done to ensure that the two VCSELs transmitted different patterns of data. Different lengths of RF cables were used to decorrelate the D and $\overline{D}$ data patterns by providing them with a random delay. VCSEL 1 and VCSEL 2 constituted channels 1 and 2 respectively. The wavelengths of the two VCSELs were tuned to match the ITU-T grid channel wavelengths for 50 GHz and 100 GHz spacing. VCSEL 1 was biased to provide a nominal central wavelength of 1550.02 nm to fit into a channel of a 50 GHz MUX. To achieve a 50 GHz spacing, VCSEL 2 was tuned to 1550.43 nm giving a 0.41 nm wavelength spacing which is equal to 50 GHz. Moreover, a 0.8 nm (100 GHz) spacing was achieved by tuning VCSEL 2 to 1550.84 nm. Both nominal central wavelengths were transmitted over a 25.5 km G.655 fibre and then demultiplexed into individual wavelengths using a 50 GHz DWDM demultiplexer (DeMUX). The quality of the individual wavelengths was evaluated using BER measurements.

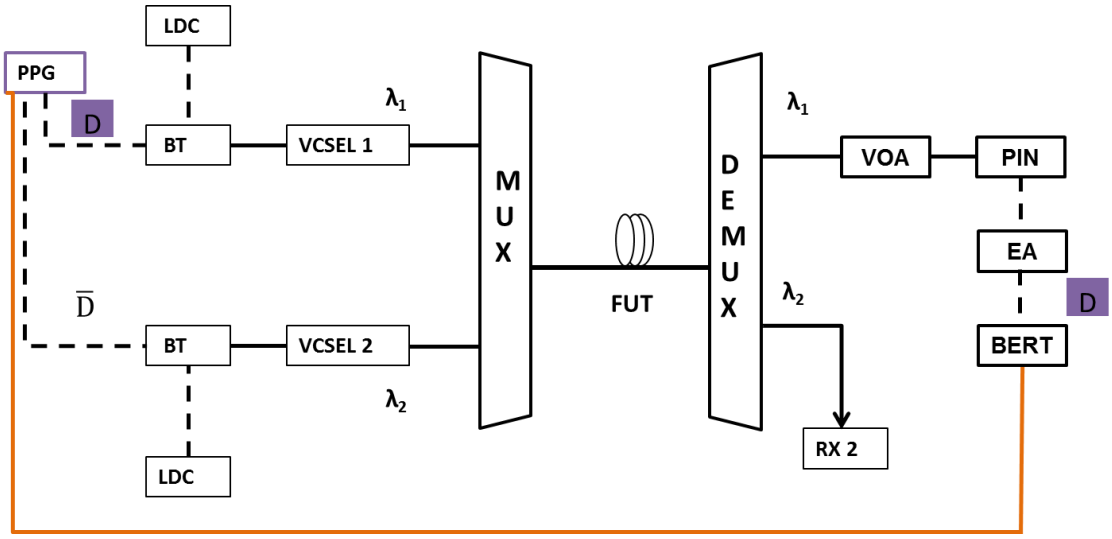

Figure 5.7: An experimental set-up demonstrating 2×10 Gb/s DWDM channels spaced at 50 GHz and 100 GHz using 1550 nm VCSELs and transmission.

To study the band-pass properties of the 8-channel 50 GHz and 100 GHz multiplexers and demultiplexers, a 1480-1650 nm broadband laser source FLS-200B with an output power of -6 dBm from EXFO Company was used. We used single channel at centre wavelength $1550 \pm 0.1\ nm$ The output optical spectrum as observed in an optical spectrum analyser (OSA) from Agilent Company is as shown in figure 5.8 (a). The channel isolation ratio for a 50 GHz and the 100 GHz multiplexers are 41 dB and 50 dB respectively. This provides high filtering capabilities of DWDM channels spaced at 50 GHz and 100 GHz. The full-width at half maximum (FWHM) of the 50 GHz and 100 GHz band-pass filters was found to be 0.21 nm and 0.64 nm respectively. A 100 GHz filter has larger FWHM and therefore allowed more optical power than a 50 GHz filter. However, the 100 GHz band-pass filter allowed more spectral components to pass through as compared to 50 GHz. In terms of spectrum usage, 50 GHz filters can accommodate twice the number of channels at 50 GHz spacing than 100 GHz filter-based multiplexers.

When an optical signal from a 1551.5 nm VCSEL was multiplexed into 50 GHz and 100 GHz MUX/DeMUX, the bandwidth of the signal was maintained by the two MUXs as shown in figure 5.8 (b). The 50 GHz and 100 GHz multiplexers can therefore be used to combine and separate signals from a 10 Gb/s VCSEL. The chirp that is associated with most VCSELs was also observed as shown indicated in figure 5.8 (b).

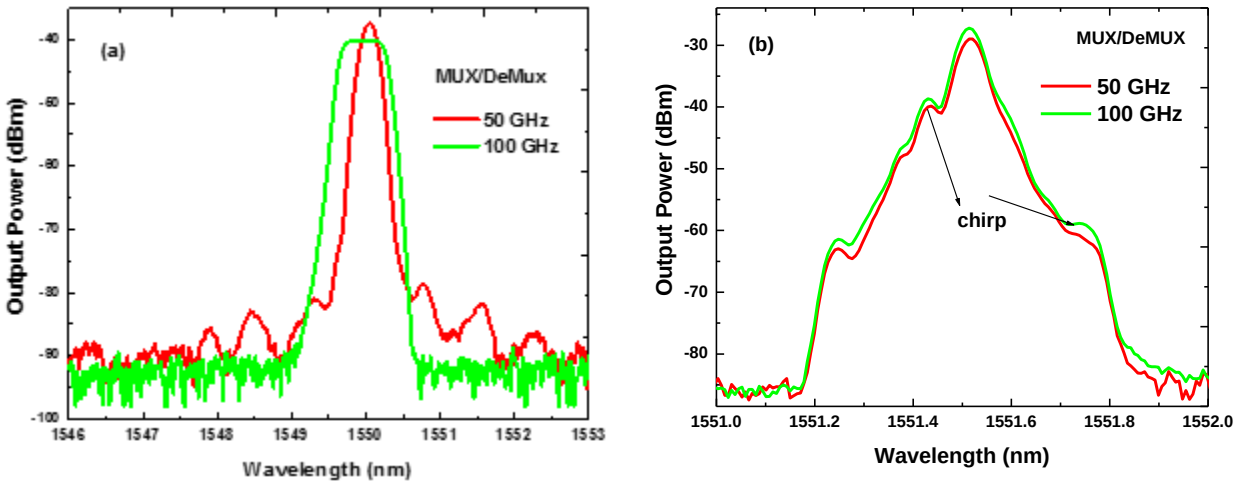

Figure 5.8: The output spectrum of a 50 GHz and 100 GHz band pass multiplexers and demultiplexers using (a) a broadband laser source and (b) VCSEL spectrum with wavelength chirps.

When the two wavelengths with a $2 \times 10\ Gb/s$ capacity were transmitted over a 25.5 km G.655 fibre, the effect of crosstalk due to the adjacent channels was studied and reported in figure 5.9. A 1550.02 nm 10 Gb/s transmission was considered as the reference wavelength while varying the wavelength of the adjacent channel at 1550.43 nm and 1550.84 nm to space the two channels at 50 GHz and 100 GHz respectively. The effect of channel spacing on adjacent channels was evaluated by BER measurements are shown in figure 5.9.

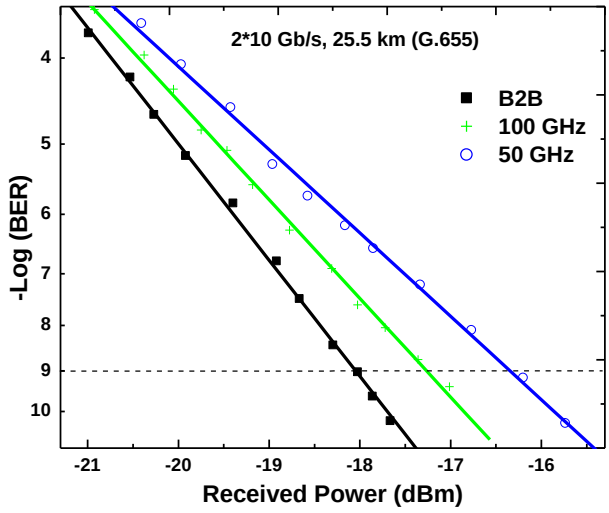

Figure 5.9: Experimental BER measurements for 2×10 Gb/s WDM transmission spaced at 50 GHz and 100 GHz transmitted over 25.5 km G.655 fibre using 1550 nm VCSELs.

It is noted that since adjusting the bias current of the VCSEL not only changes the emission wavelengths and output power, the modulation bandwidth of the laser when an RF

signal is used is also changed. As a result, error-bits might be received due to either under-modulation or over-modulation of the signal.

The sensitivity for the B2B, 100 GHz and 50 GHz for channel 1 (VCSEL 1) due to the interfering channel 2 were seen to be at -18.1 dBm, -17.3 dBm and -16.4 dBm. As a result, penalties for the different channel spacing were 1.7 dB and 0.8 dB for 50 GHz and 100 GHz spacing respectively. The penalties were due to inter-symbol interference resulting from dispersion in the fibre and the increased capacity on the fibre. Indeed, the inter-symbol interference resulted in bit-overlap as will be shown in figure in chapter 8. For a 50 GHz spaced transmission, the 1.7 dB penalty was as a result of crosstalk affecting the closely spaced adjacent signals more than in a 100 GHz spacing. The crosstalk interferences can be minimized by using narrow bandwidth band-pass filters at the receiver. The difference in penalties were also due to the different bias points and output power of the VCSELs while the wavelengths were tuned to attain 0.4 nm and 0.8 nm channel spacing. As previously discussed, increasing the bias currents of individual VCSELs not only increases the emission wavelength but also increases the output of the VCSEL.

To increase the capacity of the fibre, WDM technology using high-speed VCSELs can therefore be used to transmit user-dedicated nominal central wavelengths that fit into the ITU-T fixed and flexible frequency grid. Moreover, a DWDM system can also be implemented using VCSELs to multiplex closely spaced channels by using 25 GHz and the flexible grid systems. Crosstalk interferences will be minimized by the narrow linewidth band-pass filters with high channel isolation ratio in the 25 GHz and flexible grid multiplexers. DWDM technology is a vital element of flexible spectrum in optical networks since it allows signals to be dynamically switched and routed to minimize channel collisions and to increase the spectral efficiency by slicing the available spectrum to multiple user channels. The following sections describes how VCSELs can be used to implement bit-rate variable (BV) with 4.5 Gb/s and 10 Gb/s signal transmission.

5.1.5. High Speed 4.5 Gb/s and 10 Gb/s per Channel Bitrate Variable VCSEL Transmission for Flexible Spectrum

In optical fibre transmission, a trade-off between capacity and distance of transmission is an important element in network architecture and design. To maintain the quality of signal (QoS), quality of transmission (QoT) and to ensure that there is no denial of service, the available resources such as bandwidth is often shared amongst the users. Indeed, high speed long distance transmission is limited by attenuation and the non-linear effects such as CD,

FWM, SPM and XPM. As a result, transmission penalties on existing optical fibre networks can be reduced by varying the transmission speeds depending on the demand for bandwidth and allocation of more bandwidth to links that require more bandwidth.

In a flexible spectrum, adjustment of wavelengths and bitrates at the transmitter end is realized by using optical signals with different capacity. The PPG can provide 1 Gb/s up to 11.3 Gb/s of PRBS data. While the available VCSELs can be used to carry up to 10 Gb/s signals. By combining VCSELs capabilities and the bit-rate variable PPG, a flexible spectrum transmission can be implemented.

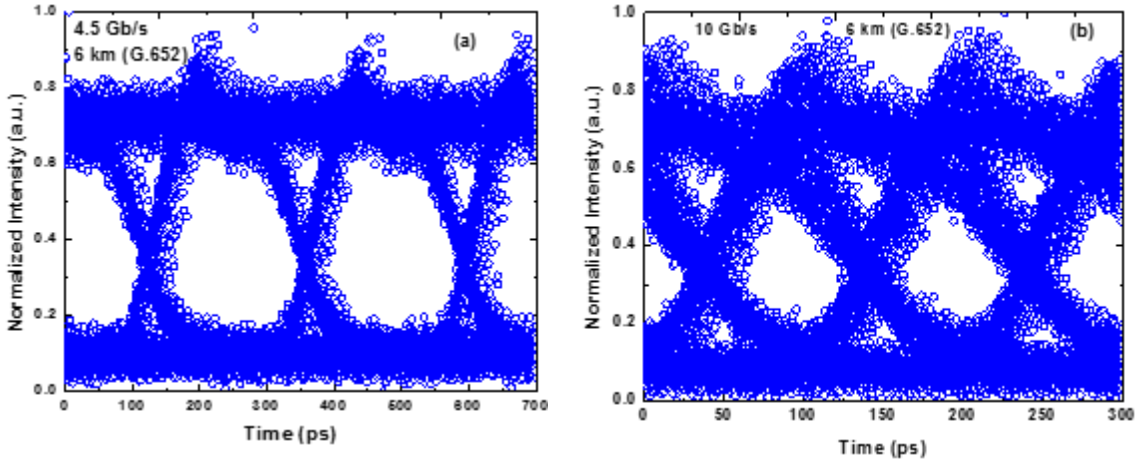

Figure 5.10: Data signal transmission using VCSEL Technology over 6 km G.652 fibre at (4.5 Gb/s) and (b) 10 Gb/s measured at an output optical power of -16.9 dBm.

To study the flexibility of bitrate allocation, a 1550 nm VCSEL was modulated with 4.5-10 Gb/s of data and transmitted over 6 km G.652 fibre. The quality of the signal was analysed using eye-diagrams as shown in figure 5.10 (a) and (b) at an error-free optical power of -16.9 dBm. A PSO-101 sampling oscilloscope from EXFO Company was used. Both 4.5 Gb/s and 10 Gb/s signals were error-free transmission as demonstrated by the clear, open and wide eye-diagrams. However, the 10 Gb/s signal showed a slightly closed eye that resulted from the received error-bits. The received error-bits were mainly as a result of the accumulated dispersion in the G.652 fibre.

Apart from nominal central wavelength tunability of the network using VCSELs, the bit-rates can also be adjusted for flexible spectrum utilization. For a VCSEL with a 5.0 nm (625 GHz), 25 and 12 flexible channels at 25 GHz and 50 GHz spacing respectively will be accommodated within the tunability range. This provides an optimized network performance in terms of bitrate, wavelength switching and capacity. With the directly modulated transmitters, we were able to characterize and optimize VCSELs for various applications in high-speed transmission, DWDM technology, long distance and flexible spectrum

transmissions. Depending on the network properties and requirements, high speed 4.5 Gb/s and 10 Gb/s transmissions can be implemented for end to end signal continuity.

5.1.6. Distributed Feed-Back (DFB) Laser Transmitter for High Speed Optical Fibre Communication Systems

DFB transmitters are high optical power and directly modulated lasers that can transmit to up to 40 Gb/s. The main advantage of DFB transmitters over other semiconductor lasers such as the VCSEL are the high output power due to the narrow linewidth of 0.04 nm, wavelength stability and they experience minimal frequency chirping. Furthermore, the emission wavelength of the DFB can be varied by varying the temperature of the DFB laser cavity. Due to these advantages, DFB lasers are therefore ideal for high-speed, WDM and long-haul optical fibre transmission.

The following study illustrates the properties, characteristics and optimization of the DFB transmitter with fibre length, power, modulation and dispersion compensation to achieve short and long-haul transmission at 10 Gb/s.

5.1.7. Bias Characteristics and Modulation of a DFB Laser

To obtain the input current-output power (I-P), the output power of a 1551.1 nm DFB laser was measured with increasing bias currents from 0 mA to 99.6 mA. The threshold current for the DFB was measured to be 18 mA and a saturation current of 94 mA. Above the threshold current level, the DFB laser demonstrated a linear I-P characteristic giving a constant increase in power when the bias current was increased as shown in figure 5.11. As a result, operating the DFB laser within this linear I-P region is an ideal property. Biasing the DFB at the middle of the linear region gives the optimum and bias point that results in a complete swing between the on-off state of the laser when an input RF modulation signal is applied. Indeed, the mid-point bias level was seen to be 56 mA emitting a 5.7 dBm output power.

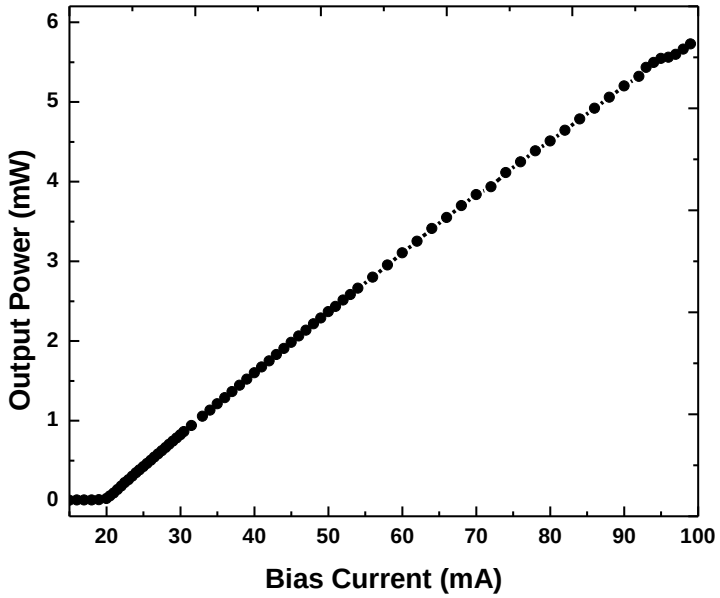

Figure 5.11: The input current (I)-output power (P), I-P bias characteristics of the DFB transmitter with threshold current level of 18 mA and 94 mA saturation current.

It was determined that by biasing the laser at the mid-point (56 mA), it would require a 0.99 $V_{r.m.s.}$ RF input signal to achieve a complete swing of the DFB laser due to direct modulation. This would therefore require a high voltage input RF signal. The effects of modulating the DFB laser at different bias current levels and using an RF signal from the BERT is illustrated in figure 5.12 (a) and (b). The eye diagrams were measured at an optical output power -15.5 dBm which was closer to the PIN error-free sensitivity at 56 mA bias.

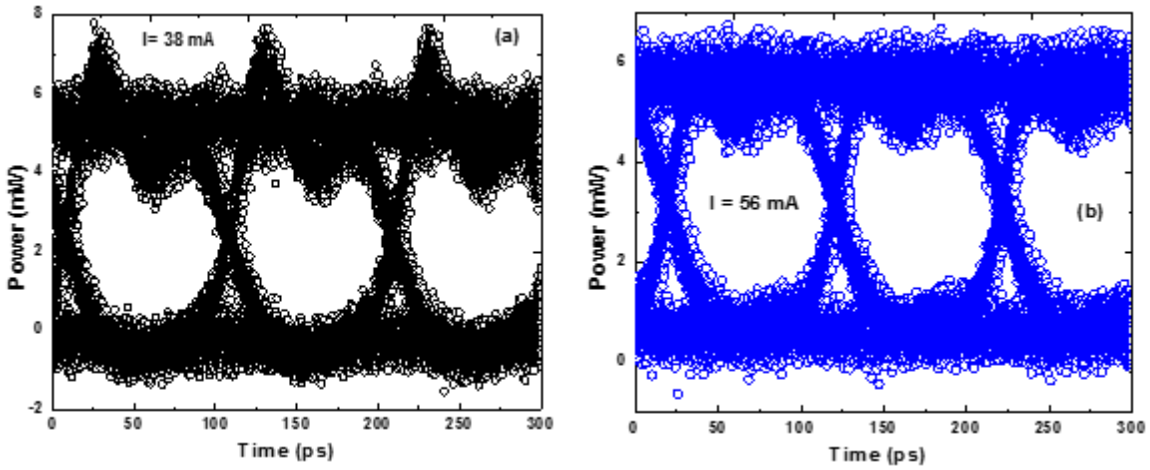

Figure 5.12: The eye diagrams of 10 Gb/s DFB signals modulated at (a) 38 mA and (b) the mid point of the linear region of the I-P, I= 56 mA at -15.5 dBm.

The maximum RF output of the PPG that was used to modulate the DFB laser was 0.354 $V_{r.m.s.}$. With a 50 Ω matching termination resistor, the equivalent swing current was

calculated to 20 mA. Indeed, the 0.354 V RF input voltage limited the bias current swing to 20 mA bias current from the threshold bias level to achieve a perfect on-off state of the laser during modulation with the 10 Gb/s NRZ data patterns. The eye-diagrams for 38 mA and 56 mA bias levels demonstrate clear and wide eyes. When the DFB laser was therefore biased at 38 mA, a 20 mA swing current was set between the threshold (off-state) and higher linear region of the I-P bias characteristics. However, this introduced chirps at the "1"-level as shown in figure 5.12 (a). Biasing the laser at the mid-point provided a clear and wide eye diagram as shown in figure 5.12 (b).

The following sections provide performance evaluation using BER measurements of the DFB transmitter for high speed and long distance transmission.

5.2. DFB Transmitters for High-Speed and Long-Haul Fibre Communication

The BER measurements to optimize modulation bias levels with the PIN photo-receiver is shown in figure 5.13. A 10 Gb/s NRZ-PRBS pattern from the PPG was used to modulate the DFB laser at 38 mA and 56 mA bias points. BER evaluation for B2B at these bias points were done to determine the sensitivity levels for the receiver. It was seen that despite the output power (4 dBm) of the DFB at 38 mA bias current, the BER performance was better than the 56 mA bias level with a 5.6 dBm output power. This was due to the 20 mA swing current that provided a voltage match with the RF input modulation voltage that provided a higher modulation index. The error-free sensitivity at the 10^{-9} BER threshold level for a 38 mA bias current was seen to be at -18.4 dBm while a 56 mA bias level had a -15.7 dBm. This provided a 2.7 dB improvement in the PIN receiver sensitivity when the DFB laser was biased at 38 mA than a 56 mA bias level due to the optimized ON-OFF operation close to the threshold level.

The 10 Gb/s modulated signal was then transmitted over a 24.7 km G.655 TrueWave low water-peak (LW)-REACH fibre and BER performance evaluation done for different bias levels. The PIN receiver sensitivity for a 38 mA biased DFB carrying a 10 Gb/s in a 24.7 km fibre transmission was measured to be -16.5 dBm resulting in a 1.9 dB penalty. The 1.9 dB power and dispersion penalty was due to the 5.8 ps/(nm.km) dispersion at the 1550 nm wavelength exerienced by the signals that resulted in bit-errors. It was also observed that despite the reduced receiver sensitivity (-14.9 dBm) at 56 mA, the 24.7 km transmission penalty was found to be 0.8 dB. This was attributed to the high intensity (5.6 dBm) from the DFB laser when 56 mA bias current was applied that enabled minimized

dispersion effects on the transmitted data over the same 24.7 km distance and therefore increased the reach.

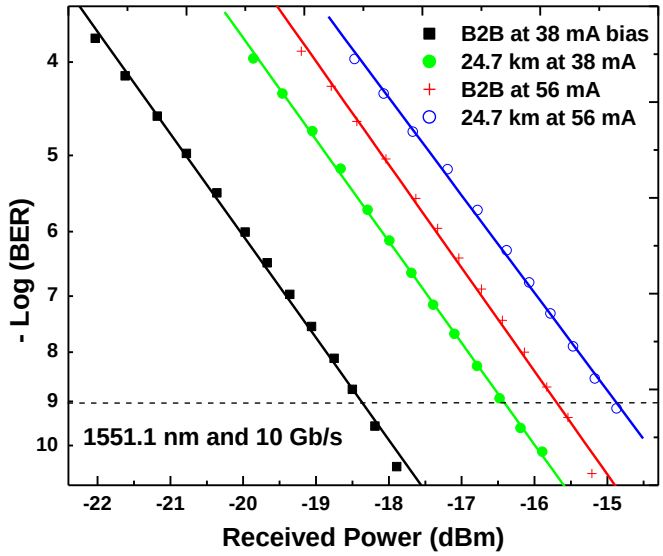

Figure 5.13: Experimental BER evaluation for 10 Gb/s DFB lasers modulated at 38 mA and 56 mA and transmission over 24.7 km G.655 TrueWave LW REACH fibre at 1551.1 nm wavelength.

The advantages of high power and wavelength stability in DFB transmitters was used to optimize them for high speed signal transmission in long distance fibre links. This was done by modulating the DFB laser with 10 Gb/s data and transmitting the signal over 50 km fibre distances. The DFB laser was biased at 38 mA bias current since its sensitivity for an error-free modulation was approximately -18 dBm which is the sensitivity for most PIN photo-receivers [78] [42] [124]. Different types of fibres with varying chromatic dispersion properties were used and their respective BER evaluation reported in figures 5.14 (a) and (b). A 1551.1 nm transmission reduced the fibre attenuation losses and non-zero dispersion shifted fibres (NZDSF) were used to minimize both dispersion and FWM effects[82], [89]. Moreover, the CD coefficients of the different G.655 fibre spools (FUTs) used were; TW-REACH (5.8 ps/(nm.km), TW-RS (2.8 ps/(nm.km) and TW-SRS (-2.8 ps/(nm.km) from OFS Company [82] [89] [90]. To extend the reach of the fibre to ~50 km, two pieces of fibre (~25 km each) were connected.

With dispersion management and compensation, longer transmission distances were attained. The sensitivity for a 50.1 km G.655 TW-REACH fibre was -12.2 dBm as shown in figure 5.14 (a). Comparing this with a 10 Gb/s B2B signal whose sensitivity was -18.5 dBm, a 6.3 dB transmission and dispersion penalty was incurred. The high penalty was due to the cumulative dispersion over the 50.1 km fibre. However, to reduce the CD penalty, the

TW-REACH fibre was combined with an inverse dispersion SRS fibre to compensate the accumulated dispersion by using the relation as described in equation 3.7 of chapter 3. The total dispersion in the 50.1 km link made up of two TW-REACH fibres was 290.6 ps. The TW-REACH fibre has the lowest CD slope of ≤0.045 ps/(nm^2.km) compared to the rest of the G.655 NZDSF fibres. As a result, combining a 24.7 km TW-REACH and 25.5 km TW-SRS fibre to achieve a 50.2 km not only extended fibre-reach but also reduced dispersion effects to have an optimized transmission. The total dispersion due to the 24.7 km REACH was 143.3 ps while a 25.5 km TW-SRS had -71.4 ps. This resulted in residual dispersion of-71.9 ps over the 50.2 km fibre link. Indeed, the sensitivity of the TW-REACH+SRS (50.2 km) transmission was seen to be -18.1 dBm. This greatly reduced the penalty from 6.3 dB to 0.4 dB due to reduced dispersion effects. Combining TW-RS and SRS fibres with 52.1 km resulted in 3.1 ps residual dispersion.

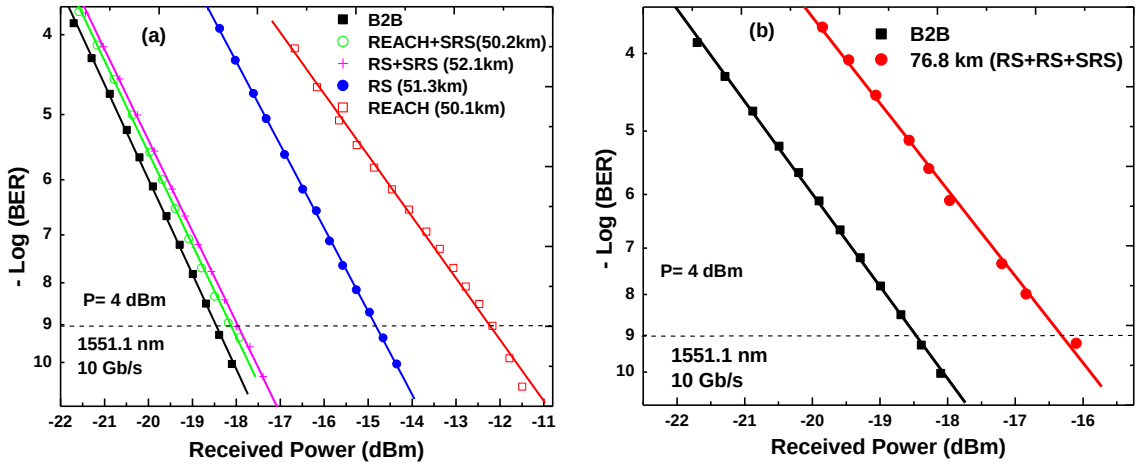

Figure 5.14: Experimental demonstration of 10 Gb/s long reach transmission optimized for (a) 50 km and (b) 76.8 km with dispersion management and compensation.

A 51.3 km 10 Gb/s transmission was also implemented using two TW-RS fibres with 2.8 ps/(nm.km) dispersion coefficient and 143.4 ps total dispersion. The PIN sensitivity for an error-free transmission over the TW-RS fibre was -14.8 dBm representing a 3.7 dB penalty was incurred. This penalty was due to bit-errors resulting from CD in the fibre. Comparing the penalties for a 51.3 km transmission over RS and 50.1 km REACH fibres without CD compensation, it was seen that despite the low dispersion slope associated with REACH fibres, TW-RS fibres had less transmission penalties and therefore performed better than TW-REACH fibre. This was due to the high dispersion effects affected by the signal over TW-REACH fibres. By compensating the CD in the TW-RS with an inverse dispersion TW-SRS fibre, the sensitivity for an error-free 52.1 km (26.6 km RS+25.5 km SRS) was seen to be -18.0 dBm as seen in figure 5.14 (a). The RS+SRS therefore incurred a 0.5 dB

penalty. The decrease in the penalty was due to the reduced 3.1 ps net dispersion. The 0.1 dB difference between REACH+SRS and RS+SRS transmission was due to the extra 2 km difference between the two aggregate transmission distances.

To further utilize the high optical power and compensation of chromatic dispersion to extend the distance of transmission of a 10 Gb/s signal without amplification, a 76.8 km fibre length was optimized and evaluated as shown in figure 5.14 (b). The sensitivity for an error-free 76.8 km transmission with CD compensated was -16.3 dBm. Therefore, with dispersion compensation, a 2.2 dB penalty was incurred for an unamplified 76.8 km 10 Gb/s data transmission over G.655 fibres.

5.3. Summary

Undistorted signal transmission to the end-user remains the primary role of the physical layer in point-to-point or point-to-multipoint networks. The QoS and QoT should always be maintained when a signal is transmitted for longer distances. This requires that the transmitters, fibres and receivers are all optimized for realization of better and end-to-end optical communication.

The next chapter provides an experimental and novel technique for achieving an all optical wavelength conversion and switching using VCSEL technology. This provides another advantage for utilising flexible spectrum rather than the fixed wavelength systems with expensive OEO conversion at the 1550 nm transmission window.

Chapter 6:

6.0 Wavelength Conversion and Switching in a Flexible Spectrum

One of the key elements of a flexible spectrum is the ability to dynamically assign transmission frequencies or wavelengths for efficient utilization of the spectrum and end-to-end connectivity. Denial of end-to-end connectivity and poor quality of signal transmission may occur as a result of attenuation, dispersion effects, fibre-cuts, channel collisions or unavailability of spectrum. This requires a cheaper and energy efficient technique that is purely optical that can convert and switch high-speed wavelengths within the low attenuation 1550 nm transmission window. Wavelength conversion does not only avoid channel collisions, but it also changes the path of signal transmission which implies that the signal can be switched or re-routed to a different path. This chapter presents for the first time to our knowledge, an all VCSEL-to-VCSEL optical wavelength conversion and transmission at the 1550 nm transmission window for high-speed optical NRZ modulated signals.

6.1. An all Optical Wavelength Conversion

A simpler, efficient and inexpensive technique to achieve wavelength conversion involves a purely optical technique that does not require optical-electrical-optical (OEO) conversion. A purely optical wavelength conversion integrates high speed optical devices to achieve high capacity and longer distance of transmission without causing deleterious signal distortion. Since most high speed long-haul transmission utilizes the low attenuation 1550 nm transmission window, the wavelength conversion technique should be flexible within the 1550 nm transmission wavelengths. Indeed, the central transmission frequencies in the flexible spectrum should also fit into the DWDM grid system for maximum utilization of the available spectrum. An all optical wavelength conversion presented in the following sections involves semiconductor lasers with the ability to convert and transmit a 10 Gb/s data signal at the 1550 nm transmission window.

6.1.1. An Experimental Demonstration of all Optical Wavelength Conversion using 1550 nm VCSELs

To achieve an all optical wavelength conversion, we for the first time using VCSELs provide an experimental demonstration as shown in figure 6.1. This wavelength conversion utilizes the low attenuation and low dispersion 1550 nm transmission window transmission that can be integrated with the Erbium-doped fibre amplifiers (EDFA) for high and distributed gains for all wavelengths in DWDM and long-haul transmission. The experimental demonstration used a purely optical mechanism with two 10 Gb/s 1550 nm window VCSEL sources to achieve wavelength conversion. The key element of the laser cavity used for conversion is its wavelength tunability and multi-mode lasing capability. The lasing (emission) wavelengths of both VCSELs were tunable with a tunability range of 5 nm by operating in the linear region of the bias current-output power characteristic as described in section 5.2 of chapter 5.

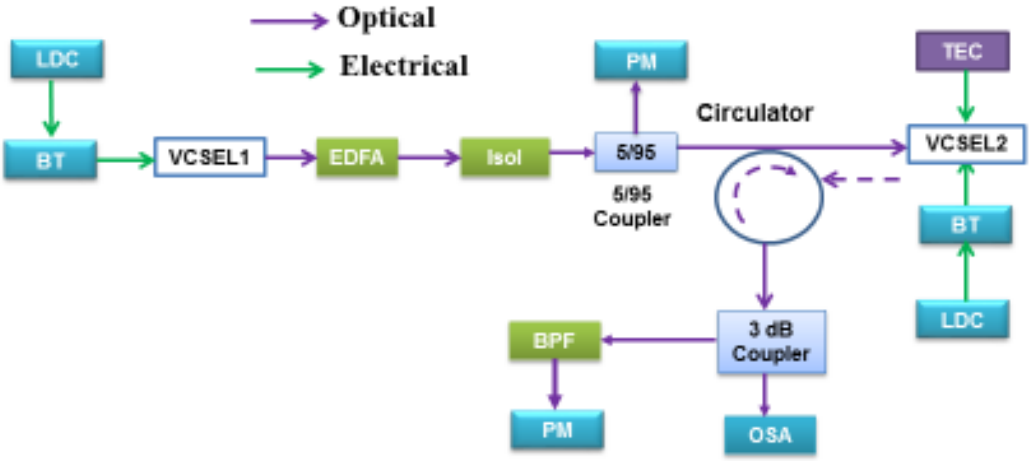

Figure 6.1: An experimental demonstration of purely optical wavelength conversion using two 10 Gb/s 1550 nm window VCSELs.

In the experimental set-up, VCSEL 1 was the incoming transmitting signal carrier referred to as a master laser, while VCSEL 2 provided an optical cavity for wavelength conversion. VCSEL 2 is referred to as the slave laser. The LDC's and TEC were used to vary the bias currents and to control the temperature of the VCSEL respectively. Both VCSELs were biased above their mid-point biasing levels with the temperature maintained at 25^0C. An EDFA was used to amplify the power of the incoming beam from the master VCSEL so as to obtain sufficient power for gain saturation of the cavity. Gain saturation of the cavity was important so as to stimulate and lase the side-mode of the slave laser cavity. An optical isolator (Isol) prevented both the backscattered and back-reflection of the injected

beam. This was performed to protect the EDFA from the backscattered power. A 5/95 optical coupler was used to monitor the injected power via the power meter (PM). Thereafter, an optical circulator directed the injected beam into and out of the cavity of the slave VCSEL and redirected the resultant light signal into the 3 dB optical coupler. The dominant mode of the slave VCSEL was thereafter filtered using a band-pass filter (BPF) in the form of a demultiplexer to measure and observe its extinction using the PM or an optical spectrum analyser (OSA). The output power and the optical spectrum of the dominant mode with increase in the incoming injection power were measured and analysed.

6.1.2. The lasing modes of a VCSEL

A VCSEL is basically a single-mode semiconductor laser with approximately 39 dB side-mode suppression ratio (SMSR) as discussed in chapter 5 and [125],[126]. As observed using an OSA, the dominant- and side-modes of the VCSEL are as shown in figure 6.2. The VCSEL was biased at 9.8 mA emitting a -2.9 dBm output power. By biasing the VCSEL at 9.8 mA, the dominant-mode was seen to be at 1552.1 nm and the side-mode at 1550.9 nm. This gave an inter-modal spacing of 1.1 nm or 137.5 GHz.

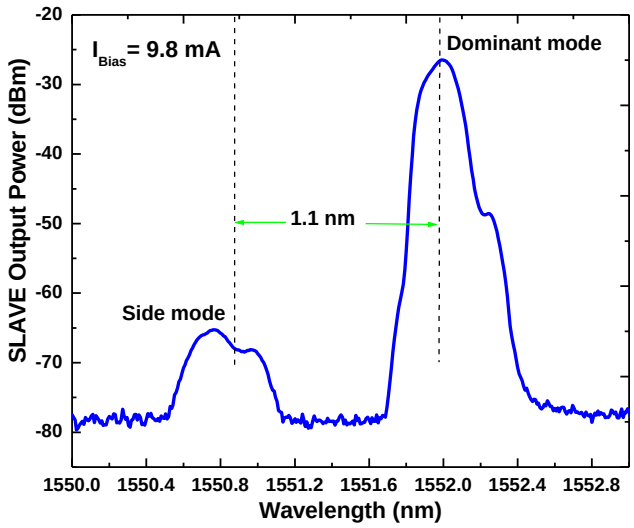

Figure 6.2: The side- and dominant modes of a VCSEL in the normal operation with 1.1 nm modal spacing.

It was important to determine the wavelengths of the side- and dominant-modes of the slave laser source since during wavelength conversion, an incoming light beam was to be injected into the side-mode of the slave VCSEL. Therefore, to convert a 1550.9 nm incoming wavelength, the side-mode of slave had to be tuned to match the wavelength of incoming beam. That is, both the incoming beam and side-mode of the slave VCSEL were to have 1550.9 nm wavelengths. The conversion process is demonstrated in the following sections.

6.2. Experimental Results Demonstrating Wavelength Conversion and Switching using VCSELs

To demonstrate wavelength conversion within the 1550 nm transmission window, a 1549.3 nm incoming master VCSEL and 1550.4 nm slave were used. The slave VCSEL was biased at 7.1 mA emitting a -5.2 dBm and the dominant- and side-modes were seen to be at 1550.4 nm and 1549.3 nm respectively as shown in figure 6.3(a). Injecting a 1549.3 nm incoming beam into a 1549.3 nm side-mode of the slave VCSEL optically locks the two wavelengths.

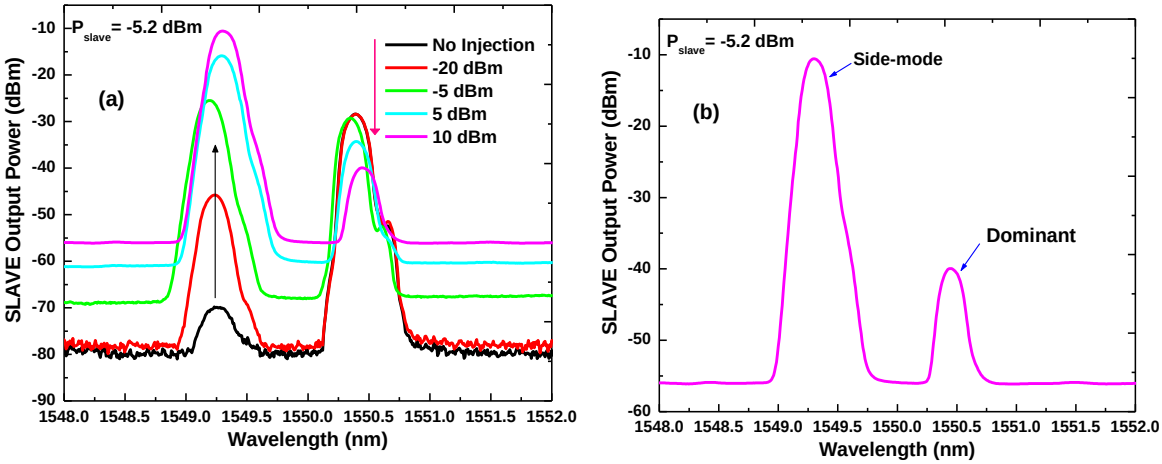

Figure 6.3: Optical spectrum from an OSA demonstrating (a) the lasing of the side-mode and the subsequent switching off of the dominant mode of slave VCSEL with increasing injected power and (b) The stimulation and lasing of the side-mode and extinction of the dominant mode of the slave at 10 dBm injection power.

The original side- and dominant modes of the slave (black-line) are as shown in figure 6.3 (a). Using the OSA, the SMSR was measured to be 41 dB. By injecting the side-mode of slave with -20 dBm and -5 dBm beams, the side-mode was stimulated and lased from -69.9 dBm to -45.7 dBm and -25.4 dBm respectively. This corresponded to 24.2 dB and 44.5 dB saturation gain. However, with a -5 dBm injection, the dominant mode was suppressed from -28.5 dBm to -29.5 dBm which represented a 1 dB extinction ratio (ER). A sufficiently high injection power of 10 dBm lased the side-mode to -10 dBm corresponding to 59.4 dB gain while suppressing the dominant mode from -28.5 dBm to -40.1 dBm with a 11.6 dB extinction ratio. The final spectrum of both the side- and dominant modes after a 10 dBm optical injection is as shown in figure 6.3 (b).

Switching off of the dominant mode and the calculated extinction ratio (ER) for different wavelengths and slave output power as measured using a PM is as shown in figures 6.4 (a)

and (b). The slave VCSEL emission wavelengths were tuned to 1550.4 nm using 7.1 mA bias with -5.2 dBm output power, 1550.8 nm using 7.5 mA bias with -4.5 dBm output power and 1551.6 nm using 8.9 mA bias with a -3.7 dBm output power. These wavelengths were used to convert 1549.3 nm, 1549.7 nm and 1550.5 nm incoming master wavelengths.

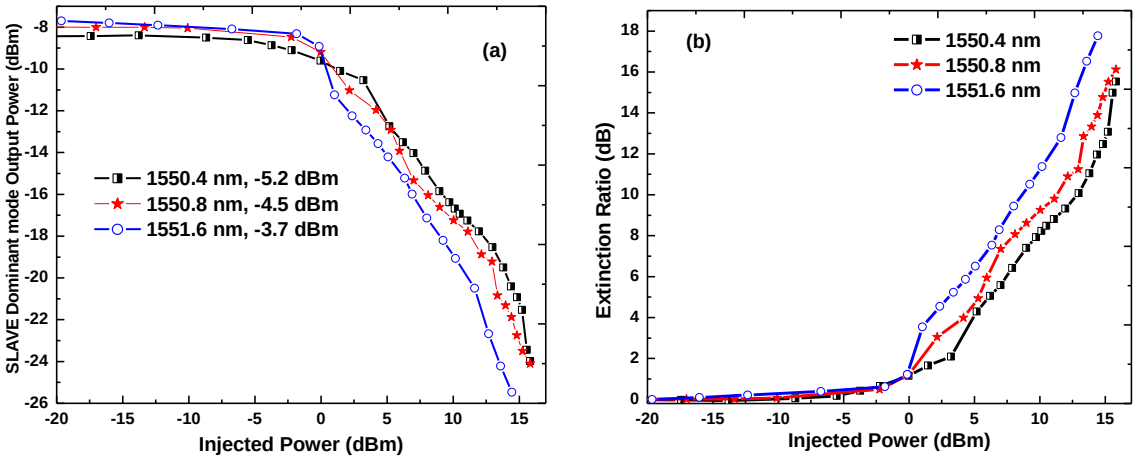

Figure 6.4: Wavelength conversion for 1550.4, 1550.8 and 1551.6 nm DWDM wavelengths using tunable VCSELs showing (a) the output power of the dominant mode of slave at different wavelengths and output power and (b) its extinction ratio with increase in injection power.

From figure 6.4 (a), the output power of the dominant modes of the three wavelengths reduced as the injection power was increased from -20 dBm to 15 dBm. For all the incoming wavelengths, the dominant modes were suppressed while lasing the side-modes when the injection power was increased. A significant reduction in the output power of the dominant mode was observed after an injection power of 0 dBm. This forms the threshold power level that resulted in gain saturation in the slave laser cavity and therefore resulting in wavelength conversion. A sufficiently high optical injection of 15 dBm reduced the dominant mode power from -8 dBm to average -24 dBm which corresponded to 16 dB ER.

The ER was calculated as the dominant-mode power difference without and with optical injection. An increase in ER as injection power was increased for the different converted wavelengths is shown in figure 6.4 (b). It is seen that injecting a 15 dBm beam into the side-mode of the slave lasers resulted in an average ER of 16 dB. In a real network scenario, the high injection powers are provided by the inbuilt amplifiers in optical switches and ROADMs that enable express signal transmission and wavelength conversion. For incoming DWDM signals, the high powers arise from EDFA amplification that enable both long distance transmission and wavelength conversion.

As previously shown in figure 6.3, the normal lasing of the VCSEL was switched from a low side-mode and a high dominant mode, to a high side- and low dominant modes due to the optical injection. This resulted in a temporary inverted VCSEL operation. In the normal operation, the dominant mode is a “HIGH” or a logical “1” while the side-mode is a “LOW” or logical “0”. But with sufficiently high injection, the dominant mode is a “LOW” or logical “0” and the side-mode is a “HIGH” or logical “1”. This results in data inversion when data was used to modulate the master VCSEL [125].

6.3. BER Measurements for Wavelength Conversion, Switching and Transmission Over Fibre

An experimental demonstration of converting a wavelength transmitting data using a VCSEL is shown in figure 6.5. The master VCSEL transmitting at 1550.4 nm with an output power of -3.7 dBm after 8.9 mA bias was modulated with 8.5 Gb/s NRZ PRBS pattern from a PPG. A -3.8 dBm 1551.5 nm slave VCSEL was used for conversion. The -3.8 dBm slave power enabled fibre transmission of the converted wavelength for longer distances (reach). For performance evaluation, the BER of a converted data signal was compared to the original B2B scenario and no transmission. The process of wavelength conversion was performed as described in section 6.2.

The master VCSEL at 1550.4 nm was modulated via a BT with 8.5 Gb/s NRZ PRBS (27-1) data (D) from a PPG. The power received by the PIN was varied using a VOA to emulate the typical losses in a transmission fibre-link. An EA was used to amplify the electrical signal coming from the PIN to meet the operational RF input power requirements of a BERT. After successful wavelength conversion, the transmitted data (D) from the master laser was compared to the received inverted data ($\overline{D}$) that was transmitted by the slave VCSEL at 1551.5 nm after conversion. The PIN receiver therefore detected a signal transmitted at a new wavelength 1551.5 nm. By combining an all optical wavelength conversion and using a BPF in the form of a wavelength demultiplexer, we were able to switch data from a 1550.4 nm to a new 1551.5 nm wavelength. As a result, for the first time, a purely VCSEL-to-VCSEL wavelength conversion and transmission was achieved within the 1550 nm transmission window. To analyse the quality of the received data signal, BER measurements were performed at 10^{-9} BER threshold level [125],[126].

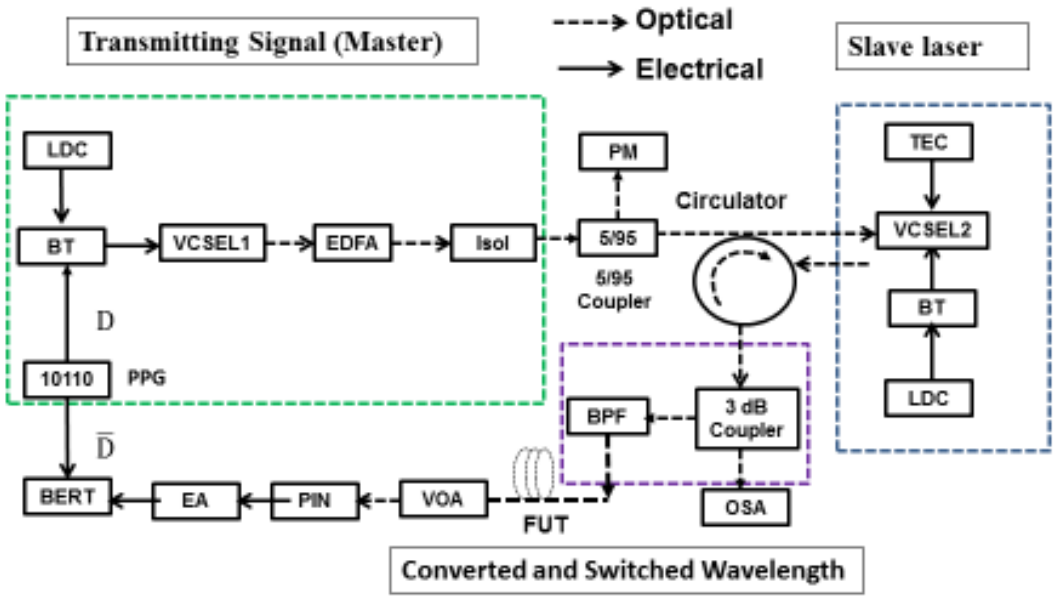

Figure 6.5: An experimental demonstration of an all VCSEL wavelength and data conversion and transmission over fibre. The incoming 1550.4 nm wavelength carries 8.5 Gb/s data. PPG is a programmable pattern generator, LDC is a laser diode controller, BT is a bias-tee, EDFA is an Erbium-doped fibre amplifier, Isol is an optical isolator, PM is a power meter, TEC is a thermoelectric controller, BPF is a bandpass filter, FUT is fibre under test, VOA is a variable optical attenuator, PIN is a positive intrinsic negative photodiode, EA is an electrical amplifier, OSA is an optical spectrum analyser and BERT is a bit-error rate tester.

To investigate transmission capability of the converted wavelength, the converted and switched signal wavelength was transmitted over G.652 and G.655 fibres (FUT). For the fibre-links used, the G.652 fibre had a 17 ps/(nm.km) dispersion co-efficient while the G.655 fibre had 5 ps/(nm.km) dispersion coefficient at 1550 nm. BER measurements were performed by comparing the original data from the master and data transmitted by the new converted and transmitted wavelength.

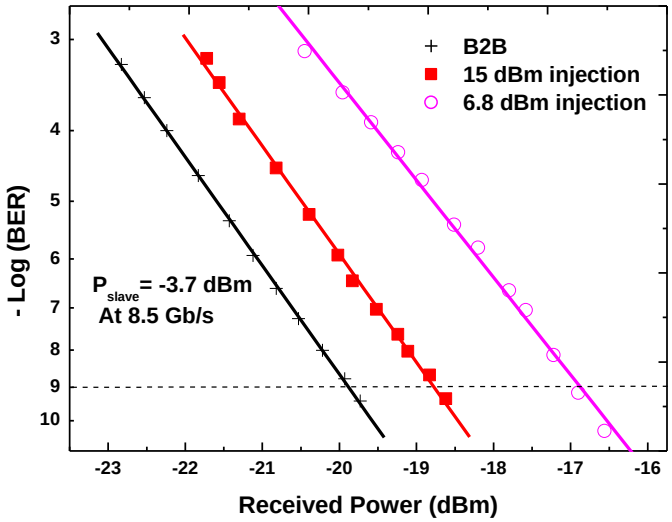

Figure 6.6: BER measurements of a data signal modulated at 8.5 Gb/s and the converted wavelength for varying injection powers. Original incoming data (B2B) from the master VCSEL and new converted signal with 6.8 dBm and 15 dBm injected power using a -3.7 dBm 1551. 5 nm slave VCSEL.

The BER measurements for converting an 8.5 Gb/s data signal by injecting the slave VCSEL cavity with increasing injection power of 6.8 dBm to 15 dBm is shown in figure 6.6. The BER for the original data from the master VCSEL was represented by the B2B. From figure 6.6, it was seen that a 6.8 dBm to 15 dBm injection power achieved an all error-free wavelength and data conversion. This error-free wavelength conversion was realized by the high extinction ratio that was obtained when the slave laser cavity was injected with a high injection beam. Indeed, a 6.8 dBm injection power produced an 8 dB ER while a 15 dBm achieved a 16 dB ER. The error-free receiver sensitivity for B2B was seen to be -19.9 dBm. After wavelength conversion with a 6.8 dBm injection power, the error-free receiver sensitivity for the inverted data was observed to be -17.0 dBm while a 15 dBm injection had a -18.8 dBm. This represented a 2.9 dB conversion penalty for a 6.8 dBm power and a 1.1 dB penalty for 15 dBm injection power. Indeed, the decrease in the receiver sensitivity was as a result of the low ER for low injection power as observed in the 6.8 dBm injection power. With low ER, the receiver strained to differentiate between the “1” and the “0” -bits. It was however noted that both receiver sensitivities for the two injection powers were within the typical PIN receiver sensitivity of ~ -18 dBm [124].

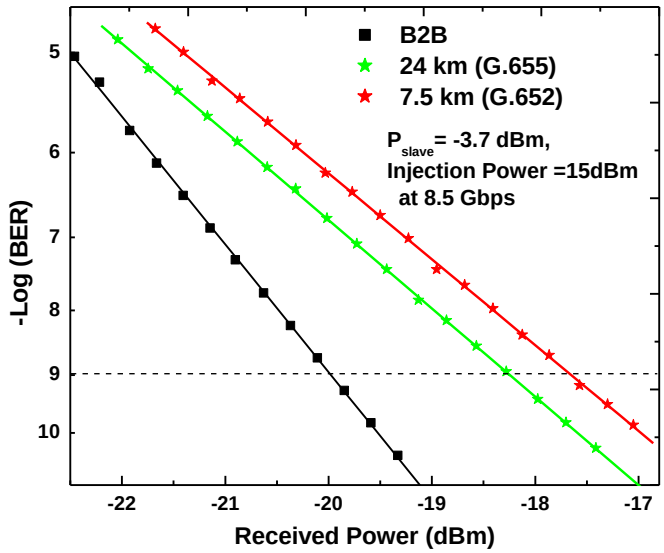

Figure 6.7: The experimental BER measurements for wavelength conversion and transmission of a 8.5 Gb/s signal over 7.5 km G.652 and 24 km G.655 fibres [125].

The transmission properties of the converted and switched wavelength are represented by the BER measurement curves in figure 6.7. In this conversion, a -3.7 dBm slave laser was injected with a 15 dBm beam. The converted wavelength was transmitted at 8.5 Gb/s over two types of fibres with varying dispersion properties. The error-free receiver sensitivity after conversion and transmission for 7.5 km over a G.652 fibre was seen to be at -17.6 dBm while a 24 km G.655 fibre was seen to be at -18.3 dBm. This translated to a 2.3 dB and 1.6 dB wavelength and transmission penalties over 7.5 km G.652 and 24 km G.655 fibres. The 2.3 dB penalty incurred in a G.652 fibre was due to the high dispersion coefficient (17 ps/(nm.km)) incurred by a 1550 nm transmission. The received error-bits were as a result of high dispersion effects resulting to data overlap. Since chromatic dispersion effects are minimized at 1550 nm transmission window in a G.655, few error-bits were received when the converted and switched data signal was transmitted over the 24 km G.655 fibre. The low dispersion coefficient (5.8 ps/(nm.km)) in a G.655 fibre resulted in less data overlap than a G.652 fibre transmission.

The residual (transmission only) penalties were measured to be 1.2 dB and 0.5 dB for the 7.5 km (G.652) and 24 km (G.655). As a result, a G.655 fibre gives a slightly better transmission performance than a G.652. This does not however, rule out the use of G.652 fibres in transmitting 10 Gb/s data signals at 1550 nm for longer distances since more sensitive receivers such as the APDs rather than the PIN can be used. The high sensitivity -28 dBm capability of the APD receiver makes it ideal for long-haul transmitted signals with low SNR that result due to attenuation and non-linear effects that are cumulative over the

length of transmission. The reach of the fibre can also be extended by compensating dispersion effects within the fibre.

6.4. Summary

This chapter has provided a novel experimental demonstration for achieving an all optical wavelength conversion and switching with fibre transmission at the 1550 nm low attenuation transmission window using the low power and tunable VCSELs. The side- and dominant- mode spacing of the used VCSELs in this experiment was measured to be 1.1 nm or 137.5 GHz. For the first time, BER measurements for wavelength conversion, inversion, switching and transmission of an 8.5 Gb/s data signal have been presented. Indeed, by using a 15 dBm injected power, a 16 dB extinction ratio (ER) of the dominant mode of a secondary slave laser providing wavelength conversion and switching has been successfully presented. The 16 dB ER provided both wavelength switching and transmission of an error-free signal for 24 km using a G.655 fibre with low chromatic dispersion at the 1550 nm transmission window despite a 1.6 dB conversion and transmission penalty. As a result of this wavelength conversion and switching technique as presented in this chapter, it is therefore capable to reconfigure a flexible optical network to minimize the probability of channel or wavelength collision. It also provides the re-use of the initial incoming wavelength in a DWDM network by assigning this available channel to a new channel for transmission. This has been realized by re-utilizing the 137.5 GHz spacing between the dominant mode of the slave VCSEL and the incoming master wavelength that was injected into the side-mode of the slave laser. Moreover, with VCSEL wavelength tunability, the central nominal frequencies of the flex-grid can be realized by adjusting the emission wavelengths of both the master and slave VCSELs. Finally, the 137.5 GHz spacing fits into the ITU-T flex-grid system for application in flexible spectrum [2].

The next chapter presents the design and performance evaluation of an optical add and drop multiplexer (OADM) implemented using a fibre Bragg grating (FBG) and a pair of optical circulators. We then discuss its suitability to wavelength management at the node of a flexible spectrum network made up of VCSEL transmitters.

Chapter 7:

7.0 Design of an Optical Add and Drop Multiplexer (OADM) for Flexible Spectrum Networks

In typical DWDM and flexible spectrum networks, wavelengths arriving at the end of transmission need to be received. A means of efficiently utilizing the spectrum is to re-use the wavelength or channel by assigning it to another user. This implies that after dropping a wavelength, another optical wavelength can be added into the available channel for transmission. This chapter reports an experimental design of a single wavelength optical add and drop multiplexer (OADM) using a pair of optical circulators and a single fibre Bragg grating (FBG). This study first demonstrates Bragg grating effect in an optical fibre using tunable laser source, a WDM laser source and a VCSEL and utilizing the wavelength that satisfies the Bragg condition to implement a wavelength-dedicated OADM. We emphasize on demonstrating our OADM using the directly modulated VCSELs transmission due to their numerous advantages discussed in chapters 3 and 5. The add and drop performance of our OADM to high-speed data signals are evaluated using BER measurements. Finally, 26 km fibre reach that is considered in this research is for considerations to metro-access distances and Gigabit passive optical network (GPON) scenario. At a network node, the OADM provides a means of channel management and efficient spectral usage in a flexible spectrum network.

7.1. Experimental Demonstration of Bragg Effect in an Optical Fibre Using Different Types of Lasers

In this study, Bragg grating effect was experimentally demonstrated by launching optical beams from different types of lasers into the fibre Bragg grating to determine the Bragg wavelength λ_B. An Agilent 81600B tunable laser source with a tunability range of 1494-1641 nm and a maximum output power of $6\,dBm$, a Thorlabs PRO8 DWDM (1550.12-1554.13 nm) DFB laser diode and VCSELs were used. The emission wavelengths from these lasers were directed into and from the FBG via an optical circulator 1. Thereafter, power of the transmitted and reflected light beams were measured using power meters (PMs) while varying either the emission wavelength and/or power of the laser as shown in figure 7.1.

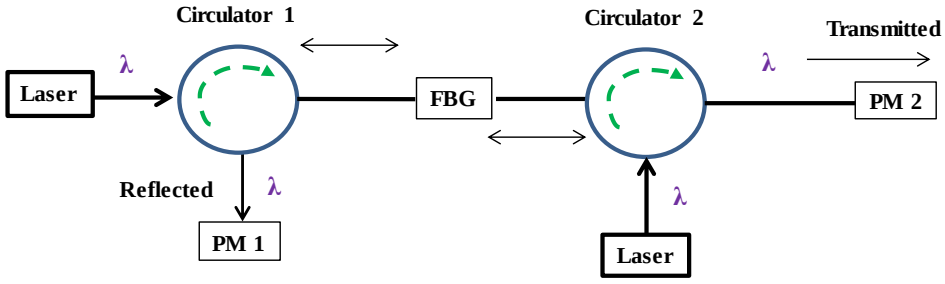

Figure 7.1: An experimental demonstration of Bragg grating effect using an optical laser, a circulator, a fibre Bragg grating (FBG) and optical power meters (PMs).

In the experimental, maximum reflection was observed at a wavelength that matched λ_B with the output power measured by PM 1, while transmitted wavelengths that did not satisfy Bragg grating condition were transmitted and power measured using PM 2. In s WDM implementation, at the Bragg wavelength, the incoming wavelength satisfying Bragg condition was therefore reflected back and eliminated from the incoming bundle of DWDM wavelengths, leaving an unused channel wavelength in transmission. To investigate the ability to insert a new signal, a second laser emitting a wavelength also satisfying λ_B was launched into the other side of the FBG via circulator 2 as shown in figure 7.1. The reflected and transmitted beams of new added wavelength were analysed by measuring their output power. Indeed, the ability of having reflected wavelengths on both ends of the FBG can be used to create an OADM.

The performance of different lasers that were used to demonstrate Bragg grating leading to the implementation of the OADM are shown in the following sections. The reflected and transmitted wavelength isolation ratios and wavelength tunability of the different lasers at the Bragg wavelength was emphasized to investigate the ideal laser for use in our OADM.

7.1.1. Fibre Bragg Grating Using a Tunable Laser (TL) Source

An Agilent 81600B tunable laser with a tunability range of 1494 nm to 1641 nm and a maximum output power of 6 dBm was used. The emission wavelength was varied from 1490 nm to 1550.7 nm and injected into the FBG as described in section 7.1, while maintaining constant powers of -5 dBm and 0 dBm. The output power for the transmitted and reflected beams were then measured and reported in figure 7.2 (a) and (b). By adjusting the wavelength of the input beam, the refractive index of the FBG changed and therefore made the signal to resonate within the period of the FBG cavity. For both input powers, it was seen that the reflected wavelength was maximum at 1549.9 nm with minimum transmitted power. This implied that at 1549.9 nm, the emission wavelength matched the λ_B

of the FBG and was therefore reflected while the other wavelengths were transmitted. The reflected and transmitted wavelength isolation ratio at the Bragg wavelength was measured to be 28 dB. As seen in figure 7.2 (a) and (b), all the incoming wavelengths in a broadband spectrum were transmitted while a wavelength satisfying the Bragg condition was reflected.

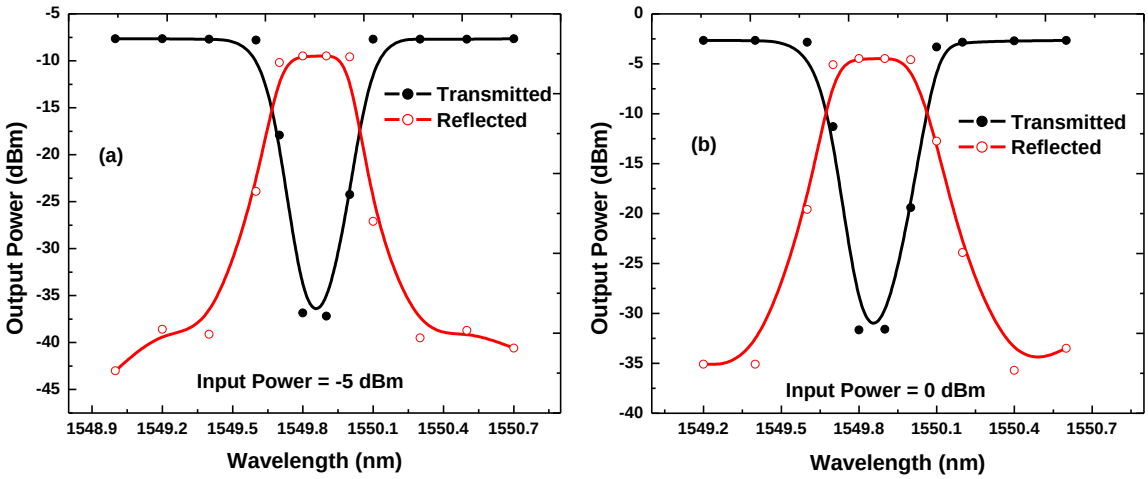

Figure 7.2: Experimental demonstration of reflected and transmitted wavelengths for; reflected (red) and transmitted (black) power as a function of wavelength at (a) -5 dBm and (b) 0 dBm laser output power using tunable laser source.

The increase in output power for both reflected and transmitted wavelengths at the Bragg wavelength with increase in injected power is shown in figure 7.3 (a) and (b). The FBG was injected with a 1549.9 nm optical beam while the laser output power was increased from -10 dBm to 6 dBm.

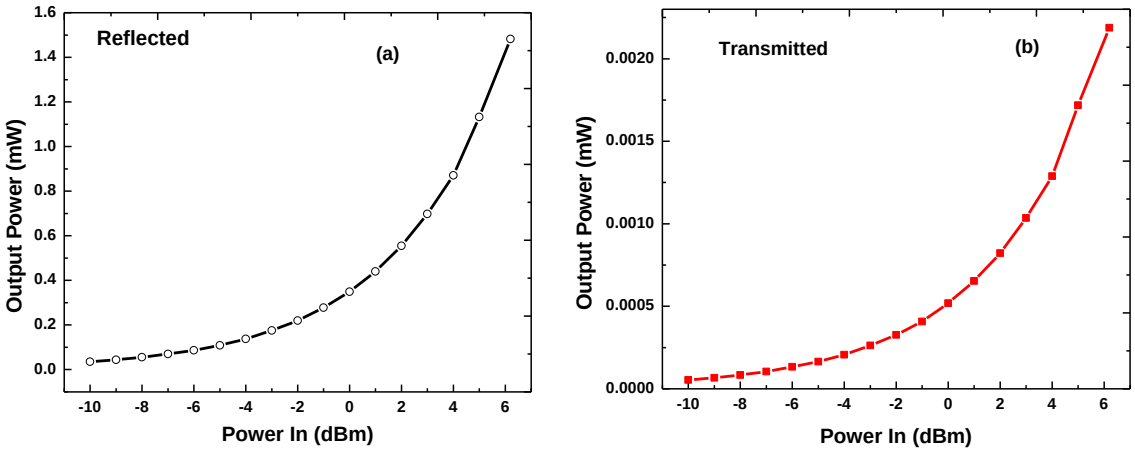

Figure 7.3: The output power of a FBG for reflected (a) and transmitted (b) at the Bragg wavelength with increasing input power.

At 1549.9 nm, the 28 dB power difference between the reflected and transmitted wavelength was also measured. This implied that the FBG reflects a 1549.9 nm wavelength

while transmitting all the other wavelengths. As a result, at the 1549.9 nm, the FBG acted as an in-line optical filter combined with a wavelength-specific reflector.

7.1.2. Demonstration of Fibre Bragg Grating Using a Thorlabs DWDM Laser Sources

The output power-wavelength spectrum from a FBG using a Thorlabs DWDM DFB laser source demonstrated a 18 dB wavelength isolation ratio at the Bragg wavelength (1549.9 nm) as seen in figure 7.4. The WDM laser source emitted a 3 dBm optical beam with 8 modules emitting wavelengths at 1549.32 nm to 1554.94 nm range.

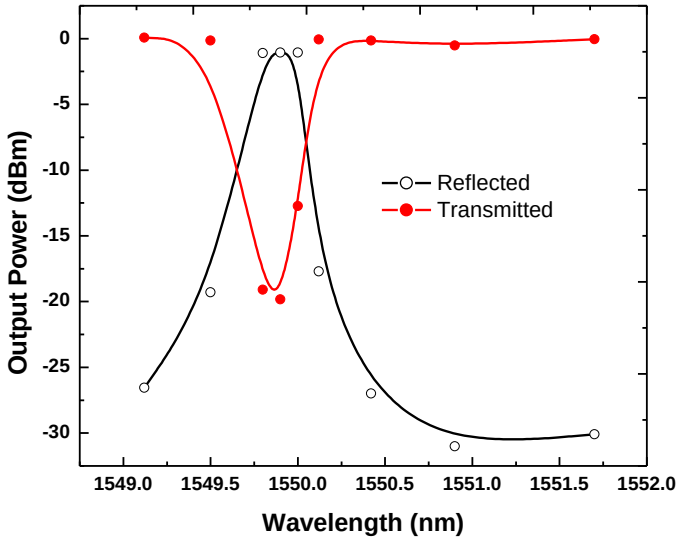

Figure 7.4: Experimental demonstration of Wavelength transmission and reflection using a fibre Bragg grating at the 1550 nm transmission wavelength and window using DWDM DFB lasers.

The output power for the reflected wavelength at 1549.9 nm was -0.9 dBm while the transmitted power was -18.9 dBm. However, the low 18 dB peak power difference was as a result of the multiple side-modes associated with the DFB lasers. It was noted that at the Bragg wavelength, DFB lasers had lower isolation ratios than the tunable laser source. This resulted in the transmission of the side-modes at the Bragg wavelength.

7.1.3. Experimental Demonstration of Fibre Bragg Grating Using VCSELs

By utilizing VCSEL wavelength tunability and its high SMSR, we were also able to experimentally demonstrate Bragg grating condition as shown in figure 7.5. By increasing the bias current above the threshold level (above 1 mA), not only did the optical power increase but also the emission wavelengths varied as illustrated. It was seen that the reflected

and transmitted beams were at 1549.9 nm as previously demonstrated by the DFB lasers in sections 7.1.1 and 7.1.2. Indeed, the 1549.9 nm Bragg wavelength was realized by changing the bias current of the VCSEL to 5.7 mA.

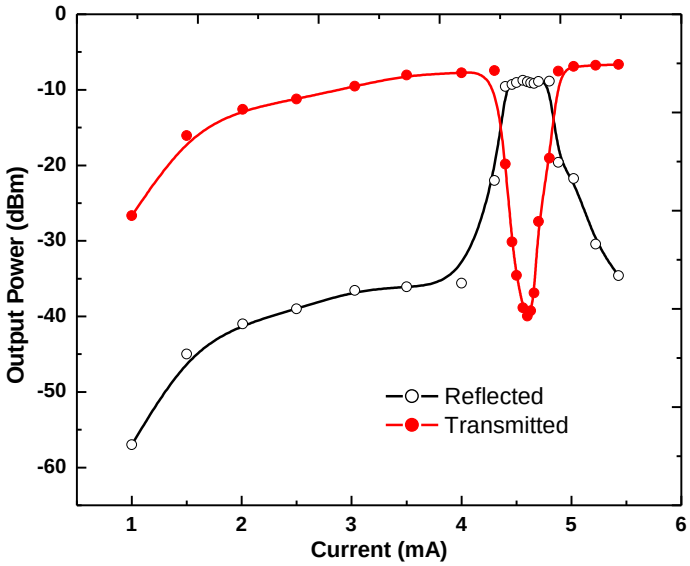

Figure 7.5: An experimental demonstrating of Bragg grating condition at 1549.9 nm using a 10 Gb/s VCSEL laser.

The difference in the output power for both transmitted and reflected beams was as a result of the output power varying with the bias current. At 1549.9 nm, the reflected and transmitted wavelength isolation ratio was 31.4 dB which was higher than the isolation ratio realized in both the tunable and DFB laser sources. This was attributed to the smaller linewidth (0.2 nm at -20 dB full width) and the high SMSR of the VCSEL used. As observed in figure 7.5, all the incoming wavelengths in a broadband spectrum are transmitted while only the wavelength satisfying the Bragg condition is reflected and hence dropped. This makes a VCSEL ideal for use in our OADM.

Since all the three transmitters (TL, DWDM DFB and VCSEL) showed slightly high wavelength isolation ratio, the reflected beam of the incoming bundle of wavelengths satisfying the Bragg condition can be filtered from the multiplexed wavelengths. Likewise, the available wavelength slot can be re-used by adding another signal transmitted by the same wavelength that was dropped by utilizing the other side of the FBG in figure 7.1. We can therefore design a high-speed purely optical add and drop multiplexer (OADM) based on a FBG and a pair of optical circulators that operates at 1549.9 nm. The following sections provide experimental implementation of the OADM and performance evaluation using BER measurements at the telecommunication acceptable 10^{-9} BER threshold.

7.2. Experimental Implementation of an OADM Using Fibre Bragg Grating Effect

To demonstrate the ability to drop and add new wavelengths satisfying Bragg wavelength λ_B, an experimental set-up as shown in figure 7.6 was implemented. An incoming 1549.9 nm wavelength from VCSEL 1 carrying 8.5 Gb/s PRBS data pattern *(D)* from a PPG was launched into a passive optical circulator 1. The optical circulator directed and redirected the reflected light beam to and from the FBG to represent the dropped signal, as shown in figure 7.6.

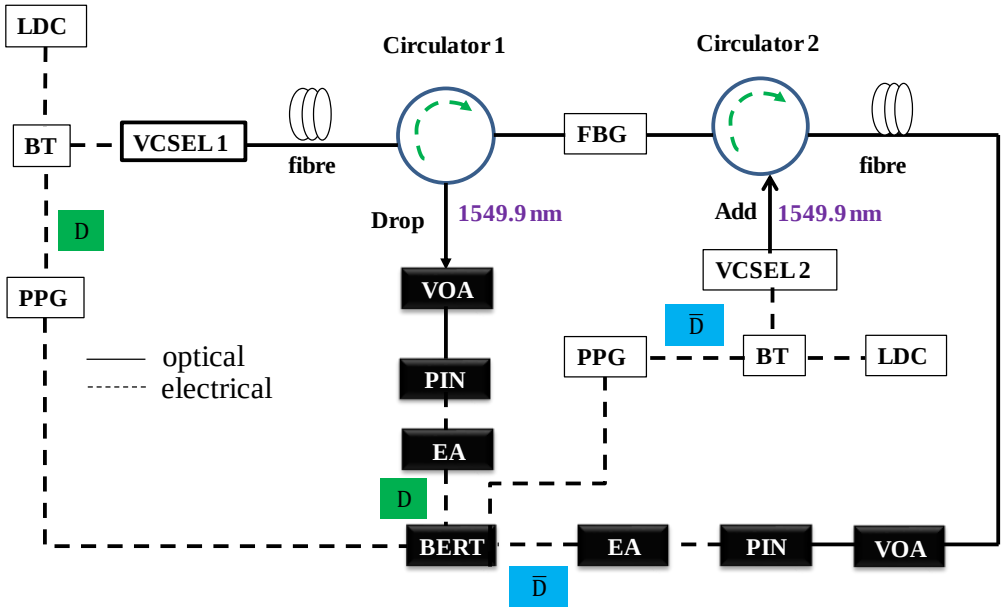

Figure 7.6: Experimental implementation of the add and drop multiplexing using fibre Bragg grating (FBG) and a pair of optical circulators and two VCSEL transmitters. VCSEL 1 carries the dropped signal wavelength while VCSEL 2 carries a new added data signal.

The received/ dropped 1549.9 nm signal was then compared to the original signal (B2B without OADM) and analysed by performing BER measurements using BERT. Moreover, to demonstrate wavelength res-use, a second 1549.9 nm VCSEL 2 was modulated with 8.5 Gb/s PRBS ($\overline{D}$) data pattern and launched (added) into the other side of the FBG by using another optical circulator 2. The reflected wavelength was then redirected by the circulator into the fibre and the received signal with ($\overline{D}$) data evaluated by BER measurements. In this study, a PIN photo-receiver was used to convert the optical signal to electrical signal.

The set-up in figure 7.6 demonstrated both the drop and add properties of an OADM that enabled wavelength re-use and therefore increase spectrum efficiency in a high-speed optical link. Indeed, spectrum efficiency was increased by re-assigning the available channel to a new user by adding a new data signal as shown by the implementation of VCSEL 2 signal carrier.

7.3. Experimental Performance Evaluation of Optical Add and Drop Multiplexing (OADM) Using BER Measurement

In evaluating the quality of the signal in an OADM system, BER measurements were performed on the drop and the add configuration of the FBG. The experimental results of the incoming 8.5 Gb/s signal from the 1549.9 nm VCSEL 1 to be dropped at one end of the FBG is shown in figure 7.7. Indeed, the original data from the PPG is represented by the B2B while the dropped signal is represented by the DROP. The receiver sensitivity for an error-free wavelength drop was seen to be -17.6 dBm and -17.3 dBm respectively. The 0.3 dB penalty was as a result of the high speed signals that affected the Bragg grating period and increased optical resonations at the Bragg wavelength.

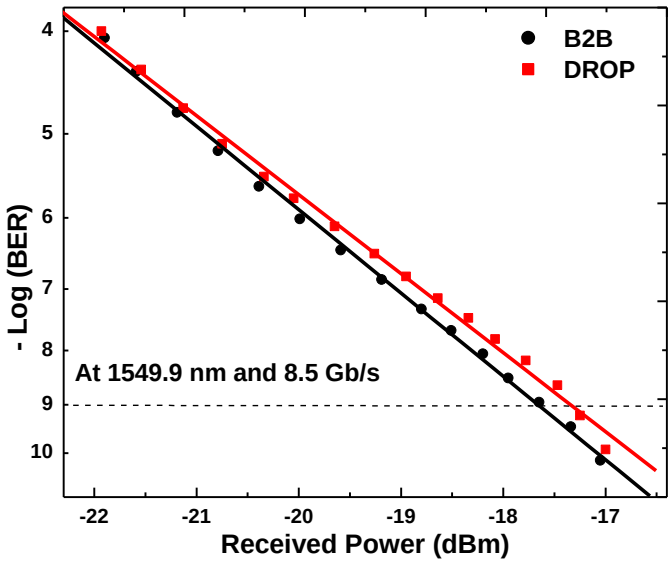

Figure 7.7: BER evaluation for B2B and drop wavelength of 8.5 Gb/s data signal using a VCSEL data carrier at 1549.9 nm without transmission.

From figure 7.7, by using a VCSEL, we were able to successfully drop a 8.5 Gb/s signal with a 0.3 dB power penalty. This penalty was less than the insertion losses for the drop channel in the industry [95], [127], [94]. The low penalty could also be attributed to the high

31.4 dB wavelength isolation ratio that was realized using VCSELs in the Bragg grating demonstration.

To demonstrate the add and drop performance of the OADM, two VCSELs both emitting a 1549.9 nm wavelength were used to transmit 8.5 Gb/s data signals from the PPG as shown in figure 7.6. Both VCSELs carried different forms of data with VCSEL 2 transmitting an exact inverse data of $\overline{D}$ decorrelated using different lengths of RF cables to provide varying delay times. This was performed to ensure that with perfect reflection and high isolation ratio at the 1549.9 nm wavelength, the FBG created a real OADM and therefore less error-bits were received as a result of interferences from the other modulated signals. The BER measurements were performed at the 10^{-9} threshold and the experimental results of the QoS shown in figure 7.8.

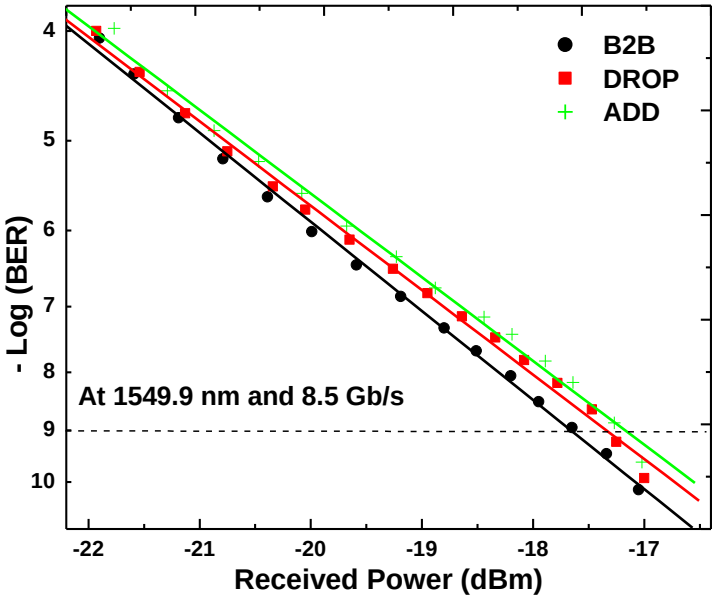

Figure 7.8: BER performance evaluation of an OADM illustrating the B2B, dropped and added signals without transmission.

The error-free receiver sensitivities were seen to be -17.6 dBm, -17.3 dBm and -17.2 dBm for the B2B, drop and add ports respectively. This represented insertion loss of 0.3 dB and 0.4 dB for the drop and add multiplexing respectively.

7.4. Performance Evaluation of OADM with High Speed Signal Transmission

When a signal is transmitted from the source to the destination, the channel is dropped to the end-user once the end-to-end communication link has been established. In a multi-node optical fibre links, several wavelengths hopping between nodes provide an end-to-end link.

Once a signal arrives at the destination, it is dropped to the receiver and the available channel assigned to a new user. In this study, high-speed data signals were transmitted over fibre and the OADM was used as a node as shown in figure 7.6.

The incoming 8.5 Gb/s data signal at 1549.9 nm was transmitted over 26.6 km NZDSF G.655 fibre with -2.8 ps/(nm.km) dispersion coefficient. The signal was then dropped and its BER measurement performed to evaluate QoS, QoT and performance of the drop port of an OADM. As seen from figure 7.9 (a), the sensitivity of an error-free original data signal (B2B) was -17.6 dBm while the dropped B2B signal without transmission was -17.3 dBm. An express channel without using an OADM after a 26.6 km fibre transmission had a sensitivity of -16.9 dBm while a dropped received signal had a -16.5 dBm. The total receiver penalty was 1.1 dB was due to the insertion loss and dispersion effects as a result of the fibre that introduced error-bits.

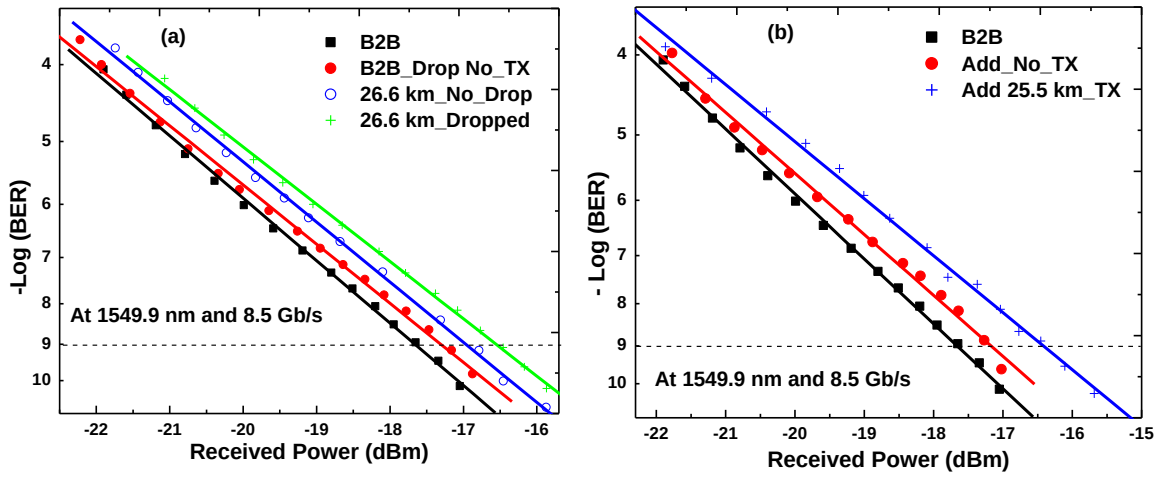

Figure 7.9: The experimental BER measurements illustrating the evaluation of the performance of an OADM created using 1549.9 nm VCSELs and a FBG. A 8.5 Gb/s data signal was transmitted over 26.6 km G.655 fibre (a) drop demultiplexing and (b) add multiplexing.

To evaluate the performance of the add multiplexing of the OADM, an inverse 8.5 Gb/s data signal from the PPG was modulated into VCSEL 2 as shown in figure 7.6. Both VCSEL 1 and VCSEL 2 were connected into the FBG to demonstrate a simultaneous experimental operation of the OADM. The error-free receiver sensitivity of the B2B was -17.5 dBm while the add port was seen to be -17.2 dBm. This resulted in a 0.3 dB add channel insertion power penalty. When the added was transmitted over a 25.5 km G.655 fibre, the error-free sensitivity was -16.4 dBm. Indeed, the 25.5 km G.655 fibre that was used to transmit the added data signal had a -2.8 ps/(nm.km) dispersion coefficient.

Consequently, a dispersion and power penalty of 1.1 dB as a result of the add multiplexing and data signal transmission over the fibre.

7.5. Summary

We have successfully designed and implemented a single 1549.9 nm OADM using a FBG using three tunable laser transmitters namely; TL, DWDM DFB and VCSELs. To demonstrate the performance of the OADM, high-speed 8.5 Gb/s data signals were modulated into 1549.9 nm VCSELs and transmitted over fibre. The data signals were then linked by an optical node created by the add and drop multiplexing of the passive OADM and transmitted over two fibre links. The 31.4 dB wavelength isolation ration of the FBG when a VCSEL was used and the 0.3 dB power penalty due to the insertion losses of the add and drop ports of the OADM makes the OADM ideal for reconfiguring an optical node. As a result, by taking the high-speed transmission capabilities of the VCSEL and the purely passive OADM that was designed, an optical node can be reconfigured by assigning and reassigning designated user wavelengths so as to improve spectrum utilization and efficiency.

The next chapter describes experimental quantification of optical impairments degrading the quality of a transmitted signal over an optical fibre. Linear and non-linear effects such as crosstalk, chromatic dispersion and polarization effects and techniques of minimizing them are discussed.

Chapter 8:

8.0 Signal Impairments and Solutions in Flexible Spectrum Networks

For high-speed fibre transmission, an optical fibre is often regarded as the most perfect medium with almost limitless bandwidth for guided transmission. However, in practice, fibre capacity is affected by several limitations such as signal impairments. As the signal transmission is extended to higher bitrates, the linear effects mainly attenuation, adjacent inter-channel crosstalk, chromatic dispersion, polarization mode dispersion (PMD) and accumulated amplified spontaneous noise (ASE) becomes detrimental to the quality of signal (QoS) and the quality of transmission (QoT). In high capacity long-haul and dense wavelength division multiplexed (DWDM) systems, non-linear effects resulting from the change in the refractive index of the fibre due to high intensity becomes the major limiting factor. These effects include stimulated Raman scattering (SRS) and stimulated Brillouin scattering (SBS), four-wave mixing (FWM), self-phase modulation (SPM) and cross-phase modulation (XPM).

The success of high-speed optical fibre transmissions therefore depends on how well these linear and non-linear effects are managed. For DWDM and flexible spectrum systems, several adjacent wavelengths are closely spaced to increase fibre capacity. However, if not properly filtered, these adjacent channels may interfere with each other resulting in crosstalk. In practice, old fibre links are often integrated with new fibres that are deployed in a typical network. Old fibre-links often have higher attenuation and higher PMD coefficients. Moreover, both aerial and cabled fibre deployments are also available for signal transmission and would therefore require network optimization. However, the concatenation of old fibres and fibre deployment schemes, aerial and cabled transmission might have varying PMD, attenuation profiles and dispersion properties. This chapter introduces and characterizes the effects of inter-channel crosstalk, dispersion and PMD effects on an optical fibre link carrying data signal. Several types of fibre links and deployments have been considered to achieve an optimized and high-speed signal transmission experiencing minimum signal impairments. It also provides techniques and solutions of minimizing and compensating these effects.

8.1. Inter-channel Crosstalk

Adjacent channel interaction or crosstalk is a common phenomenon in most communication systems [13]. Crosstalk does not only affect adjacent channels, but a single channel can also experience inter-symbol interference (ISI) [20]. In DWDM optical fibre systems, inter-channel crosstalk significantly limits the fibre capacity, QoS and QoT for closely spaced channels. For closely spaced channels, crosstalk results in channel and data overlap in the frequency domain. Indeed, crosstalk depends on a number of parameters such as bit-rate, channel spacing, signal optical power, length of the fibre and filtering properties of the multiplexers and demultiplexers [91]. As a result, fibre networks are therefore often optimized to achieve a trade-off between channel spacing and to operate within a minimum acceptable crosstalk penalty.

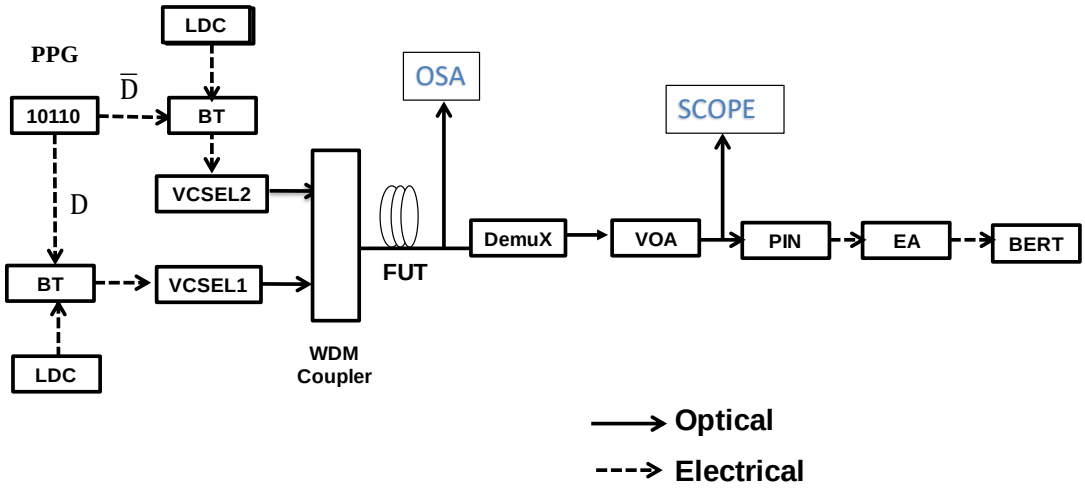

Figure 8.1: Is an experimental set up for inter channel crosstalk involving two wavelengths λ_1 and λ_2 from 1550 nm VCSELs coupled together using a passive optical coupler and transmitted over fibre under test (FUT) and separated by a demultiplexer (DEMUX). Programmable pattern generator (PPG), Bias tee (BT), Laser diode controller (LDC), Variable optical attenuator (VOA), positive intrinsic negative (PIN), electric amplifier (EA) and bit error rate tester (BERT).

In this study, an experimental demonstration of inter-channel crosstalk involving two adjacent channels is shown in figure 8.1. Two 10 Gb/s VCSELs lasing at 1550 nm with a wavelength tunability range of 5 nm were used to demonstrate inter-channel crosstalk. VCSEL 1 was considered as the main signal carrier while VCSEL 2 was regarded as the interfering channel. In this study, due to the low output power of the VCSEL, crosstalk effects arising from non-linear effects were not considered. The wavelength λ_1 for channel 1

was therefore fixed while the adjacent channel wavelength λ_2 was varied to achieve a channel spacing of 0.4 nm to 1.2 nm which represented 50 GHz to 150 GHz spacing.

A non-filter based WDM coupler was used to combine the two individual channels so as to enable inter-band and inter-spectrum interaction. The combined wavelengths were then transmitted over a fibre link under test (FUT). At the receiver-end, the spectrum for each of the two channels before and after filtering were observed using an OSA. The observed spectra for the individual wavelengths and the combined spectrum at a 0.42 nm spacing is shown in figure 8.2 (a) and (b) respectively.

To study the effects of inter-channel crosstalk on modulated signals, the two VCSELs were directly modulated with 10 Gb/s NRZ PRBS-7 (2^7-1) opposite data patterns from a PPG as shown in figure 8.1. Data patterns were decorrelated using different lengths of RF cables to introduce random time delays. Once the signal channel had been demultiplexed using a filter-based demultiplexer (DEMUX), the transmitted data was then analyzed using the received pattern sequence, eye-diagrams and BER measurements on an oscilloscope and a BERT respectively. A PIN photodiode was used at the receiver while the EA was used to amplify the converted electrical signal to the operational requirements of the BERT. BER measurements were performed at the 10^{-9} acceptable threshold level with the inter-channel crosstalk effects reported in figures 8.4-8.7.

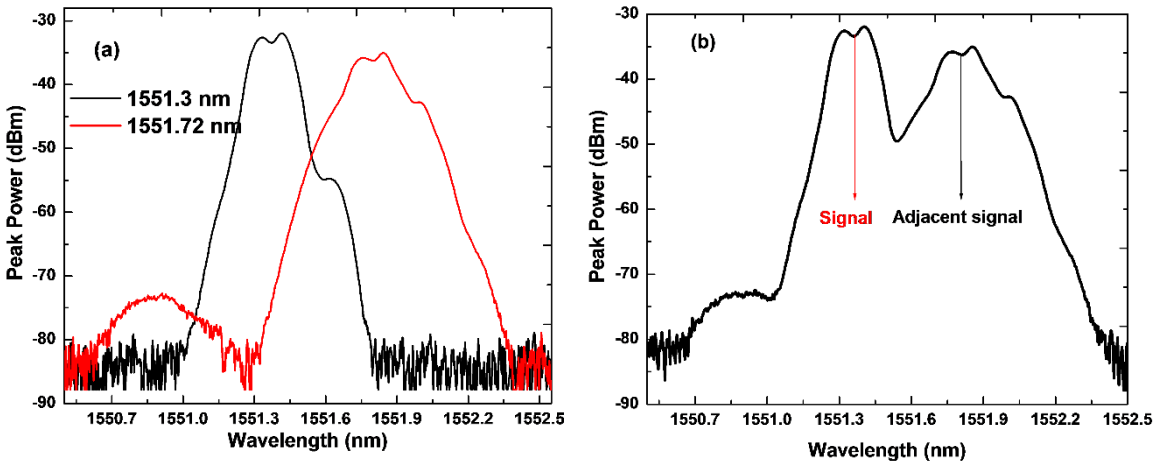

Figure 8.2: (a) The optical spectrum of two channels from two 10 Gb/s VCSEL 1551.37 nm and 1551.79 nm spaced at 0.42 nm or 50 GHz spacing (b) resultant spectrum of the two wavelengths.

The spectrum of the two signals at 1551.3 nm and 1551.72 nm with a 0.42 nm channel spacing are shown in figure 8.2 (a). It was seen that the signal channels had distinct spectra before coupling them together into the fibre. The resultant spectrum comprising of the two

channels is shown in figure 8.2 (b). With the 0.42 nm channel spacing, the two channels interacted resulting in a band-overlap at the 1550.5 nm point.

The 10 Gb/s NRZ PRBS data patterns that were used to modulate the channels 1 and 2 are shown in figure 8.3 (a) and (b) respectively. To investigate the detrimental effect of an adjacent channel on a signal, the interfering channel was over-modulated to create an error data signal represented by the overshoots contained in the NRZ pattern as seen in figure 8.3 (b). In this study, a 50 GHz filter-based DEMUX was used to separate the two wavelengths.

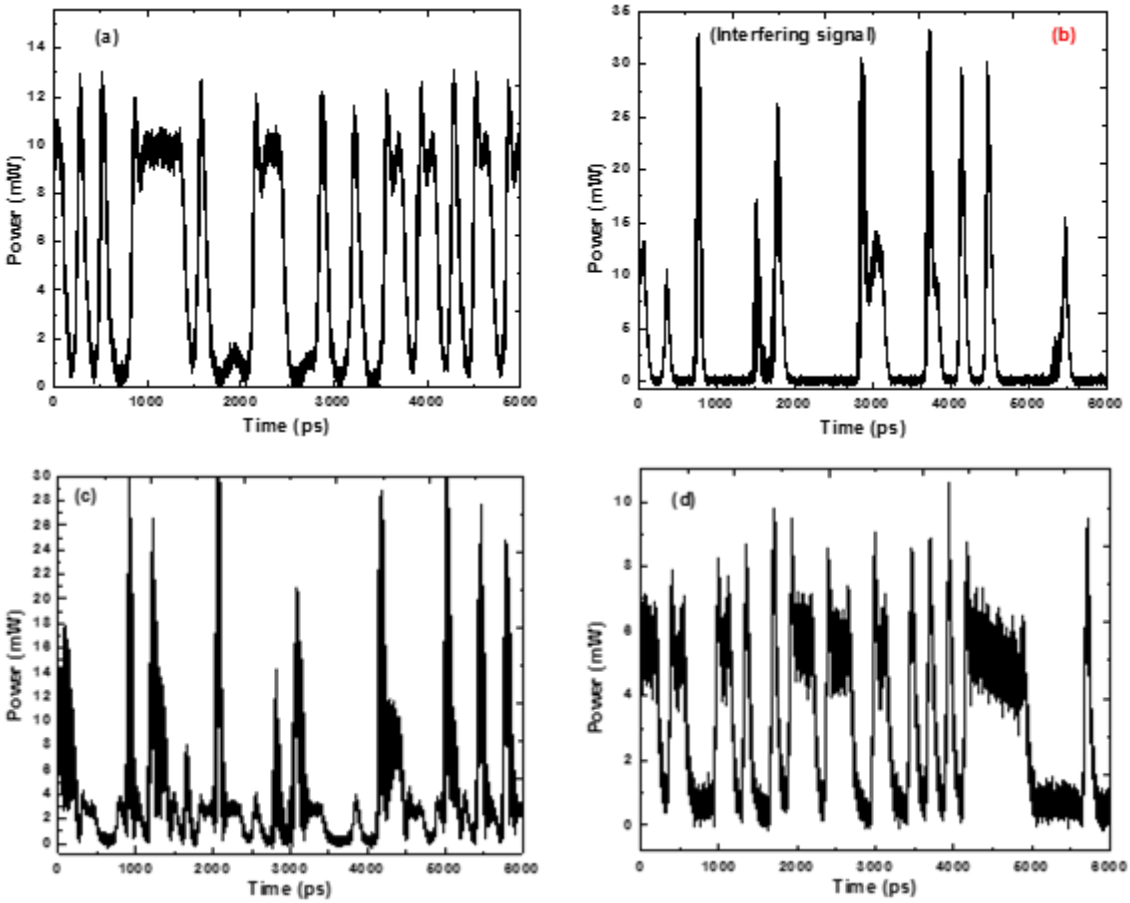

Figure 8.3: The NRZ PRBS (2^7-1) pattern sequence in a modulated VCSEL (a) Main signal, (b) adjacent interfering channel, (c) Combination of the received distorted signal without using a filter and (d) the received random bit sequence of the main signal after using a 50 GHz filter-based demultiplexer to separate the wavelengths.

The resultant sequence of the unfiltered inter-channel interaction is shown in figure 8.3 (c). The received PRBS patterns have overlapped and superimposed patterns that results in error-bits as detected by the receiver. The PIN receiver is therefore “blinded” by

the high intensity which makes it difficult for the receiver to distinguish the "1" from the "0" bits in the PRBS. The received random pattern after filtering is shown in figure 8.3 (d).

The eye-diagram for the 10 Gb/s data signal λ_1 without an adjacent interfering signal (B2B) as measured at -17.6 dBm is shown in figure 8.4 (a) while the resultant after coupling with a 50 GHz spaced channel is illustrated in figure 8.4 (b). From the wide and open eye-diagrams, it can be seen that both received signals are error-free. However, the slight eye-closure seen in figure 8.4 (b) was due to signal crosstalk resulting in error-bits received close to the BERT decision level of the eye-diagram [80].

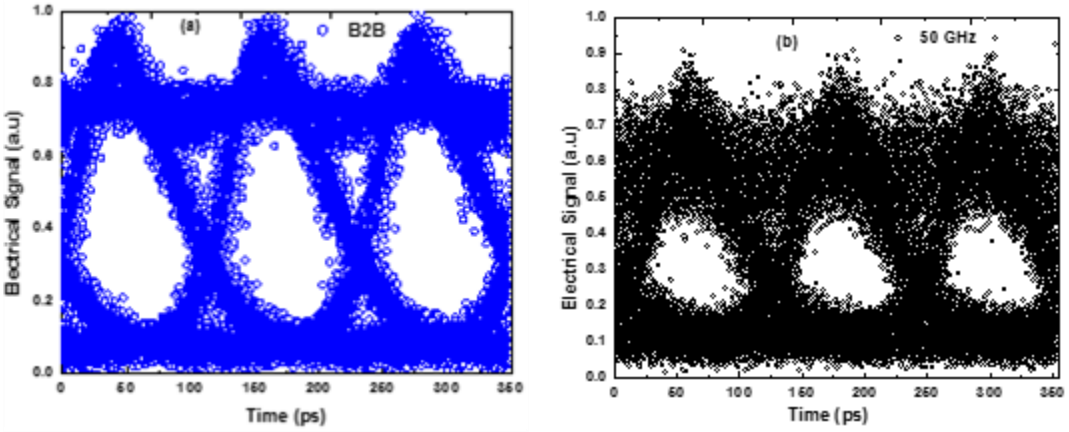

Figure 8.4: (a)The B2B signal without an interfering channel and (b) with a 50 GHz spaced adjacent signal and filtering as measured at -17.6 dBm optical power.

The BER measurements for different channel spacing are shown in figure 8.5. By increasing the bias current, VCSEL 1 was tuned to 1550.5 nm with -4.3 dBm output power while the center wavelength for VCSEL 2 was varied from 1550.9 nm to 1551.7 nm providing 0.4 nm (50 GHz) to 1.2 nm (150 GHz) channel spacing. From the BER measurements in figure 8.5 (a), it was seen that closer wavelengths introduced more errors as compared to widely spaced channels.

From figure 8.5 (a), a B2B without an interfering channel had an error-free receiver sensitivity of -19.4 dBm, while adding a 50 GHz and 150 GHz spaced adjacent channels resulted to a -17.8 dBm and -19.3 dBm sensitivities. It was seen that closer channels strained the receiver by requiring additional power to distinguish the received bits. As a result, the more power (penalty) required to distinguish the received bits as a result of the overlap and interference increased with a decrease in channel spacing as shown in figure 8.5 (a). Crosstalk was as a result of inter-symbol interference from the linear optical interaction of the two coupled signals. The closely spaced channels therefore experienced bit-overlap and

as a result, error-bits from the interfering signal were received on the main signal. A 50 GHz spacing incurred a 1.6 dB penalty whereas a 150 GHz had a 0.1 dB penalty.

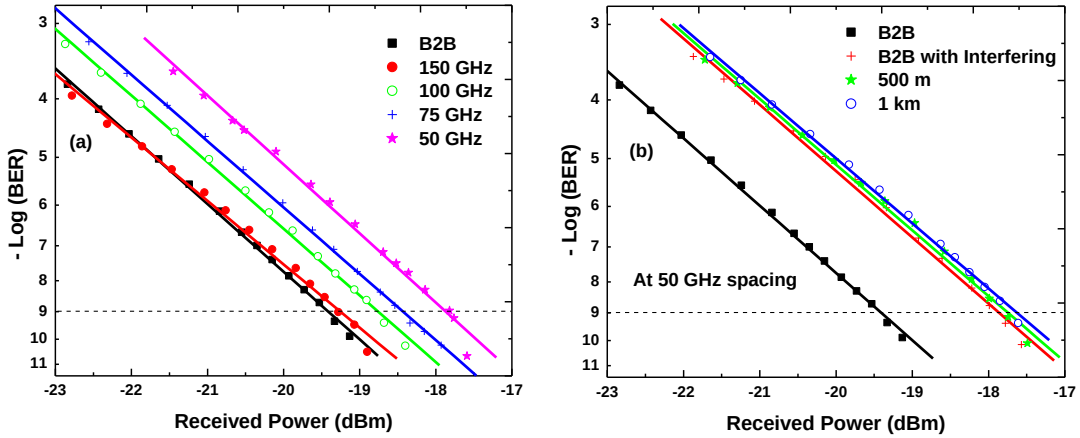

Figure 8.5: (a) Experimental BER measurements of crosstalk for channels spaced at 50 GHz to 150 GHz and (b) effects of length of fibre on adjacent 50 GHz spaced channels over G.652 fibre with 17 ps/(nm.km) dispersion.

By transmitting the two coupled data signals over a G.652 SMF with 17 ps/(nm.km) dispersion coefficient at the 1550 nm transmission window, the transmission distances of the 10 Gb/s signals were limited by crosstalk and dispersion effects. As shown in figure 8.5 (b), the receiver sensitivity for an error-free signal was seen to reduce with the increase in the length from 500 m to 1 km. The distance was limited to an error-free 1 km due to the high dispersion effects over the G.652 fibre. Indeed, the sensitivity reduced from -19.4 dBm to -17.6 dBm for a 1 km fibre transmission. The received error-bits were as a result of the accumulated dispersion effects over the fibre-link. As a result, a 1.8 dB crosstalk and dispersion penalty was incurred.

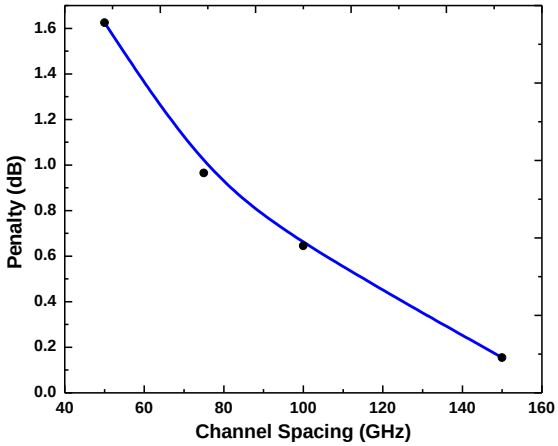

Figure 8.6: The crosstalk penalty for different channel spacing 50-150 GHz using VCSEL transmitters.

Since inter-channel crosstalk resulted in bit-errors, the crosstalk penalty reduced with increase in channel spacing 50 GHz to 150 GHz as shown in figure 8.6. Indeed, the penalty reduced from 1.6 dB to 0.1 dB when the channels spacing was increased from 50 GHz to 100 GHz. The maximum crosstalk penalty is within the maximum acceptable crosstalk penalty (2.5 dB) for 10 Gb/s multi-channel transmissions over G.652 fibres [128].

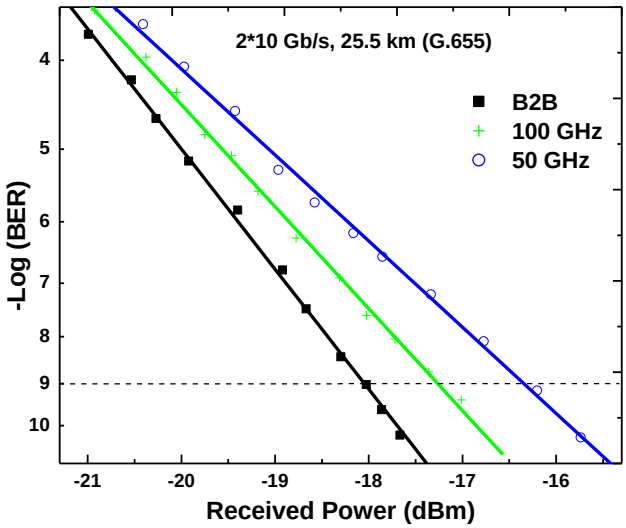

Figure 8.7: Experimental BER curves for $2 \times 10\ Gb/s$ DWDM channels multiplexed at 50 GHz and 100 GHz channel spacing and transmitted over 25.5 km G.655 fibre.

To reduce the effects of inter-channel crosstalk, the individual 10 Gb/s channels λ_1 and λ_2 were experimentally multiplexed using array waveguide grating (AWG) multiplexers instead of the passive 3 dB couplers. The AWG multiplexers offer high channel isolation ratio and are wavelength selective.

In increasing the transmission reach, the two 1550 nm signals were transmitted in a low attenuation and dispersion 25.5 km G.655 fibre. Maximum transmission reach was attained with less crosstalk and dispersion penalties due to the channel isolation provided by the multiplexer. From figure 8.7, the receiver sensitivity for an error-free signal without interfering or adjacent channel (B2B) was seen to -18.1 dBm. By introducing a 100 GHz spaced adjacent channel, the sensitivity of the main signal reduced to -17.2 dBm resulting in a 0.9 dB penalty. The 50 GHz spaced adjacent signal introduced errors to the main signal thus reducing the sensitivity to -16.3 dBm. As a result, a 1.8 dB penalty was incurred which was due to dispersion, crosstalk and the increased fibre capacity. It is therefore conclusive that using filter-based multiplexers and demultiplexers reduced the probability of the two wavelengths interfering and it increased the reach and capacity of the fibre with less crosstalk penalties.

8.1.1. Effect of Channel Spacing on Flexible Channels

A simulation to study the effects of inter-channel crosstalk on flexible spectrum channels was done. A two channel 20 Gb/s transmission was simulated using a VPI Photonics simulation tool [129] as shown in figure 8.8. Two 1550 nm tunable laser sources modulated using a 20 Gb/s NRZ PRBS (2^7-1) were multiplexed and coupled onto the fibre. The signal and interfering channels at varying spacing of Δf = 25-100 GHz were multiplexed using a WDM multiplexer into the fibre. The average power for the two channels was kept constant at 0 dBm, transmitted over a 12 km G.655 fibre and then separated using a narrow bandwidth demultiplexer. A variable optical attenuator (att) was used to attenuate the signal power getting to the receiver, thereby emulating the typical losses in a transmission fibre link. A power meter (PM) was used to measure and record the attenuated power while the oscilloscope (SCOPE) was used to observe the pattern sequence and eye-diagrams of the signal. An on-off keying (OOK) direct detection receiver was used to determine and analyse BER using a numerical analyser (NA).

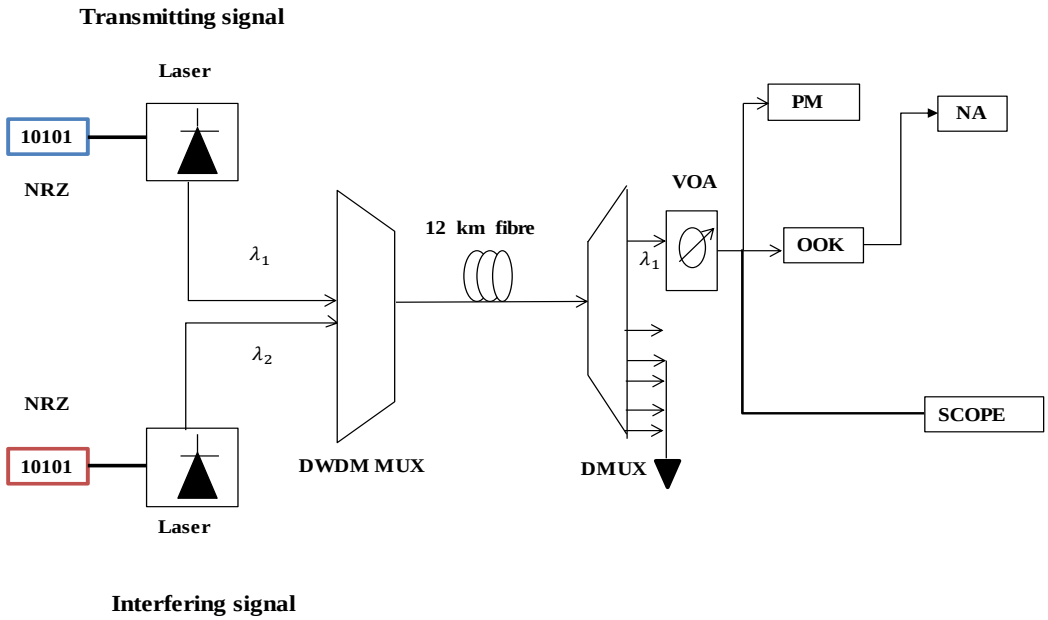

Figure 8.8: A VPI simulation of crosstalk in flexible spectrum channels with 12.5 GHz granularity for 25-100 GHz spaced channels [130] using on-off keying (OOK) direct receiver and a numerical analyser (NA) for BER quantification. Laser transmission window is 1550 nm.

The flexible channel spacing (Δf) between the signal and interfering channels was set at 25 GHz, 37.5 GHz, 50 GHz and 100 GHz to analyse the effects of inter-channel crosstalk. The centre frequency for the first channel (λ_1) was 193.1 THz while the centre frequency of the adjacent interfering channels was set to 193.1 THz+ Δf. The effect of inter-channel crosstalk and the penalty incurred in the fibre is shown in figure 8.9 (a) and (b).

For a signal without an interfering channel, the error-free receiver sensitivity at the 10^{-9} threshold level was seen to be -22.0 dBm. Introduction of an adjacent channel at different spacing causes crosstalk and therefore data errors. The error-free sensitivity for 25 GHz and 100 GHz spaced channels were seen to be -17.6 dBm and -21.9 dBm respectively. This resulted in a 0.1 dB to 4.4 dB crosstalk penalty for the 25-100 GHz spaced channels that were transmitted for 12 km in a G.655 fibre.

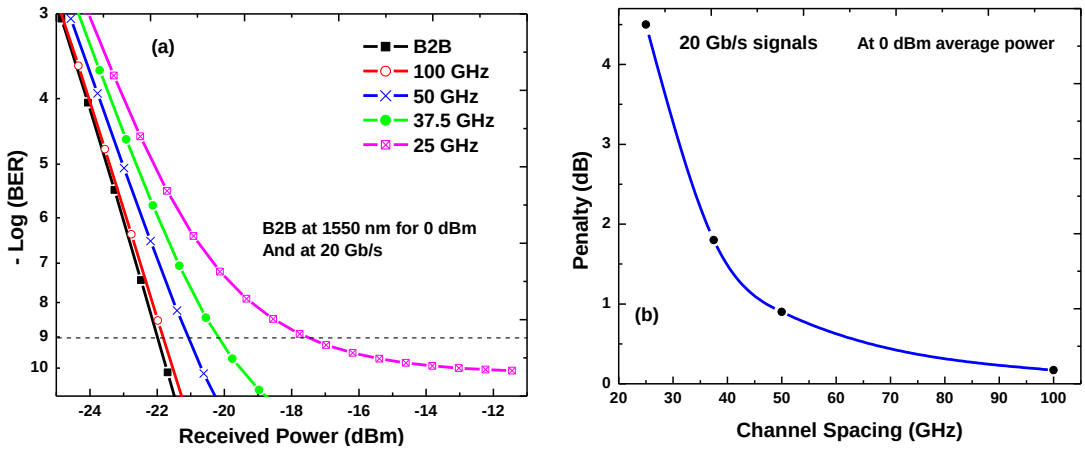

Figure 8.9: (a) Theoretical BER measurements for 25-100 GHz spaced channels at 20 Gb/s over 12 km G.655 fibre and (b) reduction in crosstalk penalty with increasing channel spacing.

Despite, the high optical signal power, the transmission distance was limited by the high 20 Gb/s transmission rate and crosstalk. The reduction in crosstalk penalty with an increase in the channel spacing as obtained from figure 8.9 (a) is shown in figure 8.9 (b) [130]. The results are from flexible spectrum channels with arbitrary spacing (25, 37.5, 50 and 100 GHz) comprised of slot sizes with 12.5 GHz granularity.

8.1.2. High Signal Power Inter-channel Interference

Figure 8.10 shows the BER simulation results for two 20 Gb/s flexible signals spaced at 37.5 GHz with different optical powers. For this study, the transmitting signal had a 10 dBm power while the interfering signal had a power range of 0 dBm to 25 dBm. Both signals were multiplexed, transmitted over 12 km G.655 fibre and demultiplexed as shown in figure 8.8. The BER measurements were taken at the 10^{-9} threshold level.

The receiver sensitivity for the B2B was seen to be -21.0 dBm as seen in figure 8.10. By introducing an adjacent channel spaced at 37.5 GHz and with an optical power of 0 dBm, the receiver sensitivity for an error-free transmitting signal was reduced to -20.6 dBm. By introducing a high power 25 dBm interfering signal, the transmission attained an error-floor. At the error-floor, the receiver could not therefore distinguish between the received "1"s and the "0"s at the telecommunication acceptable BER threshold level (10^{-9}). The high power signals introduced non-linear effects especially FWM and XPM in the fibre that resulted in more signal distortions thereby resulting in received data errors [92].

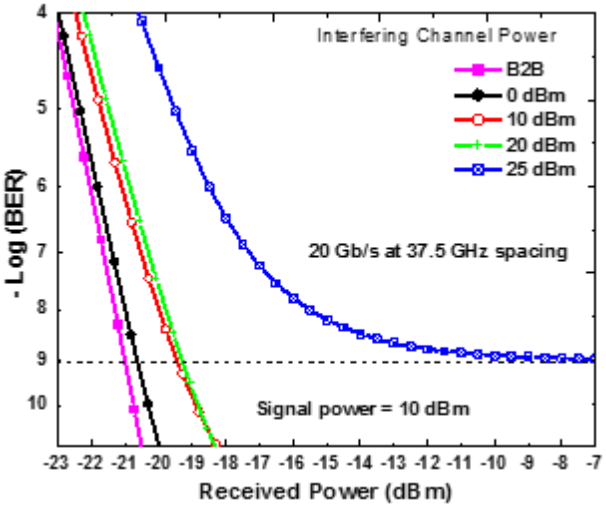

Figure 8.10: BER measurements for increasing interfering signal power at 37.5 GHz spaced 20 Gb/s channels. Transmitting signal at 10 dBm while adjacent interfering signal power increased from 0-25 dBm. Error floor attained for 25 dBm interfering signal.

To minimize crosstalk effects and penalties, channels should be separated with wide channel spacing. It is however not spectrally efficient to increase the channel spacing at the expense of reducing the number of channels that can be allocated within a bandwidth. Moreover, since crosstalk effects are affected by the signal and fibre-link properties such as fibre-length, bitrate, fibre-type, channel spacing and optical signal power, a trade-off should therefore be decided between these parameters and the optimized spectrum efficiency, capacity and maintenance of QoS and QoT [130].

8.2. Chromatic Dispersion

The increase in demand for bandwidth and longer fibre reach have forced network service providers to frequently upgrade their existing networks so as to transmit higher bit rates and fibre capacity. Therefore, to provide efficient, reliable and scalable bandwidth that meets every user's demand, the providers must verify the infrastructure of fibre deployment by checking on link attenuation, continuity, chromatic dispersion and PMD in the fibre link. This section characterizes the performances of different types of fibres with each fibre having unique dispersion coefficients, dispersion slope, attenuation and PMD. These dispersion properties depend on the wavelength of transmission and the fibre over which the signal is transmitted as discussed in section 3.2.2. The standard SMF fibres include; the non-dispersion shifted fibre (NDSF G.652) and non-zero dispersion shifted fibre

(NZDSF G.655). In this study, data is transmitted at 10 Gb/s through these fibres with the data signal being affected by different amounts of dispersion, attenuation, losses and PMD.

The optical pulse broadening results from the finite spectral linewidth of the optical source and the modulated carrier [84] as discussed in chapter 3. In this study, table 8.1 shows the dispersion coefficients, dispersion slopes and PMD coefficients for the different types of SMF fibres found at the NMMU Centre for Broadband Communication.

Table 8.1: Chromatic dispersion (CD) and PMD properties of G.652 and G.655 fibres used for fibre link optimization.

Type of Fibre	Dispersion Coefficient [(ps/(nm.km)] at		Dispersion slope $[(\mathrm{ps}/(\mathrm{nm}^2.\mathrm{km})]$	PMD coefficient (ps/√km)
	1310 nm	1550 nm		
G.652: NDSF	0	17	0.07	0.2
G.655: TW RS	-8.9	2.8	≤ 0.05	≤ 0.04
G.655: TW SRS	-8	-2.8	< 0.045	< 0.025
G.655: REACH	-5.3	5.5	≤ 0.045	≤ 0.04

Apart from the low attenuation and dispersion slopes, the G.655 fibres have non-zero dispersion so as to eliminate the effects of FWM occurring within the fibre [82], [89], [90]. In particular, a TrueWave reduced slope (TW-RS) fibre had a +2.8 ps/(nm.km) dispersion while the TrueWave submarine reduced slope (TW-SRS) had a -2.8 ps/(nm.km) dispersion [90]. The tolerable dispersion in TW-RS and TW-SRS minimises FWM and enable long-reach, DWDM and submarine transmission. The TW REACH fibre has a low attenuation at the 1450 nm Raman pump wavelength making it suitable for long reach Raman amplified and DWDM systems with enhanced low attenuation at the low water peak enabling 1310 nm to 1625 nm transmission [82].

In investigating dispersion effects, unmanaged dispersion transmissions were performed. A 1550.4 nm signal was transmitted over a G.652 fibre with a 17 ps/(nm.km) and a 1306 nm transmission over a G.655 fibre with a -5 ps/(nm.km) dispersion coefficients. The BER measurements for the two transmissions are shown in figure 8.11 (a) and (b). For a 1550.4 nm transmission, the error-free receiver sensitivity for a B2B was seen to be -18.2 dBm and the sensitivity for a maximum 12 km transmission over a G.652 fibre was -15.5 dBm as seen in figure 8.11 (a). This resulted in a 2.7 dB dispersion penalty when a 1550.4 nm signal was transmitted over a high dispersion G.652 fibre. The 12 km

transmission distance was limited by the high dispersion resulting in error-bits as experienced by a 1550 nm signal in a G.652 fibre transmission.

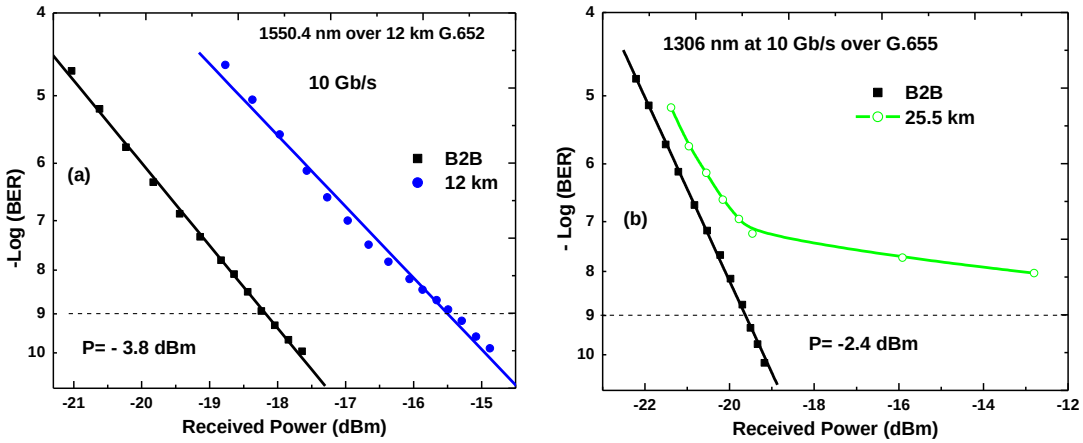

Figure 8.11: Experimental demonstration of unmanaged chromatic dispersion using BER performance of 10 Gb/s signals over (a) G.652 fibre at 1550.4 nm and (b) Error-floor over 25.5 km G.655 at 1306 nm VCSEL transmission.

Considering a 1306 nm transmission over a G.655 fibre, the BER curve attained an error-floor as shown in figure 8.11 (b). The error-bits were as a result of the high dispersion and attenuation experienced by the 1306 nm over the 25.5 km G.655 fibre. In a fibre with positive dispersion, shorter wavelengths travel faster than longer wavelengths which travel faster than shorter wavelengths in negative dispersion fibres [131]. A 1306 nm transmission therefore experienced a high negative dispersion when transmitted over a G.655 fibre and therefore travelled slower than in a G.652 transmission.

8.2.1. Optimized Transmission of flexible channels over Different Fibre Types

To achieve optimized signal transmission of flexible channels, the network links were first optimized to minimize and compensate dispersion affecting the QoS and QoT. In this study, different fibres were used to optimize data signals transmitted at 1310 nm and 1550 nm transmission windows. Indeed, 1310 nm and 1550 nm VCSELs were modulated with 10 Gb/s NRZ data sequence and transmitted over fibres, as illustrated in table 8.1 to represent signal transmission in the most commonly used 1310 and 1550 nm transmission windows. The fibre links used are 6-18 km G.652, 25.5 km G.655 SRS fibre, 26.6 km G.655 RS and over 25.3 km G.655 TW-REACH fibres.

Since a signal transmitted at 1306 nm over a G.652 experiences zero dispersion, a 10 Gb/s data signal was then transmitted in a dispersion managed and optimized fibre for

6 km to 18 km as shown in figure 8.12 (a). The sensitivity for the B2B error-free 10 Gb/s signal was seen to be -19.6 dBm. By transmitting the signal over a 6 km link, the receiver error-free sensitivity was -19.3 dBm while 18 km had a -18.5 dBm. As a result, power penalty range of 0.3 dB to 1.1 dB was incurred for up to 18 km 10 Gb/s transmission over G.652 fibres. An error-floor was attained when the signal was transmitted over 24 km. As a result, dispersion and attenuation profiles of the G.652 limited a 10 Gb/s signal to a maximum of 18 km for an error-free transmission.

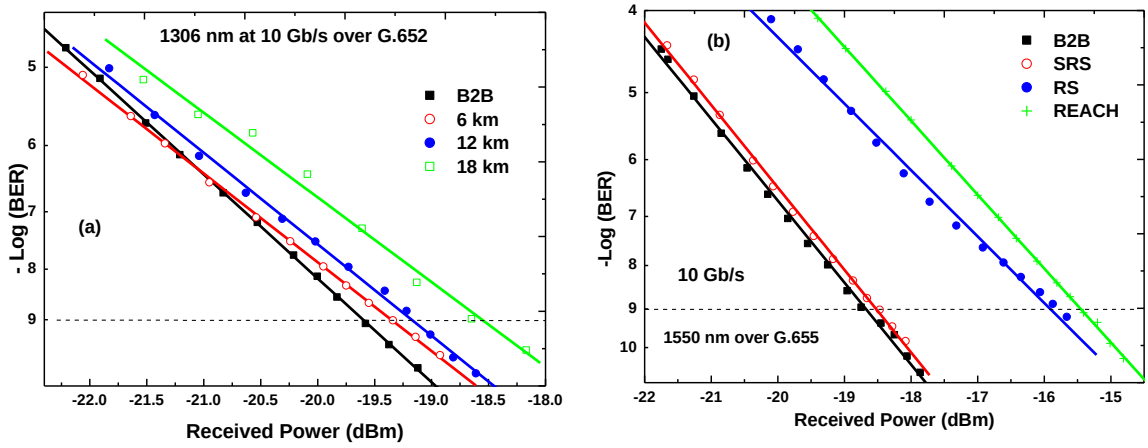

Figure 8.12: Dispersion managed 10 Gb/s VCSEL transmission (a) 1306 nm over 6-18 km G.652 and (b) 1550.4 nm over 25 km G.655 fibres.

Due to the low attenuation at the 1550 nm transmission window, data signal performance was also optimized for G.655 fibres. The BER curves for the different G.655 fibres with varying dispersion slopes and coefficients is shown in figure 8.12 (b). The average transmission distances for the three fibres was 25 km with a B2B receiver sensitivity was -18.7 dBm. An error-free sensitivity for SRS, RS and REACH fibres were seen to be -18.5 dBm, -15.9 dBm and -15.5 dBm. As a result, 0.2 dB, 2.8 dB and 3.2 dB penalties were incurred as dispersion and transmission penalties for SRS, RS and REACH fibres respectively. RS and REACH fibres have higher positive dispersion coefficients and therefore the signal experienced much broadening and error-bits than over SRS fibre.

As seen in figures 8.12 (a) and (b), dispersion management of high speed data transmission can be realized by using fibres with low dispersion properties at the 1310 nm and 1550 nm transmission windows. By minimizing the dispersion effects, longer transmission distances can therefore be attained.

8.2.2. Mitigation of Chromatic Dispersion

In increasing the distance of transmission for passive optical networks (PONs), the cumulative dispersion effects that inhibit data signal transmission can be compensated either in the physical or software domains. In the hardware and software domains, chromatic dispersion can be compensated by performing digital signal processing (DSP) of the received signal in coherent receivers [43]. In this study, instead of using the more complex DSP schemes in dispersion compensation, we eliminate the cumulative dispersion effects by combining fibres with positive dispersion and negative dispersion fibres. This technique not only increases the distance of transmission but also eliminates dispersion effects which become detrimental to bits of data in optical fibre transmission. As a result, the overall fibre reach is extended while reducing dispersion penalties.

In our experimental dispersion compensation scheme, we utilize the inverse dispersion fibre technique to nullify the cumulative positive dispersion within the transmission link. In the set-up shown in figure 8.13, a 10 Gb/s signal transmission is implemented using either 52 km RS fibre or a 52 km of (RS+ SRS). A combination of RS and SRS fibres created a positive-negative dispersion (NZDSF+IDF) compensation scheme. A 1550.4 nm VCSEL with output optical power -3.4 dBm and a PIN photo-receiver were used.

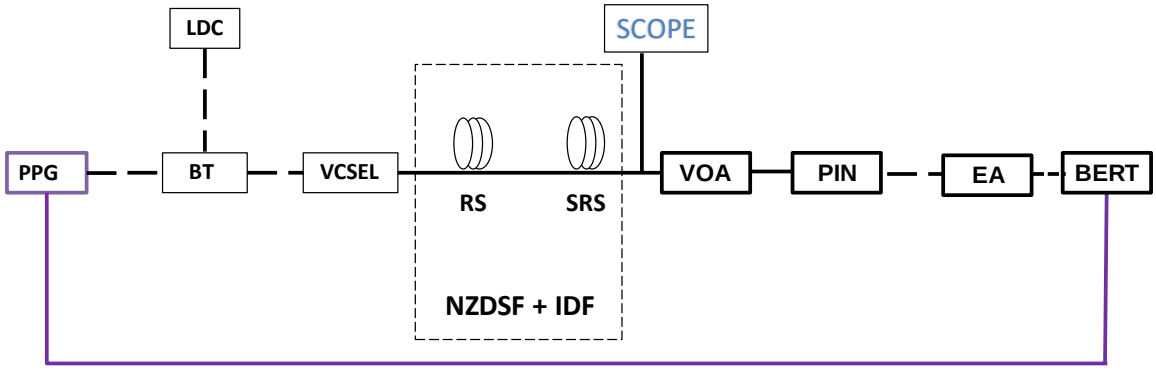

Figure 8.13: Experimental compensation of chromatic dispersion using positive dispersion and negative dispersion fibres. 10 Gb/s VCSEL transmission over 52 km reduced slope (RS) fibre and 52 km {RS+ submarine reduced slope (SRS) fibre}. Non zero dispersion shifted fibre (NZDSF) and Inverse dispersion fibre (IDF) system.

Since a NZDSF RS fibre has a +2.8 ps/(nm.km) dispersion coefficient, a signal transmitted at 10 Gb/s experiences cumulative dispersion over the transmission length. The received 10 Gb/s data signal for 52 km fibre transmission is shown in figure 8.14 (a). From

the eye-width and eye-closure, it was observed that an increased transmission distance resulted in bit-errors resulting in the overlapping of bits. This therefore strained the PIN receiver in differentiating between the received “1”s and “0”s. As seen in figure 8.15, the BER performance for the 52 km transmission over the RS fibre showed an error-free -12.2 dBm sensitivity while the error-free B2B had a -18.5 dBm. As a result, the 10 Gb/s transmission incurred a 6.3 dB dispersion penalty.

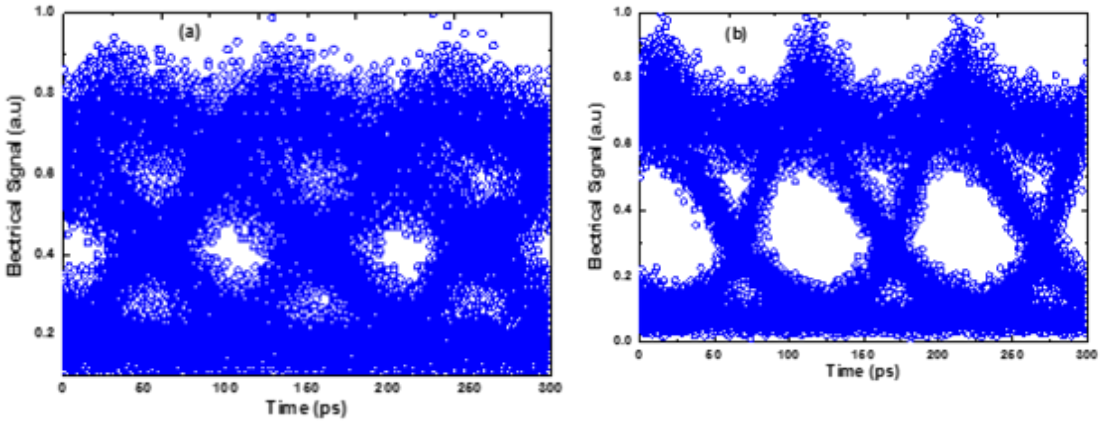

Figure 8.14: Eye-diagrams showing the received 10 Gb/s data from VCSEL for (a) 52 km uncompensated G.655 RS fibre and (b) 52 km RS+SRS dispersion compensated G.655 transmission.

To minimize the 6.3 dB dispersion penalty, a 26.6 km NZDSF RS fibre was connected to a 25.5 km NZDSF SRS fibre to make a total of 52.1 km distance of transmission. The SRS fibre used in this experiment had -2.8 ps/(nm.km) dispersion coefficient. Therefore, by combining the two fibres, the inverse dispersion fibre SRS cancelled out the accumulated dispersion thereby minimizing the number of errors resulting from broadening and overlapping of optical pulses.

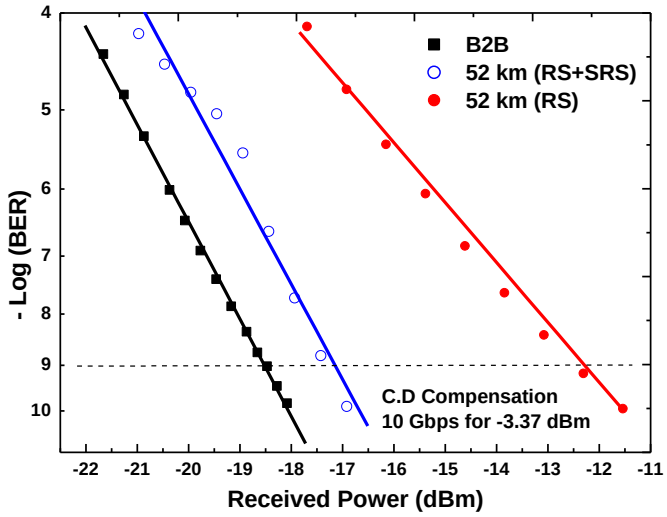

Figure 8.15: BER evaluation of experimental compensation of chromatic dispersion in a 10 Gb/s data signal using an inverse dispersion fibre, SRS to increase transmission distance to 52 km with a 1.3 dB penalty. And 6.3 dB dispersion penalty for 52 km G.655 RS VCSEL transmission.

An error-free transmission is illustrated by the clean and wide eye opening as seen in figure 8.14 (b). From the BER performance evaluation as shown in figure 8.15, the error-free receiver sensitivity after 52.1 km (RS+SRS) transmission was found to be -17.2 dBm. As a result of this dispersion compensation technique, a 1.3 dB dispersion penalty was incurred thereby reducing the 6.3 dB penalty when the signal was transmitted for 52 km in all RS fibres. To achieve a 10 Gb/s data signal transmission over 52 km at the 1550 nm transmission window, a 5 dB improvement in the receiver sensitivity was therefore achieved by utilizing dispersion compensation. An alternative method to increase transmission distances is by using a high powered laser such as the DFB to achieve high speed transmission in long-haul passive fibre links as demonstrated in section 5.2.2 of chapter 5.

8.3. Polarization Effects

PMD measurements were carried out on different types of fibre under test (FUT) using a continuous wave (CW) laser and an EXFO FTB-5500 PMD analyser module on an EXFO FTB-400 Universal Test System as shown in figure 8.16. A 1550 nm CW laser was used while single and multi-segment fibres, PMF and PMD emulator fibres were used to represent various fibre links.

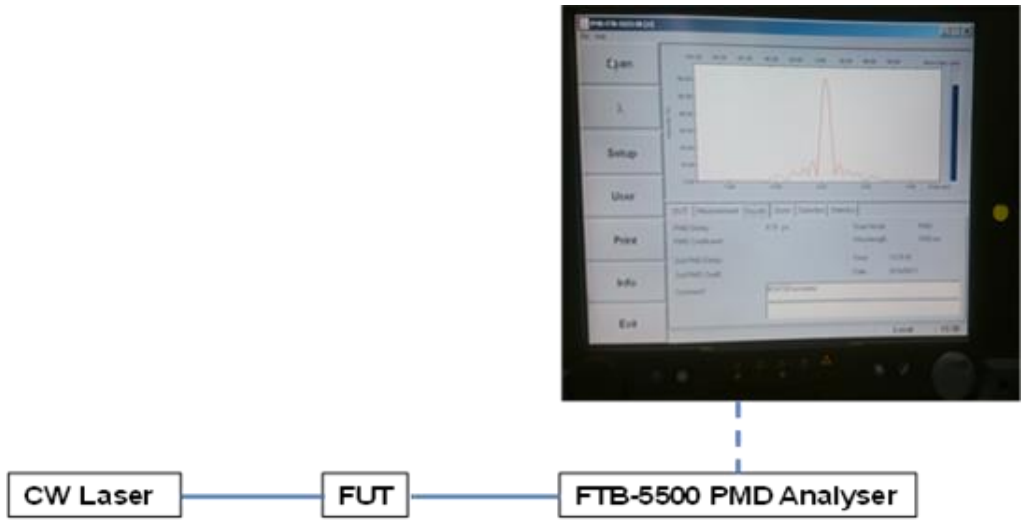

Figure 8.16: An experimental measurement of PMD along different types of fibre-links (FUT) using a continuous wave (CW) laser and an EXFO FTB-5500 PMD analyser.

For an optical signal propagating in a single segment of a standard SMF fibre, the 1st order PMD is as a result of birefringence where an optical pulse with its two distinct polarization modes (the fast and slow axis) travels with different group delays (DGD). The time difference (DGD) between these pulses represents the PMD as shown in figure 8.17 (a). PMD is often measured by determining the standard deviation of a Gaussian fit to the interferogram once the central autocorrelation peak has been removed.

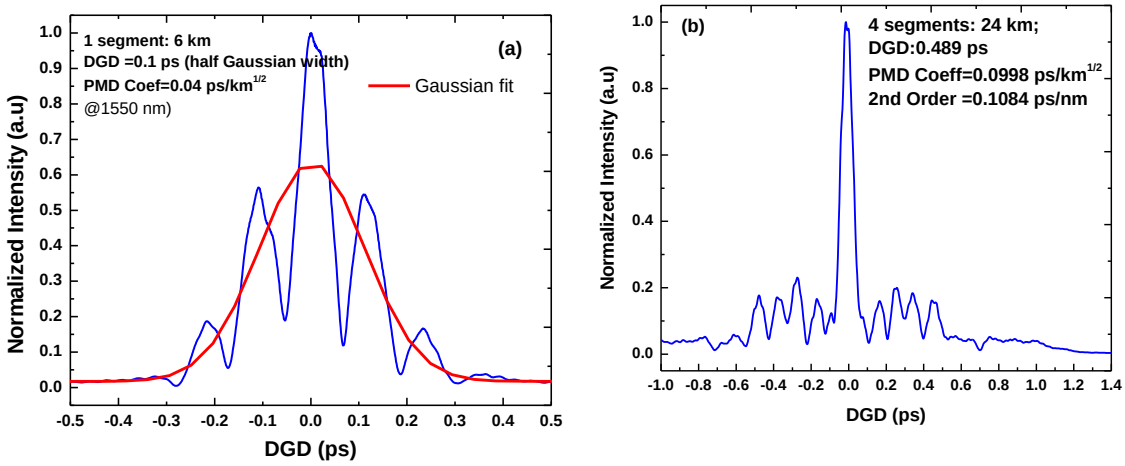

Figure 8.17: Experimental demonstration of the fast and slow pulses due with different PMD effects at 1550 nm for; (a) a single 6 km segment with DGD=0.1 ps and (b) 4 segments (24 km) with 2nd order PMD, 0.11 ps/nm.

As shown in the figure, a 6 km G.652 fibre exhibited a DGD= 0.1 ps which was half the Gaussian with or a PMD coefficient of 0.04 ps/√km at 1550 nm. Despite a single segment,

the 6 km fibre experienced spinning imperfections as a result of internal coupling locations within the fibre. However, it was experimentally depicted that the concatenation of 24 km fibre-link experienced high mode coupling as shown in figure 8.17 (b).

For a link with 4 different segments, the high 1st and 2nd order PMD is as a result of mode coupling where the principal states of polarization (PSPs) change when optical pulses are coupled onto adjacent segments of fibre. A 24 km fibre comprising of 4 segments of G.652 fibres had a 1st PMD coefficient of 0.1 ps/√km and 0.11 ps/nm 2nd order PMD as seen in figure 8.17 (b). The observed pulses are randomly distributed and therefore affects the transmission of individual bits at high speeds than the single 6 km fibre-segment.

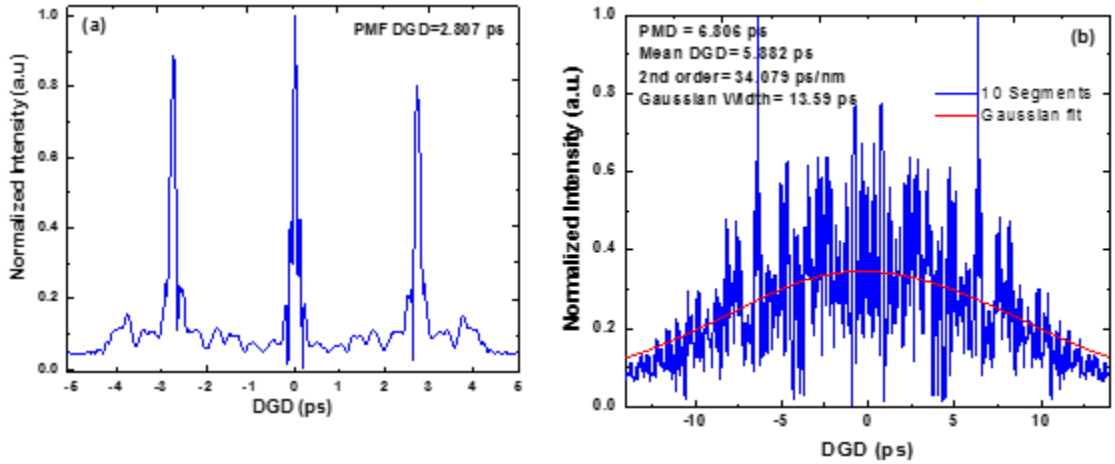

Figure 8.18: High birefringence in (a) PMF, DGD=2.81 ps and (b) High PMD emulator in a 10 segments link with DGD=6.81 ps representing an old fibre with several splicing.

For PMF fibres, the inbuilt PMD is shown in figure 8.18 (a) where the measured DGD was 2.81 ps. This high inbuilt PMD enables the PMF fibre to maintain the polarization states of a signal and as a result less error-bits due to disturbance of the fibre. A concatenation of 10 pieces of fibre to emulate a PMD emulator was created and polarization effects investigated. The PMD emulator represented a set of old fibres with numerous splicing and therefore high mode-coupling. The measured DGD as from the standard deviation of a Gaussian fit of the interferogram is as shown in figure 8.18 (b). Its mean DGD was 5.88 ps and a 1st order PMD of 6.8 ps/√km, while the 2nd order PMD was 34.1 ps/nm. As observed in the figure, the optical signal is highly affected by polarization and therefore signal distortions are experienced.

8.3.1. Quality of Signal Transmission over Aerial and Buried Fibres

In optical fibre transmission, signals can either be transmitted using overhead aerial or buried fibre deployments. In an aerial fibre, an optical fibre experiences twisting, bending, and environmental wind or thermal disturbances while a buried fibre experiences unintentional stress or strain and as a result the states of polarization of the optical signal propagating through these fibres changes. In this study, we experimentally demonstrate the change in SOPs by using a polarization scrambler (PS) or polarization controller (PC) as shown in figure 8.19 to emulate aerial or cabled fibre deployments. A 10 Gb/s modulated signal is transmitted using a 1550 nm VCSEL over a fibre under test (FUT). The signal SOPs were recorded with a polarization analyser and plotted on a Poincare sphere for analysis.

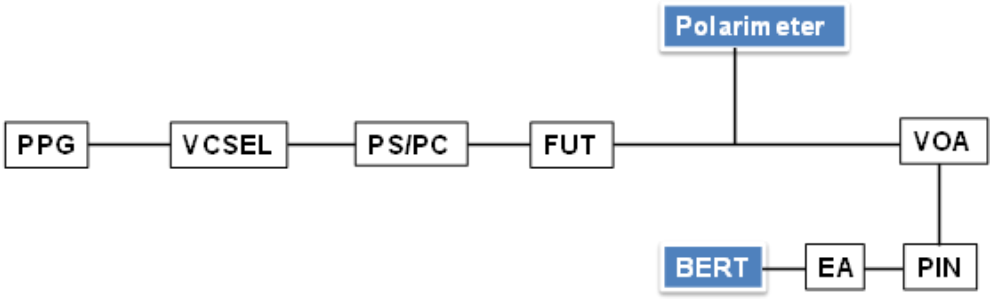

Figure 8.19: An experimental setup to characterize polarization effects on an optical fibre link (FUT) using a polarization scrambler (PS) and polarization controller (PC) to illustrate random change and fixed SOPs respectively. Random change typifies the aerial deployment while stable SOPs using a PC represents a cabled/buried fibre.

In this study, we consider 24.7 km standard SMF and a 1 m PMF fibres investigating the effects of birefringence of an optical signal transmitted through them. A polarization scrambler was used to randomly vary the states of polarization of the optical signal before injecting it into the fibre. The random evolution of the SOPs as represented by the Stokes parameters on a Poincare sphere for a disturbed SMF is shown in figure 8.20 (a). In maintaining the SOPs of an SMF, a PC was used to maximize and maintain the SOP of a signal. The SOPs for the stable SMF representing a cabled fibre without external or environmental disturbances is shown in figure 8.20 (b).

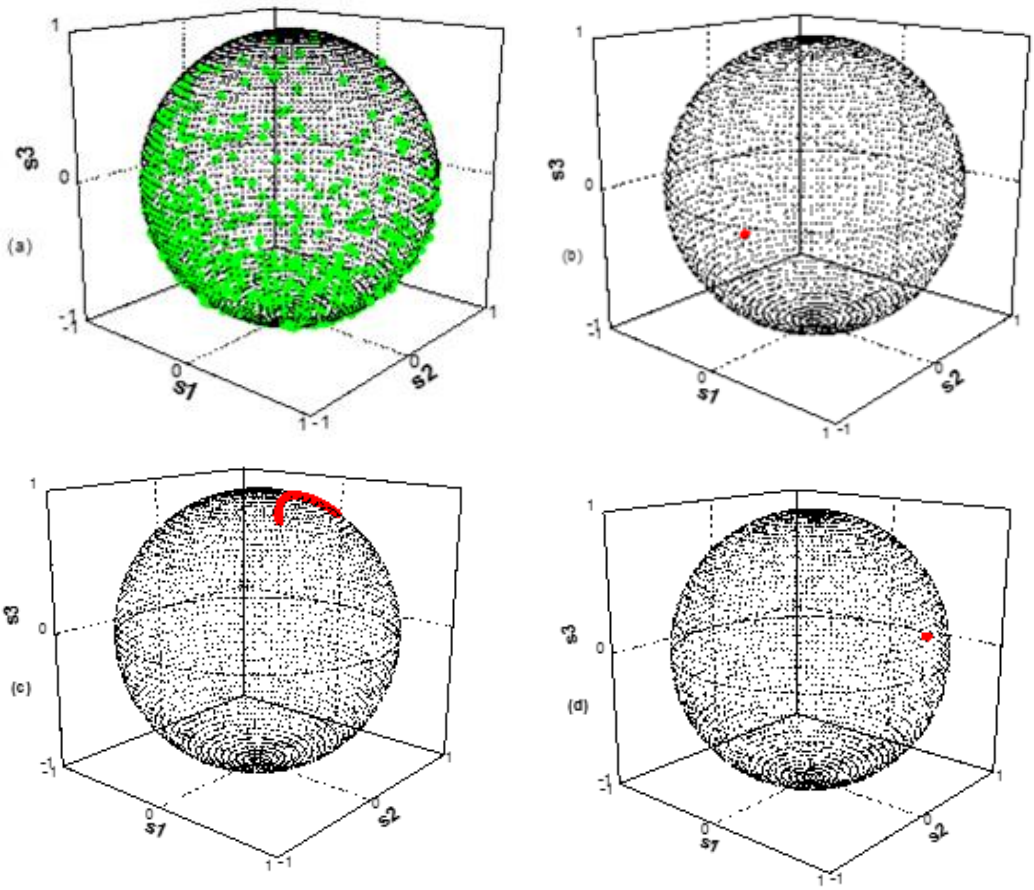

Figure 8.20: Change in states of polarization using a Poincare sphere for (a) disturbed standard SMF, (b) stable SMF, (c) Random/disturbed and (d) stable PMF.

When the SOPs of the optical signal are scrambled using the wave-plates of a PS and at a 10 KHz scrambling rate for 2 mins, the orientation of the incident SOP randomly change and therefore cover the whole surface of the Poincare sphere as shown in figure 8.20 (a). The relatively high scrambling frequency has been used to demonstrate the rapidly changing states of polarization of the signal. As a result, a change in the birefringence results in increased PMD. A scrambled PMF fibre demonstrated a stable and periodic polarization due to the inbuilt birefringence as seen in figure 8.20 (c). However, for a stable cable, the SOPs on the Poincare sphere are only on a single point or a periodic evolution of SOPs on the surface indicating a stable signal propagation. This is illustrated by figures 8.20 (b), (c) and (d) where the stability of the signal transmitted over SMF and PMF fibres experienced minimal or no effects of birefringence.

8.3.2. Stabilization and Maintaining the States of Polarization of a Signal

Signal stability and maintaining the states of polarization in a fibre-link can be done by either pre- or post-compensation techniques in physical or software domains. Post-transmission techniques involve schemes such as the fixed delay PMD compensation and the PMD nulling while the most common pre-transmission involve a PC to maintain the principle states of polarizations (PSPs) of an input signal [86]. In the fixed delay PMD compensation scheme, a combination of a PC and a short PMF is used while PMD nulling involves using a PC and a variable time delay device that is placed at the output of the transmission [72]. The delay is normally adjusted to match the accumulated DGD values within the total signal transmission link. For software domain techniques, FEC and polarization scrambling is done where distorted bits as a result of high scrambling are recovered by using FEC [48]. However, high speed scrambling has been reported to introduce jitter and therefore degrades the QoS. Other techniques involve tracking the changes in the SOPs and compensating them at the receiver-end using control algorithms [44]. These have however been least feasible based on the system complexities and the unavailability of hardware for real-time monitoring and control systems since it is not easy to predict the evolution of SOPs in a link. It is therefore practicable to stabilize the signal using PC, dispersion compensating fibres (PCFs), PMFs or compensate with FEC [132], [44].

8.4. Summary

In this chapter, the several linear and non-linear effects that affect an optical signal propagating in a fibre have been discussed and solutions on mitigating them suggested. Optimized signal transmission performances have been presented to illustrate typical optical fibre links containing high speed signals to provide an end-to-end transmission in DWDM and flexible spectrum networks. Optical fibres have been optimized with transmitter-receiver performance at the 1310 nm and 1550 nm transmission windows to achieve up to 10 Gb/s transmission speeds. Physical signal impairments such as chromatic dispersion, crosstalk and PMD affecting single wavelength, WDM and flexible spectrum signals and their mitigation and compensation techniques have been studied and reported.

The following chapter presents optimized transmission of flexible spectrum signals in a multi-node network topology containing different link properties. This include; aerial/cabled fibres, high dispersion and PMD links, DWDM channels, multi-bitrates with capability to optimize length, power, routes, capacity, resource sharing and link restoration.

Chapter 9:

9.0 Flexible Network and Optimization

Fibre capacity, spectrum efficiency and reach are the main objectives of implementing an optimized optical communication link. This chapter discusses different network properties such as transmitter, fibre-link, optical effects and receivers for optimizing signal transmission over fibre. We have experimentally shown the different attributes of a flexible spectrum network such as variable bit-rates, wavelength tunability and switching, fibre-links and multi-node hop transmission. The targeted transmission distances are for PON-based short fibre-reach, metro-access and hop in long-haul, long-haul amplified and the SKA spiral arms fibre networks. For long-haul transmissions, dispersion compensation, high power lasers and Raman amplification were used.

9.1. Designing and Building of a Flexible Network

In this study, the different types of up to 10 Gb/s transmitters and receivers as presented in chapter 5 are used at the 1310 nm and 1550 nm transmission window. Network nodes were implemented by using wavelength converters and an OADM as reported in chapter 6 and 7 respectively. Moreover, DWDM multiplexers and demultiplexers have also been used as optical nodes to provide enhanced fibre capacity. Optical signals have been transmitted over ITU-T G.652 and ITU-T G.655 SMF fibres. For optimized transmissions, optical effects such as chromatic dispersion, PMD and crosstalk have been minimized and compensated using the various techniques discussed in chapter 8.

A four node experimental demonstration was designed and implemented as shown in figure 9.1. Bitrate variable transmitters providing up to 10 Gb/s per channel/wavelength speeds at node **A** comprising long-haul incoming DWDM channels with their reachability enhanced by forward Raman amplification. Node **B** forms a wavelength selective switching (WSS) node capable of routing any of the incoming DWDM channels from node **A** to node **C** and **D**. Depending on the type of network topology, node **B** was either made up of demultiplexer, OADM or a wavelength converter. For PONs, node **B** was implemented using a distribution passive splitter while **C** and **D** represented different end-users in a fibre-linked metro-access network. Table 9.1 illustrates the various link properties that were used to create the different networks.

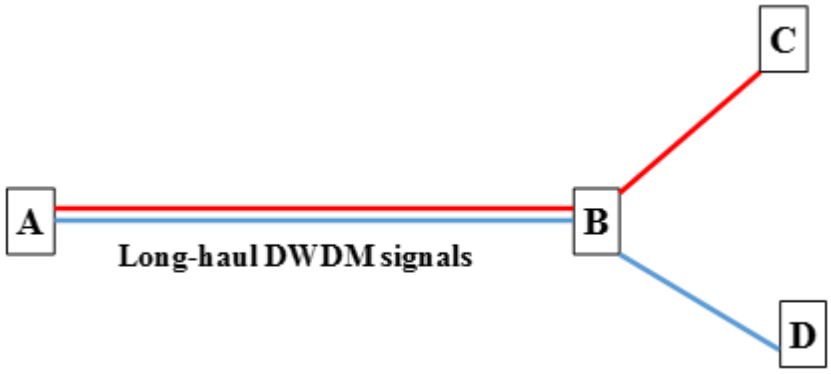

Figure 9.1: Illustration of a 4 node optical fibre network.

We have successfully achieved a novel, all optical wavelength conversion in a VCSEL-based signal transmission in an optical fibre network. The long incoming 1550 nm wavelength from node **A** has been converted with both high extinction ratio and low penalties at node **B.** The novel technique has been implemented on an 8.5 Gb/s NRZ data signal which has been switched to a new wavelength and routed to a different path (node **C**) with a total of 1.68 dB penalty for fibre-link length **B-C** of 25 km as discussed in chapter 6. With a 4.8 nm VCSEL tunability range, the wavelength conversion offers up to 4.8 nm (600 GHz) spectrum switching.

Table 9.1: The parameters for different types of fibre linked networks.

PARAMETERS	Types of Fibre Networks			
	Short-Reach	DWDM	Hops in long-haul	Long-haul
Transmitters	VCSEL	VCSEL	VCSEL and DFB	VCSEL and DFB
Transmission Window	1310 nm and 1550 nm	1550 nm	1550 nm	1550 nm
Fibre Types	G.652 and G.655	G.655	G.655	G.655
Length	6 km to 25 km	Up to 52 km	52 km and 76 km	52 km and 76 km
Receiver	PIN	PIN	PIN	PIN
Bitrate	Up to 10 Gb/s per channel	Up to 10 Gb/s per channel	Up to 10 Gb/s per channel	Up to 10 Gb/s per channel
Node **B**	Splitters, wavelength converter, switches, DWDM, OADM	Wavelength converter, switches, DWDMs, OADM	DWDM, wavelength converter, switches, OADM	DWDM, wavelength converter, switches

For WDM signals, the add and drop multiplexing has been experimentally demonstrated with a 1549.9 nm OADM. Node **B** can therefore include an OADM to provide a wavelength

drop and insertion of a new data signal into the available wavelength to ensure wavelength re-use and efficient spectrum utilization as demonstrated in chapter 7.

9.2. Optimization of the Flexible Network

The following sections demonstrate experimental illustration of how flexible spectrum signals can be transmitted in optimized optical fibre networks. 1310 nm and 1550 nm transmission windows have been optimized for up to 10 Gb/s speeds to a maximum of 76 km distances which represent access and long-haul fibre networks.

9.2.1. Short Fibre Reach for Metro-access

High speed signal transmission for typical metro-access distances is optimized by utilizing the less costly and wavelength adjustable VCSELs. Up to 10 Gb/s was transmitted for distances of 6 km to 25 km using G.652 and G.655 fibres. In a PON, 1550 nm and 1310 nm VCSELs were used to emulate downstream and upstream signal transmission respectively. Based on the dispersion management discussed in chapter 8, G.652 and G.655 fibres have been optimized for transmission.

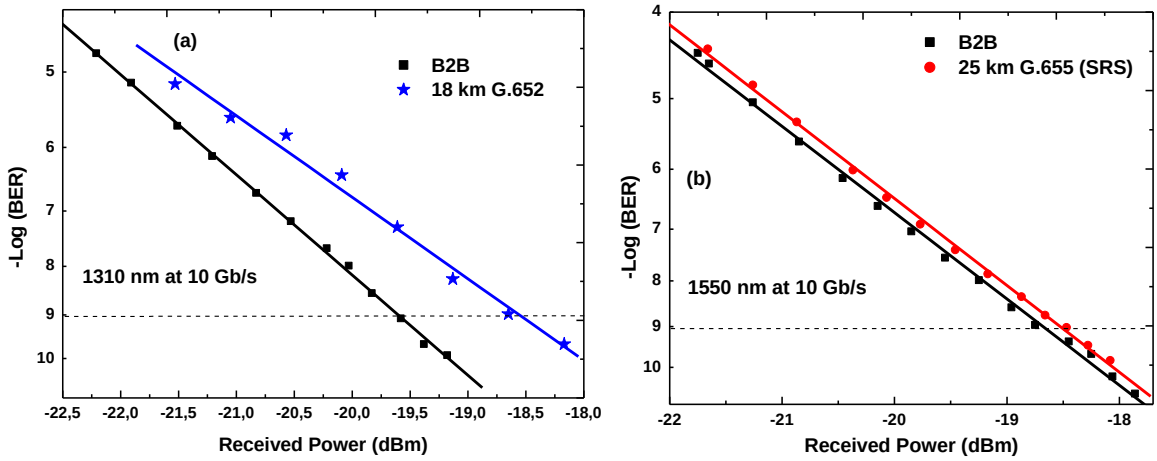

Figure 9.2: Optimized 10 Gb/s (a) 1310 nm transmission over 18 km G.652 fibre (b) 1550 nm over 25 km G.655 TW-SRS fibre with minimized chromatic dispersion effects for metro access networks.

At the 10^{-9} BER threshold level, the error-free receiver sensitivity for a 10 Gb/s 1310 nm transmission was seen to be -19.6 dBm while after an 18 km transmission over G.652 fibre, the error-free sensitivity reduced to -18.5 dBm as seen in figure 9.2 (a). This represented a 1.1 dB penalty due to dispersion effects on the high speed transmitted bits. For a 1550 nm transmission over 25 km G.655 fibre, a 0.3 dB penalty was incurred as shown in figure 9.2

(b). The low penalty was due to the low dispersion coefficient (-2.8 ps/(nm.km)). The 18 km and 25 km distances used to experimentally demonstrate high speed signal transmission represent the access distances from the OLT to the ONU of a PON in a VCSEL-based bidirectional transmission.

9.2.2. Hop in Long-haul Network

For multi-node networks with signals traversing over several nodes, high optical power 1550 nm window transmitters or compensating for signal impairments such as chromatic dispersion increases the reach and also improves receiver sensitivity. In this study, high power DFB transmitters have been optimized for hop in a long-haul 10 Gb/s transmission. With VCSEL, compensation of chromatic dispersion using negative dispersion fibres as discussed in chapter 8 is implemented.

The experimental BER measurements for the optimized hop in long-haul networks are shown in figure 9.3. Both transmitters were biased in the linear region of their input current-power characteristics. The output power for the VCSEL and DFB laser was -3.7 dBm and 4 dBm respectively and were modulated at 10 Gb/s. The modulated signal was transmitted over different fibre links comprising of G.655 fibres with varying dispersion properties and lengths up to 76 km.

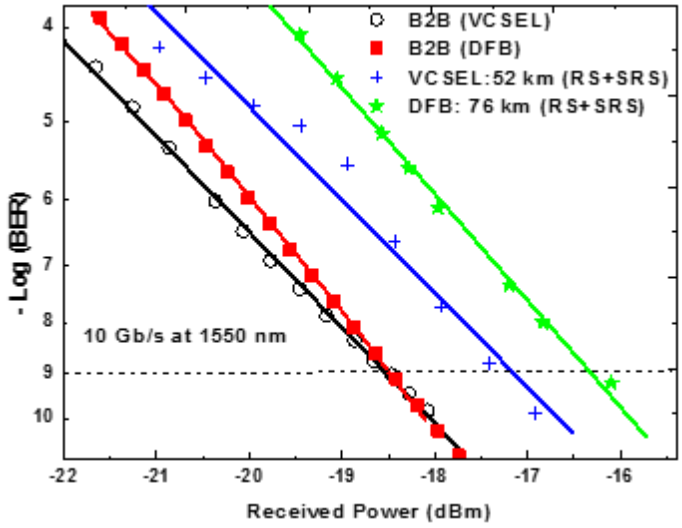

Figure 9.3: Experimental comparison of 10 Gb/s VCSEL and DFB lasers for optimized 52 km and 76 km hop in long-haul fibre networks with extended reach with dispersion compensation using negative dispersion fibres NZDSF (TW-SRS).

At 10^{-9} BER threshold level, the error-free PIN photodiode sensitivity (B2B) was seen to be -18.5 dBm for both VCSEL and DFB lasers. The error-free sensitivity after 52 km for

a 10 Gb/s signal transmission using a VCSEL was -17.2 dBm as seen in figure 9.3. This resulted in a 1.3 dB penalty due to dispersion, high speed signals and chirping on the VCSEL signal that introduced received error-bits. By combining a 4 dBm power 1550 nm window DFB laser and dispersion compensation, the fibre reach was extended to 76 km with error-free receiver sensitivity of -16.3 dBm. A 2.2 dB penalty was therefore incurred. The ITU-T G.655 TW-RS and TW-SRS fibres were optimized to reduce net dispersion effects.

We have optimized using VCSEL and DFB lasers, a 10 Gb/s signal transmission up to 76 km for a PON-based long-haul fibre-link. The low penalties make both transmitters and PIN photo-receivers ideal for hop in long-haul signal transmission and fibre networks.

9.2.3. Raman Aided VCSEL Transmission for Long-haul Amplified Networks

As demonstrated in chapter 5, VCSEL transmission is limited by its low optical power and chirping resulting in increased dispersion effects that degrade the QoS. To increase the transmission distance of a signal transmitted using a VCSEL, amplification or use of highly sensitive receivers such as APDs can be used. One of the techniques used to increase the output power of the carrier signal was to utilize forward Raman amplification which is based on stimulated Raman scattering (SRS) [77] [133]. Amplification could be performed on flexible spectrum signals before transmission if long distances are to be reached. The Raman gain peak due to SRS occurs when the signal and the pump lasers are separated by 100 nm (13.2 THz) [133]. Forward Raman amplification not only provides a higher signal gain but also provides high OSNR over the transmission distance [74]. Raman gain can be distributed over a range of closely spaced DWDM and flexible spectrum channels.

In this study, a 1550 nm window 10 Gb/s VCSEL with a tunability range of 1547-1552 nm was used as a signal carrier and amplified with a 1450 nm Raman pump laser. To investigate the Raman gain profile, the VCSEL wavelengths were adjusted by varying the bias currents from 4.5 mA to 9.8 mA providing a wavelength range of 1547-1552 nm. On-off gain and Raman gain profile was measured using an OSA and a power metre as the difference between signal powers with and without a Raman pump laser at varying wavelengths and lengths. The VCSEL was modulated at 10 Gb/s using a NRZ 2^7-1 PRBS pattern and coupled with a Raman pump via a 1450/1550 nm coupler giving a 100 nm wavelength difference. A polarization controller (PC) was used to match the SOPs of the two optical signals before coupling them. The signal was then transmitted for 52 km and

76 km over G.655 fibres. A filter-based 1450/1550 nm coupler was used to receive the transmitted signal for BER evaluation as shown in figure 9.4.

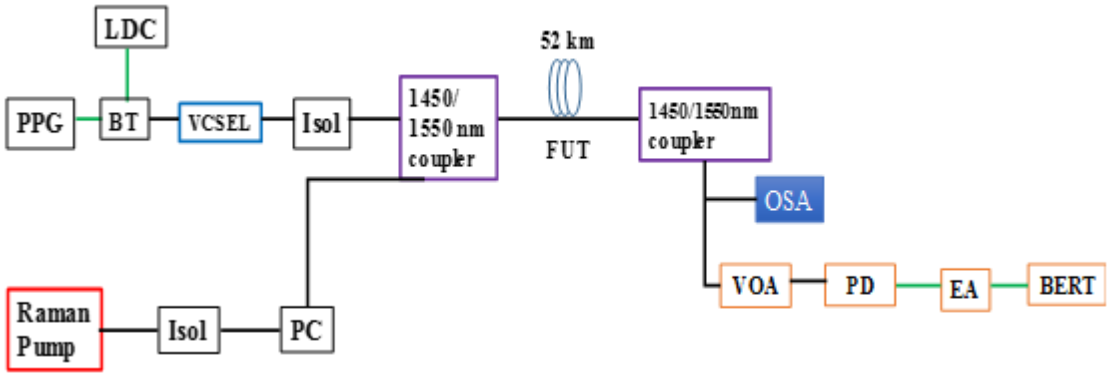

Figure 9.4: The experimental setup for demonstrating forward Raman amplification and BER measurements using a VCSEL signal carrier and a Raman pump laser.

The optical signal was amplified using a Raman pump laser in the forward direction. With high optical intensity from the Raman pump and through stimulated Raman scattering (SRS), pump energy was transferred to the longer wavelength optical signal that satisfied the Raman effect (100 nm wavelength shift). As a result, the Raman gain profile had a maximum gain peak of 5.6 dB at 1549 nm when a 25 dBm Raman pump was used as shown in figure 9.5 (a). The signal was transmitted for 76 km over G.655 fibres made up of REACH-fibre (51.5 km) and TW-SRS (24.7 km). REACH-fibres are optimized for Raman amplification [82]. Combination of the REACH-fibre and TW-SRS fibres increased the Raman gain and minimized effects of chromatic dispersion in the high speed optical signals. The mean distributed gain for the 1547-1551.8 nm bandwidth was found to be 5.2 dB.

Figure 9.5 (b) illustrates an increase in Raman gain with increasing pump power for 52 km and 76 km transmission distances. The VCSEL was biased at 7 mA and 1549.4 nm wavelength with an output power of -3.7 dBm. With a 25 dBm Raman pump, the maximum gains were 4.7 dB and 5.8 dB for 52 km and 76 km respectively. For 52 km, received signal power was increased from -21.5 dBm to -16.7 dBm. The increase in signal power enabled the PIN photodiode to operate within its sensitivity region ($-18 \pm 1\ dBm$). In a 76 km transmission, the signal output power was improved from -26.8 dBm to -21.0 dBm. The distributed flat Raman gain as shown in figure 9.5 (b) implies that VCSEL carriers in DWDM and flexible transmissions can be integrated with Raman amplifiers to extend the reach.

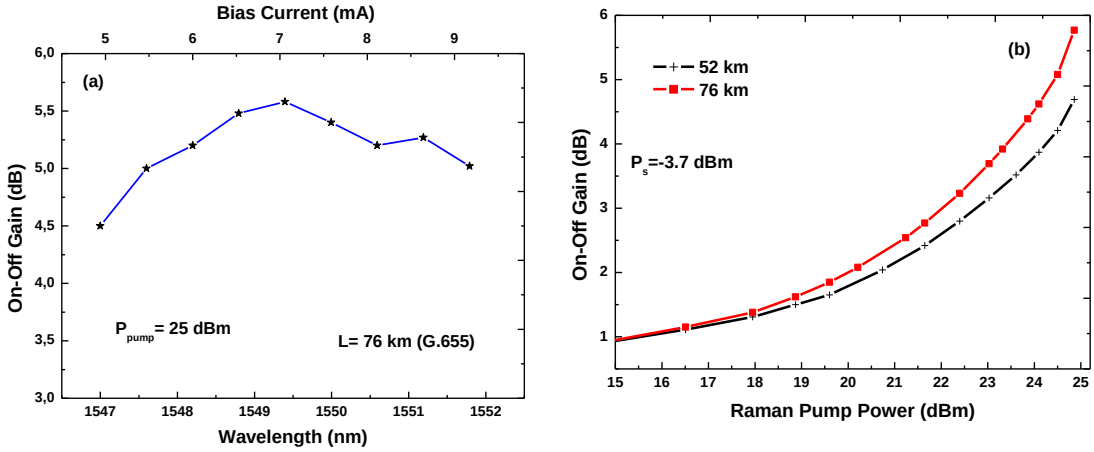

Figure 9.5: Experimental demonstration of (a) Raman gain profile and (b) On-off gain for forward Raman pumping scheme over 52 km and 76 km (TW-REACH and TW-SRS fibres) using VCSEL and Raman pump lasers.

To study the quality of transmitted data after amplification, a 10 Gb/s NRZ modulated signal with -3.7 dBm power was amplified using a forward Raman pump laser with 25 dBm power and transmitted over 52 km and 76 km and BER measurements presented as shown in figure 9.6.

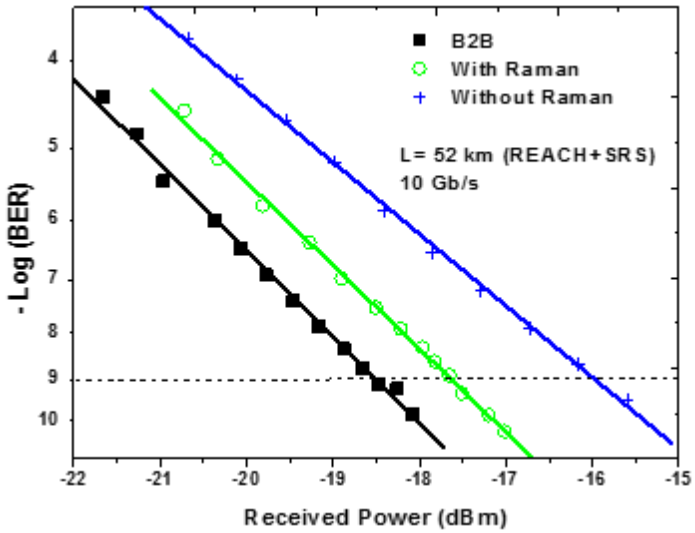

Figure 9.6: BER measurements of 10 Gb/s amplification using a 25 dBm forward Raman pump and transmission for 52 km over TW-REACH and TW-SRS fibres.

The error-free receiver sensitivity for B2B at the 10^{-9} BER threshold level, was seen to be -18.5 dBm. For a 52 km transmission without a Raman amplifier, the sensitivity was -16.0 dBm as seen in figure 9.6. The 2.5 dB reduction in the receiver sensitivity was

due to the accumulated dispersion effects and amplifier noise that affected the 10 Gb/s high speed signal resulting in a 2.5 dB penalty. The error-bits were as a result of the residual dispersion from the TW-REACH fibre after compensating with a TW-SRS fibre. With a forward Raman amplifier, the error-free receiver sensitivity was seen to be -17.7 dBm resulting in a 0.8 dB penalty as shown in figure 9.6. The 4.7 dB power gain due to Raman amplification extended the reach with minimal error-bits. For a 76 km transmission, despite the high gain and increased received power of -21.0 dBm, an error-floor was attained by the 10 Gb/s signal as a result of both high speed and dispersion effects. An APD photodiode is recommended due to its high sensitivity.

9.2.4. Raman Aided 10 Gb/s per Channel DWDM Long-Haul Networks

After the experimental demonstration of DWDM signal transmission using 10 Gb/s VCSELs as performed in chapter 5, fibre-reach was extended using Raman amplification. Using VCSEL, wavelength tunability that fit into DWDM and flexible nominal frequencies has been demonstrated. The transmission represent source-to-destination dedicated wavelength assignment. In this study, two 1550 nm window VCSELs were modulated at 10 Gb/s, multiplexed and then amplified using a forward Raman amplification as shown in figure 9.7. The DWDM demultiplexer was used as a passive network node device **B** for separating individual wavelengths to respective destinations as illustrated in figure 9.1

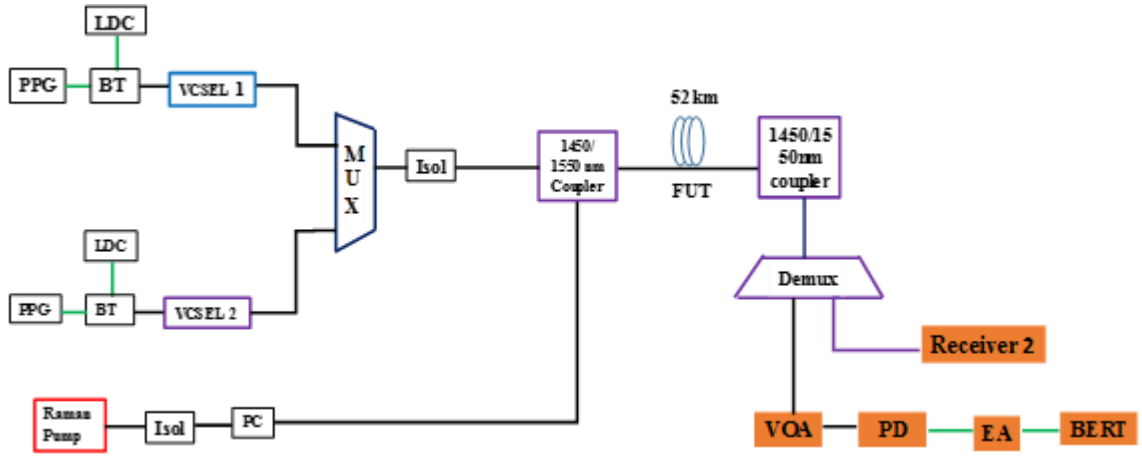

Figure 9.7: An experimental demonstration of Raman assisted DWDM transmissions for wavelength tunable and dedicated flexible spectrum networks.

VCSEL 1 was biased at 7.1 mA with nominal wavelength of 1551.7 nm. While, VCSEL 2 at 1552.1 nm with a 7.8 mA bias. VCSEL 1 and VCSEL 2 were modulated at 10 Gb/s with data D and with $\overline{D}$ respectively. Different lengths of RF cables were used to decorrelate the two data patterns so as to provide random delay times. After modulation, the

two wavelengths were multiplexed by a 50 GHz DWDM multiplexer to provide a multi-channel transmission with 50 GHz spacing. The two wavelengths were then amplified using a forward Raman pump with 25 dBm power providing a 4.8 dB distributed on-off gain as shown in figure 9.5. The signals were then transmitted for 52 km and the two wavelengths separated by a 100 GHz DWDM demultiplexer due to the unavailability of a 50 GHz DWDM demultiplexer. BER measurements were performed at 10^{-9} threshold level.

For performance evaluation, 1551.7 nm was used as the channel of interest. The PIN photodiode error-free sensitivity for B2B was seen to be -18.1 dBm. By transmitting the two channels over a 52 km fibre-link made up of TW-REACH and TW-SRS fibres without Raman amplification, an error floor was attained by the receiver as shown in figure 9.8. This was due to high dispersion and crosstalk effects that accumulated over the total length of fibre.

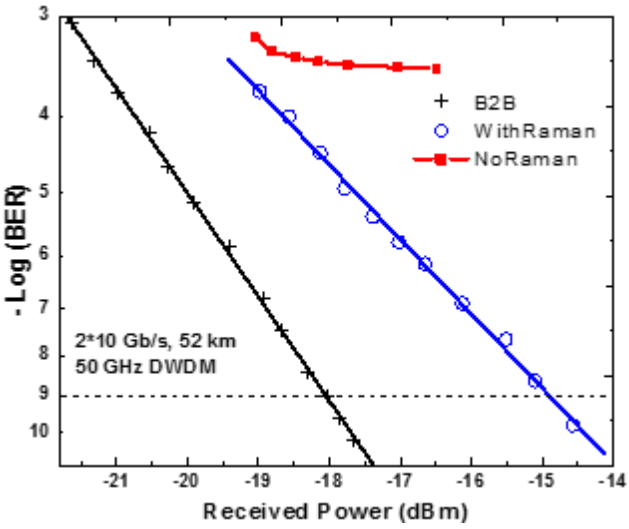

Figure 9.8: BER measurements for Raman amplified 10 Gb/s per channel DWDM channels spaced at 50 GHz using a 25 dBm forward Raman pump. An error floor is shown for 52 km transmission without Raman amplification.

The 52 km had a net dispersion of 77.0 ps that resulted in received error-bits. By amplifying the two wavelengths with a 1448 nm Raman pump at 25 dBm, the error-free sensitivity improved to -14.9 dBm. This resulted in a 3.2 dB penalty caused by dispersion effects over the fibre link. This improvement was due to signal power gains as a result of Raman amplification that enabled the long distance transmission. The high signal power reduced dispersion effects and therefore fewer error-bits were received.

Combining closely spaced DWDM channels and Raman amplification not only increased the fibre capacity but also the distance of transmission. Wavelength dedicated channels create a point to node signal distribution connections. Moreover, VCSELs have

successfully provided the ability to adjust the wavelengths matching the nominal central frequencies in fixed DWDM and flexible grid systems.

9.2.5. SKA Spiral-arms

For the SKA with 3 spiral arm configuration and a core radius of $< 2\ km$, a maximum baseline of 76 km can be covered with both data and timing and frequency reference (TFR) signals being transmitted over fibre [134], [135]. This can be implemented by high speed signal VCSEL and DFB transmitters and a PIN photodiode whose performance exhibit minimum transmission penalties over fibre. Data and timing and synchronization signals can be transmitted between the receptors and the remote signal processing stations. By using the discussed experimental demonstrations for short and long distances, signals can either be transmitted from the stations to individual receptors or broadcast to multiple dishes.

9.3. Optimization of Flexible Bandwidth for Metro-access Networks

For distribution of available resources (bandwidth), a trade-off between distance and demand is to be evaluated. With increased number of users, the shared available bandwidth and the distance to the user are optimized to reduce transmission penalties and at the same time, maintain the QoS.

In this study, we optimize the transmission bit-rate using bandwidth adjustable PPG for 4.25-10 Gb/s in point-to-point (P2P) and point-to-multipoint (P2MP) PONs. A 1550 nm transmission window VCSEL was modulated at 4.25 Gb/s and 10 Gb/s to illustrate node **A** while passive optical splitters were used as signal distribution devices and implemented as node **B** as previously illustrated in figure 9.1. In the experimental demonstration, the VCSEL was modulated by a NRZ PRBS 2^7-1 data and transmitted over 6 km G.652 and 24.7 km G.655 fibres. The transmission distances represented typical metro-access fibre lengths. Passive splitters with splitting ratio of 1:2, 1:4 and 1:8 were used to distribute the signal to P2MP as shown in figure 9.9.

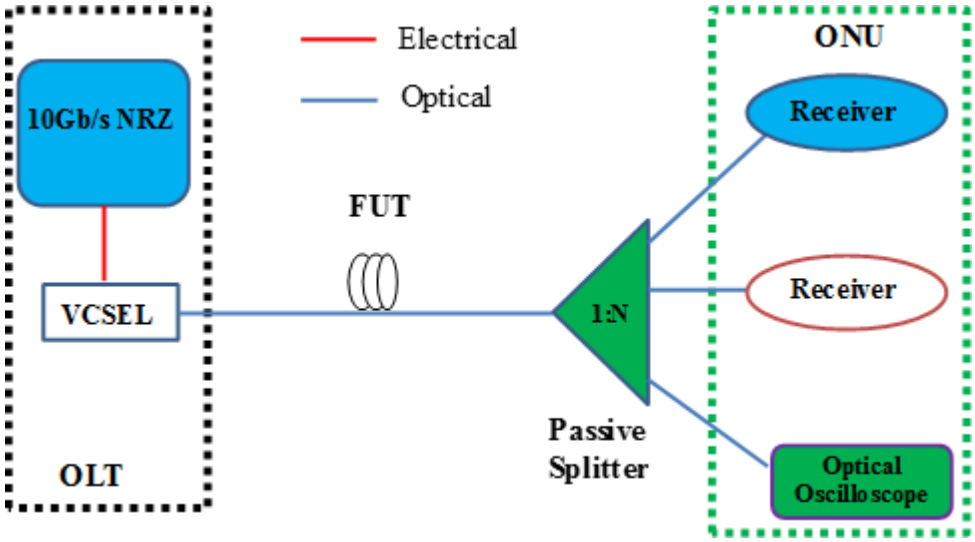

Figure 9.9: Experimental demonstration of a VCSEL-based PON with optical line terminal (OLT) made up of a VCSEL and PPG and receivers at the optical network unit (ONU) [136].

The measured insertion losses of the three splitters are as shown in table 9.2

Table 9.2: The measured insertion losses of passive splitters at 1: N (1, 2, 4, 8).

Split Ratio 1: N	Splitter Loss (dB)
1	-
2	3.8
4	8
8	11.5

The quality of the received signal after transmission was analysed using eye-diagrams, extinction ratio (ER) and the power penalty (PP) equation 9.1 and 9.2.

$$ER(dB) = 10\log(\frac{I_1}{I_0}) \quad \text{..... 9.1}$$

$$PP\ (dB) = 10\log\{\frac{(ER+1)}{(ER-1)}\} \quad \text{..... 9.2}$$

Where I_0 and I_1 are the power (in mWatt) of the "0" and "1" bit levels respectively [136].

The experimental results for optimized transmission speeds for P2P and P2MPs networks utilizing VCSEL signal carriers in 4.25 Gb/s and 10 Gb/s metro-access networks are shown in the following P2P and P2MP sections.

9.3.1. Point-to-Point Networks

The eye-diagrams for the B2B (without transmission and splitting) as measured at optical power -17.2 dBm after transmission over 24.7 km fibre for 4.25 Gb/s and 10 Gb/s are shown

in figure 9.10 (a) and b) respectively. The extinction ratio (ER) for 4.25 Gb/s and 10 Gb/s was 11.4 dB and 9.1 dB respectively. The slight reduction in the ER as seen in the reduced eye opening of a 10 Gb/s transmission in figure 9.10 (b) was as a result of dispersion effects that accumulated due to the high speed signal. It was however noted that in both transmission speeds, a P2P network provided an error-free signal at -17.2 dBm power which was within the operational standards of our PIN photodiode.

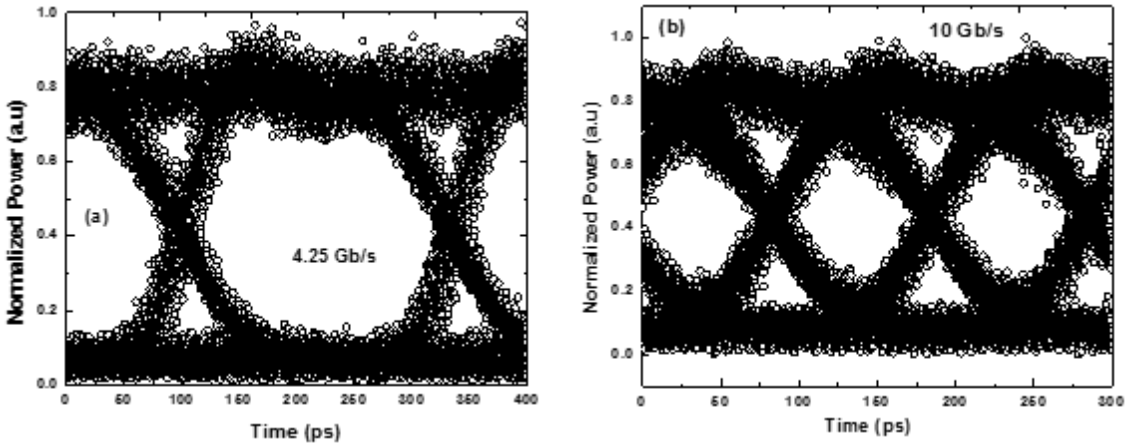

Figure 9.10: Eye-diagrams for P2P (a) 4.25 Gb/s and (b) 10 Gb/s over 24.7 km distance. The eye-diagrams of received optical signal was measured at -17.2 dBm.

For P2P network topology, signal clarity is enhanced by the trade-off between the 24.7 km distance and the dedicated signal transmission. With reduced traffic demands, the transmission speeds were flexibly adjusted using the PPG to provide the end-user with high bandwidth and ensuring that the quality of the signal is maintained.

9.3.2. Point-to-multipoint Fibre Networks

For P2MP signal distribution and transmission over 24.7 km fibre, 1:2, 1:4 and 1:8 passive splitters were used. A 4.25 Gb/s was split into 2, 4 and 8 users with the quality of the received signals analysed at -17.2 dBm as shown in figure 9.11 (a)-(c). With an increase in the splitting ratio, the eye-opening and ER of the received signals reduced. Indeed, the ER of the 4.25 Gb/s signal was 11.3 dB and 8.4 dB for 1:2 and 1:8 splitting ratios respectively. The reduction in the eye opening was as a result of reduced OSNR as the signal power was attenuated. The increase in splitting ratio strained the receiver from distinguishing the received “1” and “0” bits. However, for 1:2 and 1:8, error-free signals were received.

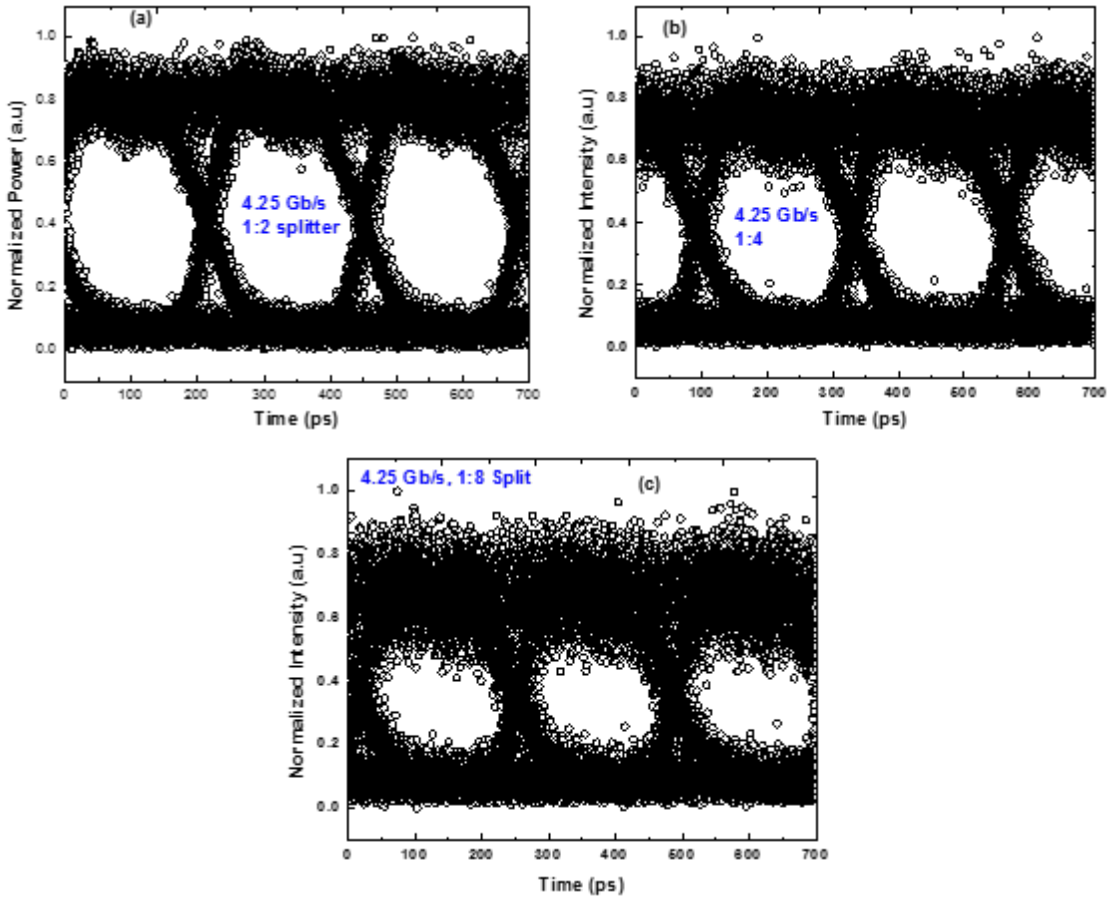

Figure 9.11:Eye-diagrams for received 4.25 Gb/s optical signal after (a) 1:2, (b) 1:4 and (c) 1:8 splitting ratio. The eye-diagrams were recorded at -17.2 dBm power.

For a high speed signal at 10 Gb/s and transmission over 24.7 km, the received signals had reduced eye openings and ERs as seen in figure 9.12. The ER for a 10 Gb/s signal after a 1:8 splitting ratio was 4 dB as seen in the reduced eye opening in figure 9.12 (c). The increased bit-rate and chromatic dispersion over the fibre-link introduced bit-overlap and therefore resulted in received error-bits.

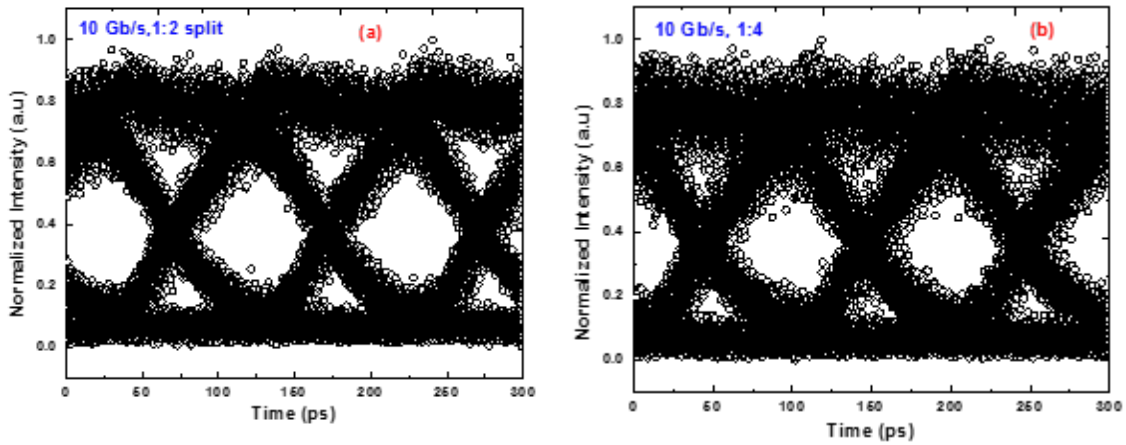

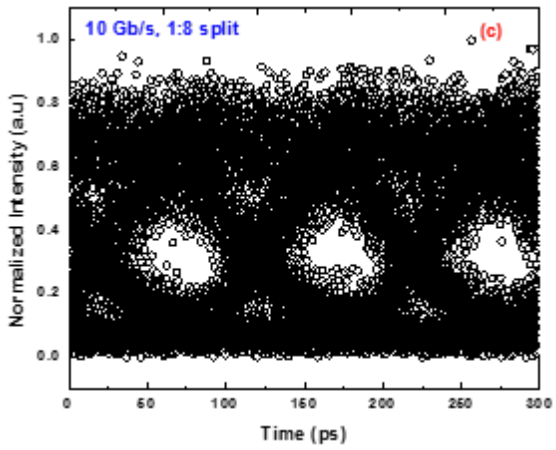

Figure 9.12: Eye-diagrams for the received 10 Gb/s optical signal at -17.2 dBm after (a) 1:2, (b) 1:4 and (c) 1:8 splitting ratio [136].

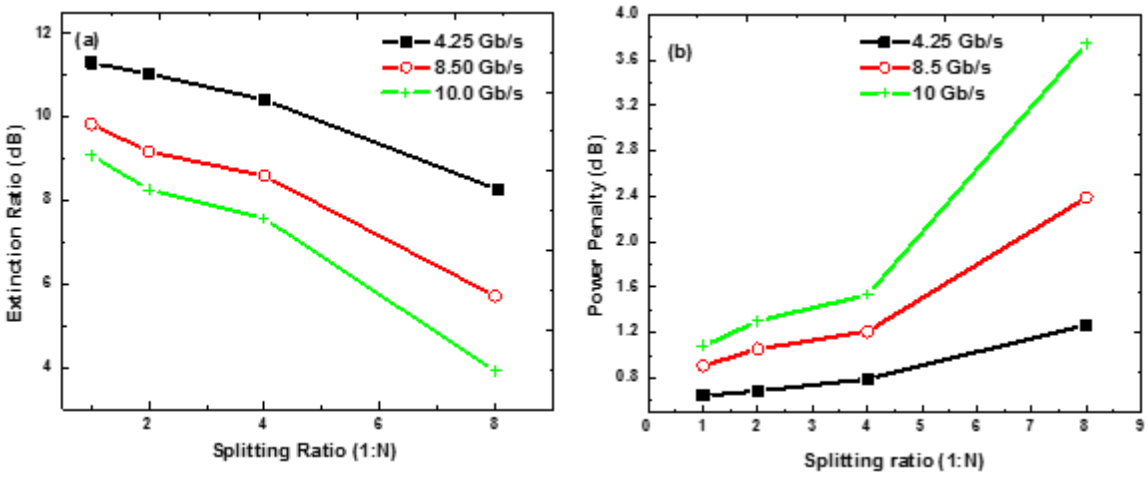

Figure 9.13: (a) Extinction ratio and (b) receiver power penalty of the received signal for different splitting ratios at 4.25, 8.5 and 10 Gb/s.

By utilizing both equations (9.1) and (9.2), the extinction ratio and the receiver power penalty as a result of the increased signal splitting ratio was calculated as shown in figure 9.13. Increase in splitting ratio resulted in reduced ER due to the slight eye-closure. As the ER reduced, the receiver strained in distinguishing the received bits. This resulted in an increase in receiver power penalty as shown in figure 9.13 (b). Considering a 1:8 splitting and a 24.7 km fibre-link, a 1.3 dB and 3.7 dB penalty was incurred for a 4.25 Gb/s and 10 Gb/s signals respectively.

It has been experimentally demonstrated that at the OLT of a GPON, the transmission bitrates can be flexibly adjusted and modulated into a VCSEL carrier and optimised to meet network and end-user demands. Sharing the available bandwidth on a single channel increases the spectrum efficiency but incurs high receiver penalties. A trade-off between distribution ratio, distance and receiver performance is to be considered. In a typical

network, the available unutilized spectrum can be flexibly assigned and distributed to users that require more bandwidth. End-users that require real-time access can be assigned more bandwidth than the best-effort service users [136].

9.4. Summary

This chapter has provided experimental findings that optimize a flexible spectrum network for short and long-haul fibre networks. Wavelength dedicated point-to-point and point-to-multipoint signal transmissions have been implemented using the low cost and power efficient VCSEL transmitters to enable up to 10 Gb/s speeds. Flexible spectrum fibre-linked nodes have been optimized for 6 km, 25 km and 76 km distances to represent metro-access and long-haul networks. In extending fibre-reach, 1550 nm transmission window, dispersion compensation and forward Raman amplification with a distributed on-off gain of 4.7 dB has been demonstrated. With dispersion compensation, a 4 dBm DFB laser has been used to transmit a 10 Gb/s signal for 76 km. These experimental results have analysed the received up to 10 Gb/s signals using PIN photo-diodes with power penalties of ≤3.7 dB. P2P and P2MP signal transmission have also been experimentally demonstrated for metro-access and SKA's fibre to the dish (FTTD) distances. The received signals have been analysed using a simple eye-diagram and extinction ratio technique that does not require the complex OEO conversion involved in BER measurements.

Chapter 10:

10.0 Conclusions and Recommendations

Optical fibre transport forms the backbone of most long-haul and metro-access networks in providing high speed signals for fixed and mobile terminals such as mobile cell towers and FTTX fibre deployments. The main aim of this thesis was to provide spectrum and energy efficient and effective reconfigurable techniques for high speed optical fibre flexible spectrum networks. Different network parameters have been optimized to facilitate signal transmission in varying network demands.

Design and implementation of a flexible spectrum network in a laboratory testbed has been performed at the Centre for Broadband Communication laboratory, at Nelson Mandela Metropolitan University. The first part of this work presents experimental characterization of the various types of transmitters and receivers optimized for the 1310 nm and 1550 nm transmission windows. The various advantages of VCSELs were optimized to provide wavelength tunable 10 Gb/s per wavelength, DWDM and flexible spectrum signal transmission over G.652 and G.655 SMFs. Transmission at the allowed central nominal frequencies of fixed DWDM and flexible grid systems have been implemented by adjusting the emission wavelengths of VCSELs. By using a PIN photo-receiver with a sensitivity of -18±1 dBm, increased dispersion penalties (maximum 2.7 dB) within the metro-access distances of 6-25 km were incurred. High optical power DFB lasers and dispersion mitigation using negative dispersion fibres were used to extend reach to 76.8 km fibre.

For routing and wavelength assignment in flexible spectrum, this work provides a novel experimental demonstration of a high speed all-optical VCSEL to VCSEL wavelength conversion and switching by optical injection at the 1550 nm transmission window. By using VCSELs with wavelength tunability range of $\sim 4.8\, nm$ (600 GHz) this work for the first time, experimentally demonstrated wavelength conversion, data inversion, transmission over 24.7 km and BER evaluation for an 8.5 Gb/s signal. This wavelength conversion and switching offers an alternative technique for re-routing signals when fibre-cuts and channel collisions occur within complex multi-node DWDM and flexible spectrum networks. For channel management, this work has designed and implemented an optical add and drop multiplexer (OADM) using a fibre Bragg grating and a pair of optical circulators and its performance evaluated. An OADM provided a technique of managing the wavelengths at an optical node by enabling simultaneous removal/drop and wavelength re-use. This cost

effective techniques are potentially suitable for implementation in VCSEL-based metro-access broadband networks.

Optical signal impairments such as crosstalk, chromatic dispersion and PMD have in this work, been studied and mitigated to improve quality of the received signal. This work suggests a trade-off between spectrum efficiency and minimized impairment penalties. In increasing fibre-reach, dispersion mitigation using negative dispersion fibres has been implemented. This work reports a 5 dB reduction in dispersion penalty of a 10 Gb/s per channel using combination of inverse dispersion fibres to mitigate dispersion effects for an extended 52 km fibre-reach. Long-haul and hop in long-haul fibre networks have been optimized using chromatic dispersion compensation and forward Raman amplification that provided an on-off gain of 4.7 and 5.8 dB distributed over 600 GHz spectral width. In VCSEL-based P2P and P2MP metro-access networks, 4.25 Gb/s and 10 Gb/s bitrates have been optimized for up to 8 distributions in a 24.7 km fibre-link with $\leq 3.7\ dB$ penalty. A simpler eye-diagram and extinction ratio technique for evaluating QoS has been proposed that avoids the complex and expensive BER measurements that require OEO conversion.

The contributions of the research in this thesis is very vital in achieving high speed and optimized signal transmission using hybrid DWDM and flexible spectrum techniques for existing and new metro-access, P2P, P2MP and in long-haul fibre-linked networks. The contributions are useful in providing cost effective and energy efficient flexible spectrum techniques for mega-projects such as the SKA-South Africa and the backbone of the national broadband networks. The fibre-link penalties can be used to develop real-time algorithms that include signal impairments in self-healing intelligent networks.

For the SKA, the reported techniques are potential and viable applications for the fibre-to-the-dish network and the long-haul data transmission from the telescopes sites to the processing centres. Possible simultaneous transmission of timing and frequency reference (TFR) and data signals in the flexible spectrum fibre network for the SKA project may in the future be studied and implemented. Higher bitrates above 10 Gb/s per channel may also be considered for networks that require high bandwidth, for which SKA is included.

Appendix A

Research outputs in journals, conferences, books of abstracts and other reports

Published/accepted/ presented articles

2016:

1. **D. Kiboi Boiyo**, G. M. Isoe, R. R. G. Gamatham, A. W. R. Leitch, and T. B. Gibbon, "A 1550 nm all Optical VCSEL-to-VCSEL wavelength conversion of a 8.5 Gb/s data signal and transmission over a 24.7 km fibre," *Proc. SPIE*, vol. 10036. SPIE, p. 100360X–1–100360X–6, 2017.
2. **Duncan Kiboi Boiyo**, T.V. Chabata, E.K. Rotich Kipnoo, R.R.G. Gamatham, A.W.R. Leitch, T.B. Gibbon, "Reconfigurable high-speed optical fibre networks: Optical wavelength conversion and switching using VCSELs to eliminate channel collisions", *Optical Fiber Technology*, Volume 33, January 2017, Pages 30-35, ISSN 1068-5200.
3. **D. Kiboi Boiyo**, G.M. Isoe, E.K. Rotich Kipnoo, R.R.G. Gamatham, A.W.R. Leitch and T.B. Gibbon, "A Signal Impairment-Aware Scheme for Next-Gen Flexible Spectrum in 10 Gb/s VCSEL Metro-Access Optical Fibre Networks", *Optical Switching and Networking*, Accepted.
4. **D. Kiboi Boiyo**, G.M. Isoe, E.K. Rotich Kipnoo, R.R.G. Gamatham, A.W.R. Leitch and T.B. Gibbon, "Flexible 1550 nm VCSEL Optical Fibre Transmission with Integrated OADM Based on Fibre Bragg Grating", *Optik- International Journal for Light and Electron Optics*, Accepted.
5. E.K. Rotich Kipnoo, **D. Kiboi Boiyo**, G.M. Isoe, T.V. Chabata, R.R.G. Gamatham, A.W.R. Leitch, T.B. Gibbon, "Demonstration of Raman-based, Dispersion-Managed VCSEL Technology for Fibre-To-The-Hut Application", *Optical Fiber Technology*, Volume 34, March 2017, Pages 1–5, ISSN 1068-5200.
6. T.V. Chabata, **D. Kiboi Boiyo**, E.K. Rotich Kipnoo, R.R.G. Gamatham, A.W.R. Leitch, T.B. Gibbon, Signal monitoring and performance stability evaluation tool in a high speed optical communication network, *Optik- International Journal for Light*

and Electron Optics, Volume 127, Issue 20, October 2016, Pages 9001-9007, ISSN: 0030-4026.

7. **D. Kiboi Boiyo**, G. M. Isoe, E. K. Rotich Kipnoo, R. R. G. Gamatham, A.W. R. Leitch and T. B. Gibbon, "Utilization of Flexible Spectrum to Optimize a 24.7 km Fibre TDM Passive Optical Network", *Proceedings of the SATNAC Conference 2016*, Fancourt, George, South Africa (4-7th Sept 2016), p.p. 8-12. ISBN: 978-0-620-72418-0.
8. G. M. Isoe, **D. Kiboi Boiyo**, S. Wassin, E. K. Rotich Kipnoo, R. R. G. Gamatham, A.W. R. Leitch and T. B. Gibbon, "Effect of 10 Gbps Data Transmission on 1.712 GHz 1309.97 nm VCSEL Based Radio Frequency Distribution over a Single Optical Fibre for the Telescope Array", *Proceedings of the SATNAC Conference 2016*, Fancourt, George, South Africa (4-7th Sept 2016), p.p. 156-159. ISBN: 978-0-620-72418-0.
9. Shukree Wassin, George M. Isoe, **D. Kiboi Boiyo**, Romeo R. G. Gamatham, Andrew W. R. Leitch and Tim B. Gibbon, "Component Power Budget Analysis and VCSEL Characterization for the Square Kilometre Array Signal and Data Transport Network", *Proceedings of the SATNAC Conference 2016*, Fancourt, George, South Africa (4-7th Sept 2016), p.p. 160-164. ISBN: 978-0-620-72418-0.
10. K.J. Leburu, G.M. Isoe, S. Wassin, **D. Kiboi Boiyo**, R.R.G. Gamatham, A.W.R. Leitch and T. B. Gibbon, "Transmission of Pulse per Second Clock Tone Signals in Optical Communication Systems over Optical Fibre and Free Space" *Proceedings of the SATNAC Conference 2016*, Fancourt, George, South Africa (4-7th Sept 2016), p.p. 21-24. ISBN: 000-0-000-00000-0 (Work in Progress).
11. **D. Kiboi Boiyo**, G. M. Isoe, S. Wassin, E. K. Rotich Kipnoo, R. R. G. Gamatham, A.W. R. Leitch and T. B. Gibbon, "An all Optical VCSEL Wavelength Conversion for Optical Fibre Access Networks", *Proceedings of the 2016 Annual Conference on Sustainable Research and Innovation*, 4-6th May 2016, JKUAT, Nairobi-Kenya, p.p. 17-20. ISSN: 2079-6226.
12. S. Wassin, G. M. Isoe, **D. Kiboi Boiyo**, E. K. Kipnoo Rotich, R. R. G. Gamatham, A. W. R Leitch and T. B. Gibbon, "The Square Kilometre Array: The Notion of Timing and Synchronization", *Proceedings of the 2016 Annual Conference on Sustainable Research and Innovation*, 4-6th May 2016, JKUAT, Nairobi- Kenya, p.p. 52-55. ISSN: 2079-6226.

13. I. M. Matere, D. W. Waswa, J. Tonui, **D. Kiboi Boiyo**, "Modeling of ring resonators as optical Filters using MEEP", *Proceedings of the 2016 Annual Conference on Sustainable Research and Innovation*, 4-6th May 2016, JKUAT, Nairobi- Kenya, p.p. 114-118. ISSN: 2079-6226.
14. **D. Kiboi Boiyo**, G. M. Isoe, E. K. Rotich Kipnoo, R. R. G. Gamatham, A.W. R. Leitch and T. B. Gibbon, "Characterization and Compensation of Fibre Link Dispersion in a 10 Gb/s Flexible Network", *61st SAIP Conference 2016*, 4-8th July 2016, Kramer Law building, University of Cape Town, Cape Town, South Africa-Poster.
15. G. M. Isoe, **D. Kiboi Boiyo**, S. Wassin, P. P. Dlamini, E. K. Rotich Kipnoo, R. R. G. Gamatham, A.W. R. Leitch and T. B. Gibbon," Effect of 1.712 GHz RF-Clock Signal Distribution on 10 Gbps 1550.89 nm VCSEL Based Transmission over Single Optical Fibre for Square Kilometre Telescope Array", *61st SAIP Conference 2016*, 4-8th July 2016, Kramer Law building, University of Cape Town, Cape Town, South Africa.
16. P.P. Dlamini, **D. Kiboi Boiyo**, T. B. Gibbon, R.R.G. Gamatham, A.W.R. Leitch, "Laser Effect on the RF Signal Stability for Clock Signal Distribution over Optical Fibre", *61st SAIP Conference 2016*, 4-8th July 2016, Kramer Law building, University of Cape Town, Cape Town, South Africa.
17. S. Wassin, G. M. Isoe, **D. Kiboi Boiyo**, E. K. Kipnoo Rotich, R. R. G. Gamatham, A. W. R Leitch and T. B. Gibbon, "Power Budget Analysis of Passive Components along an Optical Fibre Link of a Frequency Dissemination System within the MeerKAT Telescope Array", *61st SAIP Conference 2016*, 4-8th July 2016, Kramer Law building, University of Cape Town, Cape Town, South Africa.
18. K.J. Leburu, **D. Kiboi Boiyo**, G.M. Isoe, S. Wassin, R.R.G. Gamatham, A.W.R. Leitch and T. B. Gibbon, "Advantages of Free Space Optics over Optical Fibre for Clock Tone Distribution in a 2.5 GHz Transmission Link", *61st SAIP Conference 2016*, 4-8th July 2016, Kramer Law building, University of Cape Town, Cape Town, South Africa-Poster.

2015:

1. **D. Kiboi Boiyo** and T.B. Gibbon, "Advanced Modulation Techniques in a 80 Gb/S Flexible Spectrum for SKA High Speed Data Transport", *SKA SA-HCD 2015*

Postgraduate Bursary Conference, Stellenbosch, Cape Town, 30th Nov- 8th Dec 2015).

2. **D. Kiboi Boiyo**, T.B. Gibbon and A.W.R. Leitch, "Reconfigurable Optical Networks for Next Generation Optical Fibre Transmission", *8th African Laser Centre Student Workshop,* Zevenwacht, Stellenbosch, South Africa (2nd- 4th Dec 2015).
3. **D. Kiboi Boiyo**, T.V. Chabata, E.K. Rotich Kipnoo, R.R.G. Gamatham, A.W.R. Leitch and T.B. Gibbon, "Crosstalk Penalties in Optical Fibre Transport for Next-Generation Flexible Spectrum Networks", *Proceedings of the SATNAC Conference 2015,* Arabella, Hermanus, Western Cape, South Africa (6-9th Sept 2015), p.p. 21-24. ISBN: 978-0-620-67151-4.
4. T.V. Chabata, **D. Kiboi Boiyo**, E.K. Rotich Kipnoo, R.R.G. Gamatham, A.W.R. Leitch and T.B. Gibbon, "Directly Modulated 10.3 Gb/s Coherent Detection Scheme for Passive Optical Access Network in the Fibre-to-the-Hut Technology*", Proceedings of the SATNAC Conference 2015,* Arabella, Hermanus, Western Cape, South Africa (6- 9th Sept 2015), p.p. 37-40. ISBN: 978-0-620-67151-4.
5. **D. Kiboi Boiyo**, T.V. Chabata, Romeo Gamatham, A.W.R. Leitch and T.B. Gibbon, "Reconfigurable Wavelength Selective Switching for 10 Gbps Optical Fibre Ring Networks", *60th SAIP Conference 2015*, Boardwalk, Port Elizabeth, South Africa (29th June – 3rd July 2015).
6. T.V. Chabata, **D. Kiboi Boiyo**, E.K. Rotich Kipnoo, R.R.G. Gamatham, A.W.R. Leitch and T.B. Gibbon, "Performance Comparison between the Traditional Intensity Modulation Direct Detection and Coherent Detection in a High Speed Optical Fibre Communication System", *Proceedings of the 60th SAIP Conference 2015*, Boardwalk, Port Elizabeth, South Africa (29th June – 3rd July 2015), p.p. 399-403, ISSN: 978-0-620-70714-5.
7. G.M. Isoe, E.K. Rotich, **D. Kiboi Boiyo**, R.R.G. Gamatham, A.W.R. Leitch, T.B. Gibbon, K.M. Muguro, D.W. Waswa, "Noise figure and pump reflection power in SMF-reach optical fibre for Raman amplification," in *AFRICON, 2015,* Addis Ababa, Ethiopia, vol., no., pp.1-5, 14-17th Sept. 2015.

2014:

1. **D. Kiboi Boiyo**, E.K. Kipnoo, R.R.G. Gamatham, A.W.R. Leitch, T.B. Gibbon, "Effects of Crosstalk on a 20 Gb/s Flexible Grid 12 km Optical Fibre Transmission",

SKA SA-HCD 2014 Postgraduate Bursary Conference, Stellenbosch, Cape Town, 4-8th Dec 2014.

2. **D. Kiboi Boiyo**, E.K. Kipnoo, R.R.G. Gamatham, A.W.R. Leitch, T.B. Gibbon *"*Evaluation of Efficient Guard Bands on Flexible Grids in an Optical Fibre Transmission", *Proceedings of the ALC Annual Workshop 2014*, p.p. 30, Rabat, Morocco (3-5th November 2014).
3. **D. Kiboi Boiyo**, E.K. Rotich Kipnoo, R.R.G. Gamatham, A.W.R. Leitch, T.B. Gibbon, "Towards Investigating Transmission Penalties in a Flexible Spectrum Optical Network", *Proceedings of the SATNAC Conference 2014*, the Boardwalk, Port Elizabeth, Eastern Cape (31st Aug-3rd Sept 2014), p.p. 459-460. (WIP Paper). ISBN: 978-0-620-61965-3.
4. **D. Kiboi Boiyo**, E.K. Rotich Kipnoo, A.W.R. Leitch, T. B. Gibbon, "Flexible Spectrum and the Effects of Crosstalk on a 20 Gbps Signal over 12 km Optical Fibre", *59th SAIP Conference 2014*, Johannesburg (7-11th July 2014) -Poster.
5. G. M. Isoe, K. M. Muguro, D. W. Waswa, D. Osiemo, E. Kirui, H. Cherutoi, **D. Kiboi Boiyo**, E. Rotich Kipnoo, "Forward Raman Amplification Characterization in Optical Networks", *Proceedings of 2014 International Conference on Sustainable Research and Innovation*, Volume 5, 7-9th May 2014. ISSN: 2079-6226.

Bibliography

[1] M. Jinno, H. Takara, B. Kozicki, Y. Tsukishima, Y. Sone, and S. Matsuoka, "Spectrum-efficient and scalable elastic optical path network: Architecture, benefits, and enabling technologies," *IEEE Communications Magazine*, vol. 47, no. 11. pp. 66–73, 2009.

[2] ITU-T, "G.694.1: Spectral grids for WDM applications: DWDM frequency grid," *Ser. G.694.1*, pp. 1–16, 2012.

[3] N. Sambo, F. Cugini, G. Bottari, G. Bruno, P. Iovanna, and P. Castoldi, "Lightpath provisioning in wavelength switched optical networks with flexible grid," *2011 37th Eur. Conf. Exhib. Opt. Commun.*, pp. 1–3, 2011.

[4] F. Cugini, G. Meloni, F. Paolucci, N. Sambo, M. Secondini, L. Gerardi, L. Poti, and P. Castoldi, "Demonstration of flexible optical network based on path computation element," *J. Light. Technol.*, vol. 30, no. 5, pp. 727–733, 2012.

[5] A. Farrel, D. King, Y. Li, and F. Zhang, "Generalized Labels for the Flexi-Grid in Lambda Switch Capable (LSC) Label Switching Routers," Work in Progress, Label 5, 2015.

[6] G. Bennett and S. Melle, "Superchannels, flex-grid, multilayer switching key developments for next-gen transport networks," *Lightwave*, vol. 30, no. 2, p. 17, Mar. 2013.

[7] M. Jinno, B. Kozicki, H. Takara, A. Watanabe, Y. Sone, T. Tanaka, and A. Hirano, "Distance-adaptive spectrum resource allocation in spectrum-sliced elastic optical path network," *IEEE Commun. Mag.*, vol. 48, no. 8, pp. 138–145, 2010.

[8] ITU-T, "G.694.2:Spectral grids for WDM applications: CWDM wavelength grid," *International Telecomunication Union*. p. 12, 2003.

[9] P. J. Winzer and R.-J. Essiambre, "Advanced Optical Modulation Formats," *Proc. IEEE*, vol. 94, no. 5, pp. 952–985, 2006.

[10] M. Seimetz and R. Freund, "Next generation optical networks based on higher-order modulation formats, coherent receivers and electronic distortion equalization," *Elektrotechnik und Informationstechnik*, vol. 125, no. 7, pp. 284–289, 2008.

[11] E. Lach and W. Idler, "Modulation formats for 100G and beyond," *Opt. Fiber Technol.*, vol. 17, no. 5, pp. 377–386, 2011.

[12] S. Walklin, "Flexible Spectrum Networks Are Not All That Flexible," *White Paper*, no. September. Optelian, USA, 2013.

[13] I. T. Monroy and E. Tangdiongga, *Crosstalk in WDM communication networks*, no. SECS 678. Boston: Kluwer Academic, 2002.

[14] D. J. Geisler, R. Proietti, Y. Yin, R. P. Scott, X. Cai, N. K. Fontaine, L. Paraschis, O. Gerstel, and S. J. B. Yoo, "The first testbed demonstration of a flexible bandwidth network with a real-time adaptive control plane," *2011 37th Eur. Conf. Exhib. Opt. Commun.*, vol. 1, no. d, pp. 1–3, 2011.

[15] P. Wright, A. Lord, and L. Velasco, "The network capacity benefits of Flexgrid.," in *ONDM*, 2013, no. c, pp. 7–12.

[16] T. Foggi, G. Colavolpe, A. Bononi, and P. Serena, "Spectral Efficiency Optimization in Flexi-Grid Long-Haul Optical Systems," pp. 1–7, 2014.

[17] K. Christodoulopoulos, I. Tomkos, and E. A. Varvarigos, "Elastic Bandwidth Allocation in Flexible OFDM-Based Optical Networks," *J. Light. Technol.*, vol. 29, no. 9, pp. 1354–1366, May 2011.

[18] M. Angelou, E. Palkopoulou, D. Klonidis, K. Christodoulopoulos, A. Klekamp, F. Buchali, E. Varvarigos, and I. Tomkos, "Quantifying Spectrum, Cost, and Energy Efficiency in Fixed-Grid and Flex-Grid Networks." 2012.

[19] J. M. Simmons, "Flexible Optical Networks," in *Optical Network Design and Planning*, Second., Springer International Publishing, 2014, pp. 401–440.

[20] N. Massa, "Fiber Optic Telecommunication," *Fundamentals of Photonics*. University of Connecticut, Massachusetts, pp. 293–347, 2008.

[21] H. Khodakarami, B. S. G. Pillai, B. Sedighi, and W. Shieh, "Flexible optical networks: An energy efficiency perspective," *J. Light. Technol.*, vol. 32, no. 21, pp. 3356–3367, 2014.

[22] D. Amar, E. Rouzic, N. Brochier, J.-L. Auge, C. Lepers, and N. Perrot, "Spectrum Fragmentation Issue in Flexible Optical Networks: Analysis and Good Practices," *Photonic Netw. Commun.*, vol. 29, no. 3, pp. 230–243, Jun. 2015.

[23] A. Pagés, J. Perelló, and S. Spadaro, "Lightpath fragmentation for efficient spectrum utilization in dynamic elastic optical networks," *2012 16th Int. Conf. Opt. Netw. Des. Model. ONDM 2012*, 2012.

[24] A. N. Patel, P. N. Ji, J. P. Jue, and T. Wang, "Defragmentation of Transparent Flexible Optical WDM (FWDM) Networks," in *Optical Fiber Communication Conference/National Fiber Optic Engineers Conference 2011*, 2011, p. OTuI8.

[25] P. Roorda, "Critical Issues for the Flexible Spectrum Network," *White paper, Lumentum*. 2015.

[26] A. Kretsis, K. Christodoulopoulos, P. Kokkinos, and E. Varvarigos, “Planning and operating flexible optical networks: Algorithmic issues and tools,” *IEEE Commun. Mag.*, vol. 52, no. 1, pp. 61–69, 2014.

[27] O. G. de Dios and R. Casellas, “Framework and Requirements for GMPLS-based control of Flexi-grid DWDM networks,” *draft-ietf-ccamp-flexi-grid-fwk-07*, no. August 30. Work in Progress, 2015.

[28] V. López, Ó. G. D. E. Dios, O. Gerstel, and N. Amaya, “Target Cost for Sliceable Bandwidth Variable Transponders in a Real Core Network,” *Proc. Futur. Netw. MobileSummit 2013 Conf.*, pp. 1–9, 2013.

[29] H. Takara, B. Kozicki, Y. Sone, T. Tanaka, A. Watanabe, A. Hirano, K. Yonenaga, and M. Jinno, “Distance-adaptive super-wavelength routing in elastic optical path network (SLICE) with optical OFDM,” *Eur. Conf. Opt. Commun. ECOC*, vol. 1–2, pp. 2–4, 2010.

[30] M. Jinno, H. Takara, Y. Sone, K. Yonenaga, and A. Hirano, “Multiflow optical transponder for efficient multilayer optical networking,” *IEEE Commun. Mag.*, vol. 50, no. 5, pp. 56–65, 2012.

[31] N. Sambo, P. Castoldi, A. D’Errico, E. Riccardi, A. Pagano, M. S. Moreolo, J. M. Fabrega, D. Rafique, A. Napoli, S. Frigerio, E. H. Salas, G. Zervas, M. Nolle, J. K. Fischer, A. Lord, and J. P. F. P. Gimenez, “Next generation sliceable bandwidth variable transponders,” *IEEE Commun. Mag.*, vol. 53, no. 2, pp. 163–171, 2015.

[32] M. S. Moreolo, J. M. Fabrega, L. Nadal, F. J. Vilchez, and G. Junyent, “Bandwidth variable transponders based on OFDM technology for elastic optical networks,” *Int. Conf. Transparent Opt. Networks*, pp. 4–7, 2013.

[33] T. Gyselings, G. Morthier, and R. Baets, “Crosstalk analysis of multiwavelength optical cross connects,” *J. Light. Technol.*, vol. 17, no. 8, pp. 1273–1283, 1999.

[34] S. V Kartalopoulos and I. C. Society, “Optical Cross-Connects,” in *Introduction to DWDM Technology: Data in a Rainbow*, SPIE Optical Engineering Press, 2000, pp. 141–150.

[35] M. Jinno, H. Takara, B. Kozicki, Y. Tsukishima, Y. Sone, and S. Matsuoka, “Spectrum-efficient and scalable elastic optical path network: Architecture, benefits, and enabling technologies,” *IEEE Commun. Mag.*, vol. 47, no. 11, pp. 66–73, 2009.

[36] B. Barua, “Evaluate the Performance of Optical Cross Connect Based on Fiber Bragg Grating Under Different Bit Rate,” *Int. J. Comput. Sci. Inf. Technol.*, vol. 3, no. 5, pp. 123–136, 2011.

[37] L. Eldada, “Optical add / drop multiplexing architecture for metro area networks.” SPIE, pp. 2–4, 2008.

[38] C. A. Al Sayeed, A. Vukovic, and O. W. W. Yang, “Performance optimization of PLC-based ROADM subsystem in ring-to-ring interconnection,” *IEEE Int. Conf. Commun.*, vol. 6, no. c, pp. 2764–2769, 2006.

[39] Infinera, “Transmode’s Flexible Optical Networks,” *Application Note*. [Online]. Available: https://www.infinera.com/wp-content/uploads/2015/12/AN_Flexible_Optical_Networks_A-2.pdf. [Accessed: 03-Aug-2016].

[40] C. Rottondi, M. Tornatore, F. Puleio, S. Raavi, A. Pattavina, and G. Gavioli, “On the benefits of lightpath re-provisioning in optical mesh networks,” in *IOFC/NFOEC*, 2012.

[41] Xtera, “New Flex-Rate Channel Card for Flexible, High-Performance 100G/400G Optical Networking,” 2015. [Online]. Available: http://www.xtera.com/new-flex-rate-channel-card-for-flexible-high-performance-100g400g-optical-networking/. [Accessed: 04-Aug-2016].

[42] M. Azadeh, “PIN and APD Detectors,” in *Fiber Optics Engineering*, Boston, MA: Springer US, 2009, pp. 157–175.

[43] T. Xu, G. Jacobsen, S. Popov, J. Li, E. Vanin, K. Wang, A. T. Friberg, and Y. Zhang, “Chromatic dispersion compensation in coherent transmission system using digital filters.,” *Opt. Express*, vol. 18, no. 15, pp. 16243–16257, 2010.

[44] A. Kaur, “Polarization Mode Dispersion compensation in WDM system using dispersion compensating fibre,” *nternational J. Eng. Res. Appl.*, vol. 2, no. 2, pp. 668–673, 2012.

[45] D. Kreutz, F. M. V. Ramos, P. E. Verıssimo, C. E. Rothenberg, S. Azodolmolky, and S. Uhlig, “Software-Defined Networking : A Comprehensive Survey,” in *Proceedings of the IEEE*, 2015, vol. 103, no. 1, pp. 14–76.

[46] J. Leguay, M. Draief, S. Chouvardas, S. Paris, G. S. Paschos, L. Maggi, and M. Qi, “Online and Global Network Optimization: Towards the Next-Generation of Routing Platforms,” pp. 1–16, 2016.

[47] S. Perrin, “Next-Generation ROADM Architectures &Benefits,” 2015.

[48] V. Lopez, B. Huiszoon, J. Fernandez-Palacios, O. Gonzalez De Dios, and J. Aracil, “Path computation element in telecom networks: Recent developments and standardization activities,” in *2010 14th Conference on Optical Network Design and*

Modeling, ONDM 2010, 2010.

[49] Q. Zhu and L. Pavel, "Enabling Differentiated Services Using Generalized Power Control Model in Optical Networks," *IEEE Trans. Commun.*, vol. 57, no. 9, pp. 2570–2575, 2009.

[50] M. Klinkowski and K. Walkowiak, "Routing and spectrum assignment in spectrum sliced elastic optical path network," *IEEE Commun. Lett.*, vol. 15, no. 8, pp. 884–886, 2011.

[51] J. Zhang, Y. Zhao, and Y. Wang, "Spectrum consecutiveness based routing and spectrum allocation in flexible bandwidth networks," in *CHINESE OPTICS LETTERS*, 2012, vol. 10, pp. 1–4.

[52] Y. Wang, J. Zhang, Y. Zhao, J. Wang, and W. Gu, "ACO-based routing and spectrum allocation in flexible bandwidth networks," *Photonic Netw. Commun.*, vol. 25, no. 3, pp. 135–143, 2013.

[53] Coriant, "Coriant Transcend^{TM} SDN Solution." [Online]. Available: http://www.coriant.com/products/transcend-sdn.asp. [Accessed: 10-Nov-2016].

[54] I. Kaminow and T. Li, *Optical Fiber Telecommunications IV-B: Systems and Impairments*, 4th ed. Academic Press, 2002.

[55] R. L. Freeman, *Fundamentals of Telecommunications*, 2nd ed. John Wiley & Sons, 2005.

[56] H. J. R. Dutton, *Understanding Optical Communications*, 1st ed., vol. 1. Raleigh, North Carolina: IBM Corp, 1998.

[57] B. B. T. R. Agarwal, "Transmission Media," in *Data Communication And Computer Networks*, 1st ed., Vikas Publishing House Pvt Limited, 2009, pp. 29–54.

[58] M. Curran and B. Shirk, "Basics of Fiber Optics." Fiber Systems Int.

[59] G. P. Agrawal, *Fiber-Optic Communication Systems*, 4th ed. John Wiley & Sons, 2012.

[60] G. P. Agrawal, "Optical Transmitters," in *Fiber-Optic Communications Systems*, 3rd ed., John Wiley & Sons, 2002, pp. 77–132.

[61] Vertilas GmbH, "Communications VCSEL Product Catalog," *Rev. 5.0, 18.05.2007*, 2007. [Online]. Available: http://www.vertilas.com/sites/default/files/Downloads/vertilas_communications_v5_0_0.pdf. [Accessed: 31-May-2016].

[62] Raycan, "VCSEL Technology." [Online]. Available: http://www.raycan.com/tech.html. [Accessed: 11-Apr-2016].

[63] R. Michalzik, *VCSELs: Fundamentals, Technology and Applications of Vertical-Cavity Surface-Emitting Lasers*. Springer, 2012.

[64] R. E. Michalzik K. J., "Operating principles of VCSELs," in *Verical-Cavity Surface-Emitting Laser Devices*, vol. 6, no. 6, H. E. L. et al., Ed. Germany: Springer Berlin Heidelberg, 2003, pp. 53–98.

[65] Finisar, "Application Note: Optical modes in VCSEL," 2007. [Online]. Available: https://www.finisar.com/sites/default/files/downloads/application_note_vcsel_optical_modes.pdf. [Accessed: 31-May-2016].

[66] K. Iga, "Surface-emitting laser - its birth and generation of new optoelectronics field," *IEEE J. Sel. Top. Quantum Electron.*, vol. 6, no. 6, pp. 1201–1215, 2000.

[67] M. Grabherr, S. Intemann, S. Wabra, P. Gerlach, M. Riedl, and R. King, "25 Gbps and beyond: VCSEL development at Philips," *Proc. SPIE*, vol. 8639, p. 86390J, 2013.

[68] W. Hamad, S. Wanckel, and W. Hofmann, "Small-Signal Analysis of Ultra-High-Speed VCSELs," vol. 52, no. 7, pp. 5–6, 2016.

[69] T. B. Gibbon, K. Prince, T. T. Pham, A. Tatarczak, C. Neumeyr, E. Ronneberg, M. Ortsiefer, and I. T. Monroy, "VCSEL transmission at 10 Gb/s for 20 km single mode fiber WDM-PON without dispersion compensation or injection locking," *Opt. Fiber Technol.*, vol. 17, no. 1, pp. 41–45, 2011.

[70] Raycan, "Key Issues for Long-Wavelength VCSELs." [Online]. Available: http://www.raycan.com/tech_3.html. [Accessed: 11-Apr-2016].

[71] RayCan, "VCSEL: Linking the world," 2011. [Online]. Available: http://www.raycan.com/image/pdf/Raycan-product 2011.pdf. [Accessed: 31-May-2016].

[72] M. Azadeh, *Fiber Optics Engineering*, Optical Ne. California: Springer US, 2009.

[73] NTTElectronics, "NEL Laser diodes," no. 1112A. p. 2005, 2005.

[74] P. J. Winzer, "Modulation and multiplexing in optical communications," *IEEE LEOS NEWSLETTER*. Bell Labs, Alcatel-Lucent, Holmdel, New Jersey, p. 10, 2009.

[75] G. Breed, "A Tutorial Introduction to Optical Modulation Techniques," no. May. Summit Technical Media, LLC, 2007.

[76] S. Reddy, L. Taira, and M. Resso, "Signal Integrity Concerns when Modulating Laser Transmitters at Gigabit Rates," in *DesignCon2002*, 2002.

[77] G. P. Agrawal, *Nonlinear Fiber Optics*, 4th ed. Academic Press, 2007.

[78] J. E. Bowers and Y. G. Wey, "Chapter 17 High-Speed Photodetectors," in *Handbook of Optics: Fundamentals, Techniques and Design*, 1995, pp. 1–29.

[79] E. A. Varvarigos and K. Christodoulopoulos, “Algorithmic aspects in planning fixed and flexible optical networks with emphasis on linear optimization and heuristic techniques,” *J. Light. Technol.*, vol. 32, no. 4, pp. 681–693, 2014.

[80] G. Breed, “Using the Eye Diagram,” *High Freq. Electron.*, no. November, pp. 50–53, 2005.

[81] G. Chauvel, “Dispersion in Optical Fibers.” Anritsu Corporation, 2008.

[82] OFS, “TrueWave REACH fiber Low Water Peak.” OFS FITEL, LLC, Oct 2014, 2014.

[83] Y. Kazuo, I. T. U. International telecommunication Union, and P. systems development, “New functionalities for advanced optical interfaces (Dispersion compensation),” Fujitsu, Report, 2002.

[84] G. P. Agrawal, *Applications of Nonlinear Optics*, 4th ed. San Diego: Academic Press, 2007.

[85] G. Keiser, *Optical Fibre Communication*, 3rd ed. Singapore: Mc-Graw-Hill, 2000.

[86] Jyotsana, R. Kaur, and R. Singh, “Performance comparison of pre-, post- and symmetrical-dispersion compensation techniques using DCF on 40 Gbps OTDM system for different fibre standards,” *Optik (Stuttg).*, vol. 125, no. 9, pp. 2134–2136, 2014.

[87] N. I. Eappen and A. Sangeetha, “Analysis and performance comparison of inverse dispersion compensation technique for standard optical fibers,” in *2014 First International Conference on Computational Systems and Communications (ICCSC)*, 2014, pp. 364–369.

[88] T. V. Chabata, D. K. Boiyo, E. K. R. Kipnoo, R. R. G. Gamatham, A. W. R. Leitch, and T. B. Gibbon, “Signal monitoring and performance stability evaluation tool in a high speed optical communication network,” *Opt. - Int. J. Light Electron Opt.*, vol. 127, no. 20, pp. 9001–9007, 2016.

[89] OFS, “TrueWave RS Fiber Low Water Peak,” OFS FITEL, LLC, USA, Report, 2014.

[90] OFS, “Truewave Ocean Fibers SRS,” OFS FITEL, LLC, USA, Report, 2013.

[91] G. P. Agrawal, “Crosstalk Penalty in Multichannel Ask Heterodyne Lightwave Systems,” *J. Light. Technol.*, vol. 7, no. 12, pp. 2064–2071, 1989.

[92] D. K. Boiyo, E. K. R. Kipnoo, R. R. G. Gamatham, A. W. R. Leitch, and T. B. Gibbon, “Towards Investigating Transmission Penalties in a Flexible Spectrum Optical Network,” *Southern Africa Telecommunication Networks and Applications Conference (SATNAC)*, no. September. Port Elizabeth, pp. 459–460, 2014.

[93] M. Recalcati, F. Musumeci, M. Tornatore, S. Member, S. Bregni, S. Member, A. Pattavina, and S. Member, "Benefits of Elastic Spectrum Allocation in Optical Networks with Dynamic Traffic," *Commun. (LATINCOM), 2014 IEEE Latin-America Conf.*, pp. 1–6, 2014.

[94] ITU-T, "G.671: Transmission characteristics of optical components and subsystems," 2012.

[95] M. Kagawa, H. Tsukada, and M. Yoneda, "Optical add-drop multiplexers for metro/access networks," *Furukawa Rev.*, no. 23, pp. 59–64, 2003.

[96] K. E. Stubkjaer, A. Kloch, P. B. Hansen, H. Poulsen, D. Wolfson, K. S. Jepsen, A. T. Clausen, E. Limal, and A. Buxens, "Wavelength Converter Technology," *IEICE TRANS. ELECTRON*, vol. E.82-C, no. 2. pp. 338–348, 1999.

[97] Y. Wu, X. Xiong, Y. Zhu, J. Meng, and J. He, "All-optical Wavelength Conversion Using Optical Injection Induced Wavelength Switching in V-cavity Laser," in *PIERS Proceedings*, 2014, pp. 915–919.

[98] K.-H. Lee, Y.-S. Cho, S. Kim, and W.-Y. Choi, "A tunable-output wavelength converter based on a self-seeded Fabry-Perot laser diode with a chirped fiber grating," *Microw. Opt. Technol. Lett.*, vol. 37, no. 1, pp. 35–36, 2003.

[99] S. L. Jansen, S. Member, H. Chayet, E. Granot, S. Ben Ezra, D. D. Van Borne, P. M. Krummrich, D. Chen, G. D. Khoe, and H. De Waardt, "Wavelength Conversion of a 40-Gb / s NRZ Signal Across the Entire C -Band by an Asymmetric Sagnac Loop," in *IEEE PHOTONICS TECHNOLOGY LETTERS*, 2005, vol. 17, no. 10, pp. 2137–2139.

[100] COMMSCOPE, "Design Guide: Passive Optical LAN (POL)," 2015.

[101] ITU-T, "G.655: Characteristics of a non-zero dispersion-shifted single-mode optical fibre and cable," 2009.

[102] A. Kajee, "Open Access Network Models for South Africa, a Socio Economic Development Perspective," no. December, 2013.

[103] S. Khan, "South Africa's National Broadband Policy Purpose – SA Connect," no. October. Research ICT Africa, 2015.

[104] SANReN, "Backbone – SANReN," 2016. [Online]. Available: http://www.sanren.ac.za/backbone/. [Accessed: 11-Aug-2016].

[105] A. Jagun, *The Case for "Open Access" Communications Infrastructure in Africa: The SAT-3 / WASC cable - Senegal Case Study*. Strathprints, 2008, pp. 1–34.

[106] B. Akoh, P. Lange, E. Osiakwan, and R. Southwood, *The case for Open Access*

communications infrastructure in Africa : impact of international submarine cable infrastructure [SAT- 3 / WASC] in four African countries. .

[107] Steve Song, “African Undersea Cables – Many Possibilities,” 2016. [Online]. Available: https://manypossibilities.net/african-undersea-cables/. [Accessed: 10-Aug-2016].

[108] MyBroaband, “This is what South Africa’s Internet actually looks like,” 2014. [Online]. Available: http://mybroadband.co.za/news/internet/98178-this-is-what-south-africas-internet-actually-looks-like.html. [Accessed: 10-Aug-2016].

[109] SANReN, “SA NREN International Capacity – SANReN,” 2016. [Online]. Available: http://www.sanren.ac.za/sa-nren-international-capacity/. [Accessed: 11-Aug-2016].

[110] Lloyd Gedye, “Fibre optic turf war pushes speeds up and prices down,” 2016. [Online]. Available: http://mg.co.za/article/2016-03-31-fibre-optic-turf-war-pushes-speeds-up-and-prices-down. [Accessed: 11-Aug-2016].

[111] Department of Communications, “National Broadband Policy for South Africa,” *Government Gazette - 3 April*, no. February. p. 28, 2013.

[112] ACCAN and ISOC-AU, “National Broadband Network : A Guide for Consumers,” no. April. 2011.

[113] NBN-Co, “Half Year Results 2016 Presentation Agenda.” 2016.

[114] ZTE, “End to End Design for Australia NBN Co Network.” 2009.

[115] NBN-Co, “NBN Co Network Design Rules,” no. December. NBN Co Ltd, p. 50, 2011.

[116] SKATelescope, “SKA Telescope: Amazing Facts,” 2016. [Online]. Available: https://www.skatelescope.org/amazingfacts/. [Accessed: 12-Aug-2016].

[117] SKATelescope, “Africa - SKA Telescope,” 2016. [Online]. Available: https://www.skatelescope.org/africa/. [Accessed: 15-Aug-2016].

[118] SKA, “AFRICA ’ S MeerKAT RADIO TELESCOPE.” CSIR, 2015.

[119] SKA, “MeerKAT – SKA SA,” 2016. [Online]. Available: http://www.ska.ac.za/science-engineering/meerkat/. [Accessed: 15-Aug-2016].

[120] T. B. Gibbon, E. K. Rotich Kipnoo, R. R. G. Gamatham, A. W. R. Leitch, R. Siebrits, R. Julie, S. Malan, W. Rust, F. Kapp, T. L. Venkatasubramani, B. Wallace, A. Peens-Hough, and P. Herselman, “Fiber-to-the-telescope: MeerKAT, the South African precursor to Square Kilometre Telescope Array,” *J. Astron. Telesc. Instruments, Syst.*, vol. 1, no. 2, p. 28001, Apr. 2015.

[121] SKATelescope, “Signal Transport and Networks - SKA Telescope,” 2016. [Online]. Available: https://www.skatelescope.org/signal-processing/. [Accessed: 12-Aug-2016].

[122] Signal and Data Transport Consortium, “SADT Technical Information Pack,” no. January. Rev 2.0, pp. 1–89, 2016.

[123] R. Schilizzi, “Big Pipes for Big Data : Signal and Data Transport in the SKA Data Transport and Synch & Time,” no. March. 2013.

[124] H. Nie, “High performance, low-cost PIN, APD receivers in fiber optical networks and FTTx applications,” *14th Annu. WOCC*, 2005.

[125] D. K. Boiyo, T. V Chabata, E. K. R. Kipnoo, R. R. G. Gamatham, A. W. R. Leitch, and T. B. Gibbon, “Reconfigurable high-speed optical fibre networks : Optical wavelength conversion and switching using VCSELs to eliminate channel collisions,” *Opt. Fiber Technol.*, vol. 33, pp. 30–35, 2017.

[126] D. K. Boiyo, G. M. Isoe, R. R. G. Gamatham, A. W. R. Leitch, and T. B. Gibbon, “A 1550 nm all Optical VCSEL-to-VCSEL wavelength conversion of a 8.5 Gb/s data signal and transmission over a 24.7 km fibre,” *Proc. SPIE*, vol. 10036. SPIE, p. 100360X–1–100360X–6, 2017.

[127] TelecomEngineeringInc, “DWDM Lite ™ OADM Brochure Completely passive DWDM optical add / drop multiplexer,” *Product Catalogue*. [Online]. Available: http://www.telecomengineering.com/downloads/pdf/DWDM/OADM DWDM Lite Product Catalog.pdf. [Accessed: 15-Jul-2016].

[128] ITU-T, “G.695: Optical interfaces for coarse wavelength division multiplexing applications.” 2010.

[129] VPIphotonics GmbH, “VPI TransmissionMaker,” 2016. [Online]. Available: http://www.vpiphotonics.com/index.php. [Accessed: 21-Jul-2016].

[130] D. K. Boiyo, T. V. Chabata, R. E. K. Kipnoo, R. R. G. Gamatham, A. W. R. Leitch, and T. B. Gibbon, “Crosstalk Penalties in Optical Fibre Transport for Next-Generation Flexible Spectrum Networks,” *Southern Africa Telecommunication Networks and Applications Conference (SATNAC)*. Arabella, Hermanus, Western Cape, South Africa, pp. 21–24, 2015.

[131] C. Brandon and E. Al, *Advanced Fiber Optic Testing High-Speed Fiber Link and Network Characterization*, vol. 2. JDS Uniphase Corporation, 2010.

[132] J. H. Winters, R. D. Gitlin, and S. Kasturia, “Reducing the effects of transmission impairments in digital fiber optic systems,” *IEEE Commun. Mag.*, vol. 31, no. 6, pp.

68–76, 1993.

[133] C. Headley and G. P. Agrawal, *Raman Amplification in Fiber Optical Communication Systems*. Elsevier Academic Press, 2005.

[134] P. Diamond, “Square Kilometre Array: Strategic Overview,” 2013.

[135] SKA-CSTF, “SKA array configuration studies – a guide for SKA site proposers,” vol. 2005.

[136] D. K. Boiyo, G. M. Isoe, E. K. R. Kipnoo, R. R. G. Gamatham, A. W. Leitch, and T. B. Gibbon, “Utilization of Flexible Spectrum to Optimize a 24.7 km Fibre TDM Passive Optical Network,” in *Southern Africa Telecommunication Networks and Applications Conference (SATNAC)*, 2016, no. September, pp. 8–12.